PhD Program in Molecular Medicine

Cycle: XXXII

A.Y. 2018/2019

PhD Thesis

Insights into the tumor suppressor KCASH2: new functions and mechanisms of regulation

Candidate:

Annapaola Angrisani

PhD. Program Coordinator:
Prof. Isabella Screpanti

Tutor:
Prof. Enrico De Smaele

TABLE OF CONTENTS

ABSTRACT

Medulloblastoma (MB) is the most common malignant childhood brain tumor. About 30% of all MBs belong to the I molecular subgroup, characterized by constitutive activation of the Sonic Hedgehog (Hh) pathway. The Hh pathway is involved in several fundamental processes during embryogenesis and in adult life and its deregulation may lead to cerebellar tumorigenesis. Indeed, Hh activity must be maintained via a complex network of activating and repressor signals.
One of these repressor signals is KCASH2, belonging to the KCASH family of protein, which acts as negative regulators of the Hedgehog signaling pathway during cerebellar development and differentiation. KCASH proteins possess a well conserved N-terminal BTB domain but an heterogenous C-terminus, suggesting the presence of peculiar functions or different mechanisms of individual KCASHs functional regulation.

In order to better characterize the physiologic role and modulation mechanisms of KCASH2, we have searched through a proteomic approach for new KCASH2 interactors, identifying Potassium Channel Tetramerization Domain Containing 15 (KCTD15) and Mitotic Arrest Deficient2-like 1 (MAD2).
KCTD15 is able to directly interact with KCASH2, through its BTB/POZ domain. This interaction leads to increase KCASH2 stability which implies a reduction of the Hh pathway activity and a reduction of Hh-dependent MB cells proliferation. Here, we report the identification of KCTD15 as a novel player in the complex network of regulatory proteins which modulate Hh pathway, this could be a promising new target for therapeutic approach against MB.
MAD2 is the main player in the spindle assembly complex (SAC), essential for chromosomal stability during cell mitosis, preventing defected cellular divisions that may lead to aneuploidy. Nowadays, no mechanisms have been provided for the MAD2 regulation, although it has been suggested that MAD2 may be degraded following ubiquitination by an unknown E3 ligase. Our work fills this gap, identifying in Cul3-KCASH2 the E3 ligase involved in MAD2 degradation process. Our data suggested that KCASH2 overexpression, affecting MAD2 protein levels, alters SAC formation during cell cycle, promoting mitotic defects that may give rise to chromosomal aberration and aneuploidy. The discovery of a mechanism able to modulate MAD2 protein levels and, indirectly, SAC checkpoint functionality and cell cycle progression may have important implications both in therapeutic approaches directed to the reconstitution of a normal SAC function and in approaches aiming to increase chromosomal instability to a level not sustainable by tumor cells, leading to their death.
Finally, we have investigated the KCASH2 transcriptional regulation aimed to discover new potential therapeutics mechanisms for all that tumor types in which KCASH2 is low expressed. We have

analyzed its proximal promoter region and performed bioinformatics analyses in order to identify putative transcription factors involved in KCASH2 regulation. Here, we have identified SP1, considered unanimously a hallmark of cancer, as a key transcriptional regulator that is involved in KCASH2 expression modulation in different cancers.

The work presented here draw a more complex, although not yet complete, picture of the biological role of KCASH2, unveiling its additional functions as a new putative "guardian" of genomic stability and identifying two novel mechanism of regulation of its expression in KCTD15 and SP1.

INTRODUCTION

1. KCASH2 AS A MODULATOR OF THE HEDGEHOG SIGNALING PATHWAY

In our laboratory we have discovered and characterized the KCTD Containing-Cullin3 Adaptors, Suppressors of Hedgehog (KCASH) family of proteins. The family is composed by three human potassium (K+) channel tetramerization domain (KCTD) containing proteins: REN^{KCTD11} also referred as KCASH1, KCTD21 also indicated as KCASH2 and KCTD6, renamed KCASH3 (De Smaele et al., 2011).
This family of proteins has been first identified as a negative regulator of the Hedgehog (Hh) signaling pathway, playing an important role in the control of the developmental and tumorigenic processes driven by this pathway.

1.1. The Hedgehog signaling pathway

The evolution has worked with a rather limited number of signaling pathways to generate the notable variety and complexity of forms and functions that we see today. Four decades of intensive research have identified the key molecular players that underpin these mechanisms and have unveiled the plethora of processes that they control (Ingham et al., 2011). The majority of cell signaling processes regulates development and understanding how these pathways have evolved to perform their function can illuminate the origin of morphological diversity, as well as the molecular and cellular basis of development and disease.

One such pathway is the evolutionarily conserved Hedgehog (Hh) signaling **(figure1)** which regulates cell functions that are vital for normal embryonic development and adult tissue homeostasis (Niyaz et al., 2019). During vertebrate development, Hh signaling plays an essential role in orchestrating the cell specification and cell division programs required to form an organism (Petrova et al., 2014). In the adult, Hh continues to signal to discrete populations of stem and progenitor cells within various organs, including the brain (Ahn et al., 2005), skin (Brownell et al., 2011), prostate (Peng et al., 2013) and bladder (Shin et al., 2011) among others. Indeed, Hh ligands diffuse to form spatial gradients that provide positional information across a field of progenitor cells to inscribe a pattern of cell fates on a developing tissue. A hallmark of Hh signaling is its ability to act as a system that drives distinct outcomes depending on the strength and duration of signaling activity in target cells, and not a binary ON/OFF switch (Kong et al., 2019). The Hh signaling ability to control distinct cell fates depending

on its concentration opens important questions: how Hh gradients are generated and maintained during development, how the responses to Hh signaling change over time and how different threshold are transduced to elicit distinct developmental outcomes (Jiang and Hui C, 2008). All these questions are yet under investigation.

The *Hh* gene was first discovered in Drosophila as a "segment-polarity" gene that controls Drosophila embryonic cuticle pattern (Nüsslein-Volhard and Wieschaus, 1980). The origin of the name "Hedgehog" derives from the short and "spiked" phenotype of Hh mutant Drosophila larvae cuticle. Soon after the molecular identification of Drosophila *Hh* gene (Lee et al., 1992), vertebrate homologs of *Hh* were identified in chick and mouse and were involved in limb and the neural tube patterning (Riddle et al., 1993).
Of note, while Drosophila has a single *Hh* gene, mammals have three paralogous genes, called Sonic Hedgehog (SHh), Indian Hedgehog (Ihh), and Desert Hedgehog (Dhh), which possess different functions and expression patterns (Echelard et al., 1993):
- Dhh plays a role in germ-cell proliferation towards the late stages of spermatogenesis, testis determination, androgen synthesis and is involved in sex differentiation.
- Ihh is a master regulator of endochondral bone development (McMahon et al., 2003), regulating the proliferation and differentiation of chondrocytes. Moreover, together with SHh, it is involved in midline specification (St-Jacques et al., 1999).
- finally, SHh has the most critical roles in development, acting as a morphogen implicated in establishing the early left-right/ anterior-posterior axis in the limbs and in regulating ventral cell fates in the central nervous system.
The vertebrate Hh proteins can act over a field of cells that are many cell diameters away from the source of the protein. This long-range signaling requires a sensitized signal transduction dependent on the primary cilium (Corbit et al., 2005; Bangs and Anderson, 2017). The primary cilium is a single, small, hair-shaped projection that emanates from the surface of nearly all non-dividing mammalian cells. Mutations in different proteins required for cilia formation have distinct effects on Hh signaling: some of them block responses to Hh ligands, other ones cause ligand-independent pathway activation and yet others change the spatial organization of pathway activation.

Hh proteins signal via two transmembrane proteins, Patched (Ptch) and Smoothened (Smo).
Unlike most receptors, Ptch activity turns off the downstream pathway in the absence of ligand and Hh binding relieves that repression. The Ptch protein does not share the typical topology of receptors for secreted polypeptides: indeed, it belongs to the integral-membrane proteins family, formed by two large extracellular loops and 12 transmembrane domains, and it presents a sterol-sensing domain

(SSD). Likewise, Smo encodes a transmembrane protein that is similar to the large family of G protein-coupled receptors and to members of the Frizzled family serpentine proteins (Ayers and Thérond, 2010).

All Hh ligands must bind and inhibit the Ptch function to trigger signaling in target cells. Vertebrates, unlike Drosophila, have two Ptch genes (Ptch1 and Ptch2) but Ptch1 is the major regulator of signaling *in vivo*. In the absence of Hh ligand, Ptch1 localizes to the cilium whereas Smo is excluded and is typically localized to the transition zone at its base. The Hh ligands, instead, elicit their effect by directing Ptch1 to the endosomes (and lysosomal degradation) and Smo to the cilium tip, activating the intracellular signaling cascade. Three distinct co-receptors (Cdo, Boc, and Gas1) facilitate high-affinity binding of mature Hh ligand to Ptch, thereby enhancing Hedgehog signal strength.

Of note, Ptch1 expression is activated by Hh signaling, resulting in a negative feedback loop: Hh ligands inactivate Ptch1 and derepresses Smo, increasing transcription of Ptch1 which, in turn, inhibits Smo (Huangfu and Anderson, 2006).

Unlike Gli1, that functions exclusively as a transcription activator, the transcription factors Gli2 and Gli3 perform the dual function as repressor (GliR) and activator (GliA) of Hh target genes. In the off-state of Hh pathway, Gli3 protein appears to continuously cycle through the primary cilium where it undergoes proteolytically cleavage into a C-terminally truncated repressor form lacking the transactivation domain. The Gli3 repressor form translocases to the nucleus where it binds to the promoter of Hh target genes and shuts off their transcription. The balance between Gli3 activator and repressor is fine-tuned by sequential post-translational events mediated by kinases (PKA, Gsk-3β and Ck1) and phosphatases (Abe and Tanaka, 2017).

Another fundamental critical negative pathway regulator is Suppressor of Fused (SuFu), a protein localized both in the nucleus and the cytoplasm which controls the Hh pathway by directly binding to Gli proteins. When the Hh signaling is absent, SuFu restrains Gli1, Gli2 and 3 in the cytoplasm, promoting Gli2 and Gli3 processing into repressor form. On the other hand, SuFu may stabilize Gli2 and Gli3, protecting them from degradation by the E3-Ubiquitine ligase SPOP. Hh-mediated Smo activation releases Gli1, Gli2 and Gli3 from cytoplasmic sequestration by SuFu, allowing the TFs to move to the nucleus inducing gene targets transcription (Carpenter and Lo, 2012).

In addition to the canonical activation of GLI by the Hh-Ptch-Smo route, which is typical of normal cells and ciliated tumors, SMO-independent stimulation of GLI activity are observed in cancer (Gu and Xie, 2015; **figure2**). These non-canonical mechanisms are involved both in transcriptional activation of GLI genes and in post-translational modifications of GLI proteins, representing a

heterogeneous mosaic of alterations that contribute to the development of several types of cancer with elevated GLI activity (Brechbiel et al., 2014). Often in a given cancer type, canonical and non-canonical Hh pathway activation co-exist. In some cancer types, more than one mechanism of non-canonical Hh activation occurs simultaneously.

In fact, an important mechanism of Hh pathway regulation is represented by ubiquitination-related posttranslational modifications of signaling key components (Canettieri et al., 2010; De Smaele et al., 2011; Gulino et al., 2012; Infante et al., 2019). The complex of these regulatory circuitries finely tunes Hedgehog signaling providing a tight control of developmental processes, the subversion of which leads to medulloblastoma tumorigenesis.

Numerous studies have highlighted the importance of molecular crosstalk between the Hedgehog and other signaling cascades, interactions that can modulate signal strength and determine specificity of molecular and cellular phenotypes (Dennler et al., 2007; Beauchamp et al., 2009). Indeed, recent studies show that Hh signaling elements talk to several other cofactors belonging to major pathways, such as Notch, Wnt, and transforming growth factor β (TGF-β). The integration of several signaling pathways is a key step able to determine a more aggressive behavior of tumor cells and their resistance to pharmacological approaches. Interestingly, Notch, Wnt, and TGF-β pathways are able to promote/sustain oncogenesis through synergistic associations with Hh signaling in several types of tumors (as reviewed in Pelullo et al., 2019).

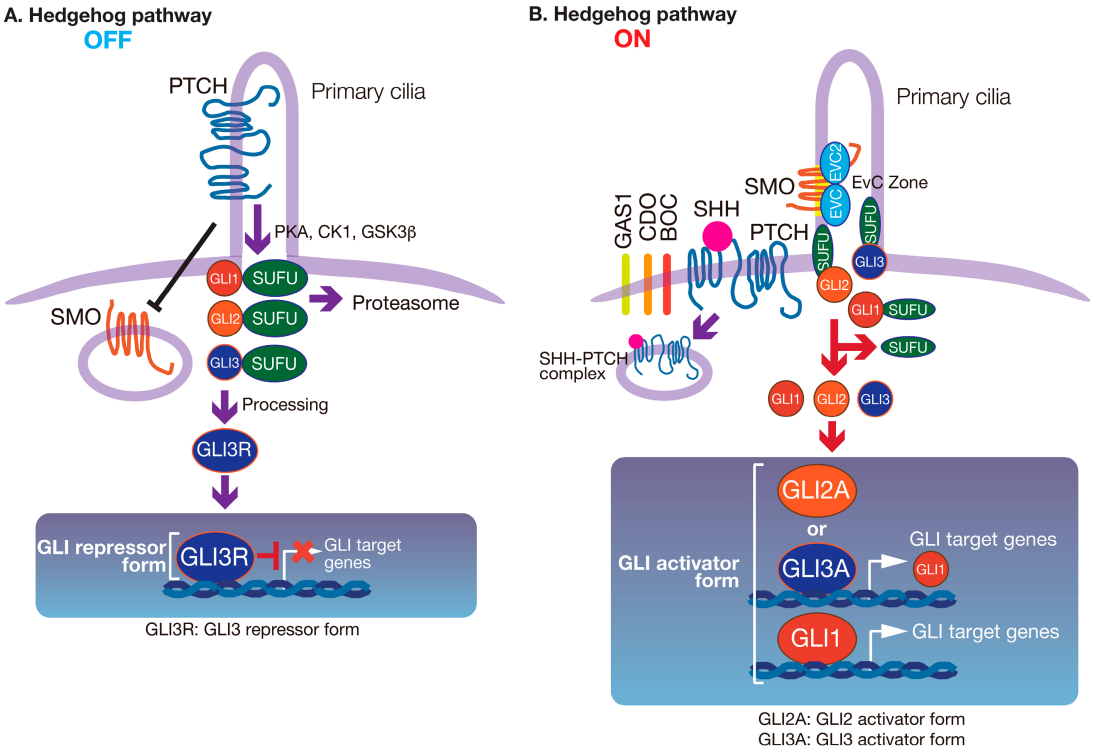

Figure 1. The Hedgehog signaling pathway

A) In the absence of Hedgehog (HH) ligand, PTCH blocks the ciliary localization of SMO; a repressor form of GLI (mainly GLI3R) suppresses the induction of GLI target genes.

B) Signaling is activated in the presence of HH ligand. The binding of HH ligand to PTCH prevents PTCH inhibition of SMO and SMO then interacts with EVC–EVC2 complex and translocates into primary cilia to be fully activated. SMO then activates mainly GLI2. GLI2 up-regulates the GLI1 expression, as well as GLI target genes.

From Yoshinori and Tanaka, 2017.

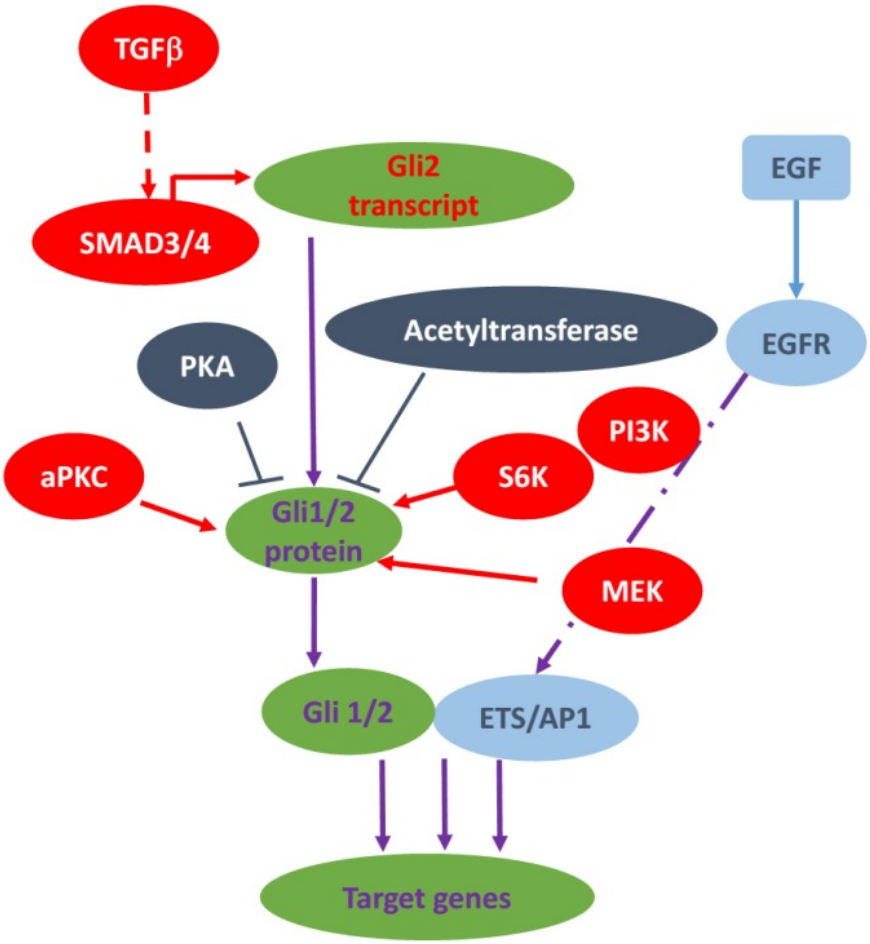

Figure 2. A diagram of typical non-canonical Gli1/2 signaling

From Gu and Xie, 2015.

1.2. Hedgehog signaling in development and cancer

During embryonic development, the Hedgehog signaling regulates proliferation and differentiation in a time- and position-dependent fashion (Ingham and McMahon, 2001). Some of the Hh pathway members have been implicated as key mediators, acting as morphogenic factors promoting dose-dependent induction of differentiation and/or cell fate. They also have an effect as mitogens, controlling cell proliferation, survival, and organogenesis in different anatomical regions of vertebrates and as an induction signal of the ventral neural tube, development of the anterior-posterior axis of extremities and somatic ventral structures (Ruat et al., 2012).

In the central nervous system (CNS) Hh signaling orchestrates many aspects of cerebellar development and maturation. In particular, it regulates the growth of granule cell progenitors (GCPs) in the cerebellar external germinal layer: in this context, SHh is produced by Purkinje neurons and induces GCPs proliferation (Dahmane et al., 1999; Wechsler-Reya and Scott, 1999) and Bergmann glia differentiation (Stecca et al., 2010).
Although the Hedgehog signaling activity is significantly lower in the adult compared with the embryo, it is still relevant in several organs and tissues. Hh plays an important role in the maintenance and proliferation of continuously renewing tissues such as the gut epithelium (van den Brink et al., 2004) and skin (Teglund and Toftgård, 2010) and is reactivated at sites of tissue damage and repair (Mirsky et al., 1999; Parmantier et al., 1999; Beachy et al., 2004). Furthermore, Hh signaling controls proliferation, migration and survival of numerous cell types, such as retinal precursor cells, optic nerve, myoblasts, astrocytes and neural progenitor cells (NPCs; Varjosalo and Taipale, 2008).

The first description of the role of the Hh pathway in neoplastic transformation arose from observations in central nervous system tumors, glioblastomas and melanomas associated with a genetic amplification of GLI-1 (Gailani et al., 1997). Later, PTCH1 mutations were associated with over-activation of the Hh pathway in basal cell carcinoma and medulloblastoma (Johnson et al., 1996; Xie et al., 1998).

Constitutive Hh signaling triggers a strong cellular mitogenic response that ultimately may favor abnormal proliferation, leading to tumorigenesis.
Four basic models have been proposed to describe the different mechanisms of Hh pathway activation in cancer (**figure 3**; Rubin and de Sauvage, 2006; Scales and de Sauvage, 2009).
The type I cancers are characterized by pathway-activating mutations and are, thus, Hh ligand independent, such as basal cell carcinomas (BCC) and Medulloblastoma (MB). Since these tumors

are ligand independent, therapeutic Hh pathway inhibitors must be designed to act at or below the level of SMO in order to be effective (Johnson et al., 1996).

Type II cancers are ligand dependent and autocrine (or juxtracrine), meaning that Hh is both produced and responded to by the same (or neighboring) tumor cells, supporting both tumor growth and survival. These tumors present a functional PTCH receptor that activates the downstream pathway. This kind of abnormal Hh pathway activation has been detected in a variety of tumors including lung, stomach, esophagus, pancreas, prostate, breast, liver and brain (Karhadkar et al., 2004; Sicklick et al., 2006; Clement et al., 2007). Type II cancers can be effectively suppressed by Hh neutralizing antibodies or SMO antagonists.

Type III cancers are also ligand dependent but paracrine, in that Hh produced by the tumor epithelium is received by cells in the stroma which feed other signals back to the tumor to promote its growth or survival (Scales and de Sauvage, 2009). Inhibition of Hh signaling in the stroma effectively restrained the growth of tumor xenografts.

The last model is reverse paracrine signaling, in which Hh is secreted from the stroma and is received by the tumor cells. So far, this has only been observed in hematological malignancies such as multiple myeloma, lymphoma and leukemia, in which the Hh secreted from the stroma seems to be essential for the survival of the cancerous B cells, via upregulation of the antiapoptotic factor Bcl2 (Dierks et al., 2007; Hegde et al., 2008).

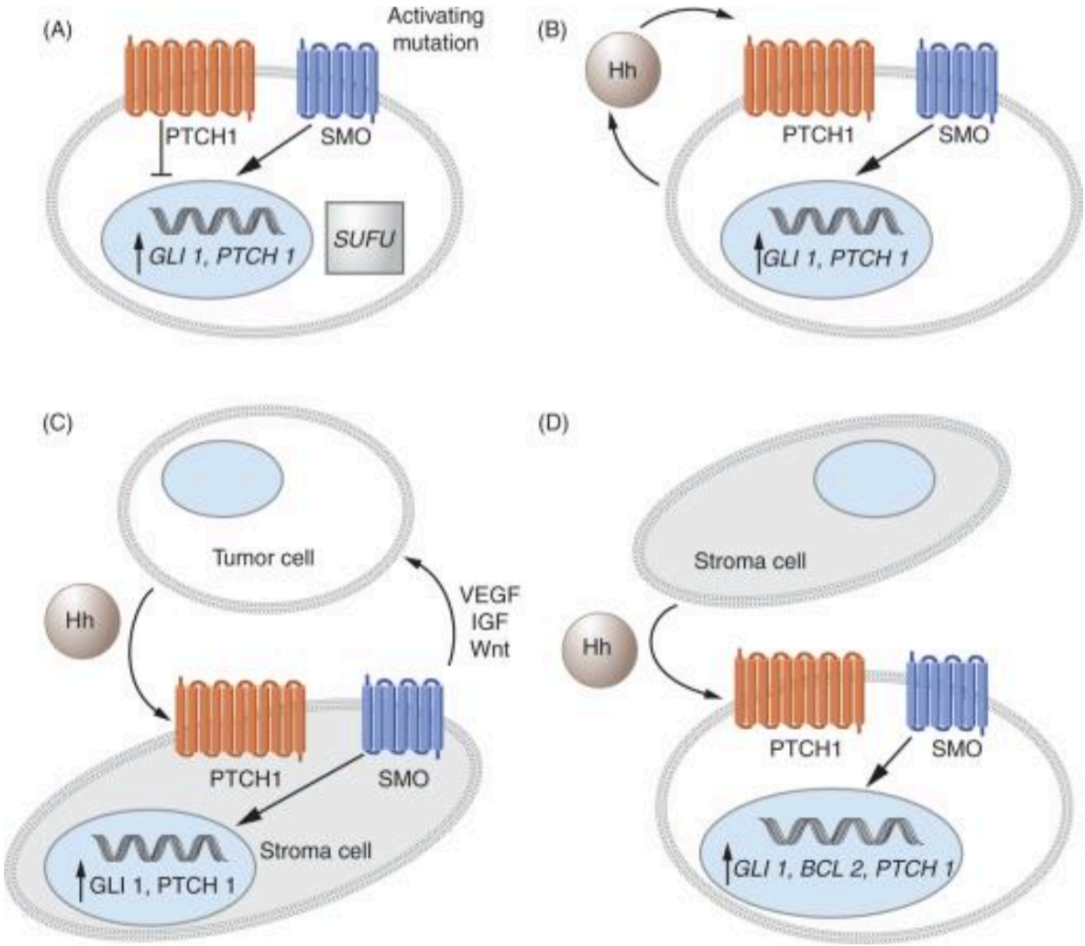

Figure 3. **Model of different Hh signaling pathway in cancer**

A) Type I cancer: Hh ligands independent, characterized by HH pathway-activating mutations.

B) Type II cancers, autocrine (or juxtacrine) ligand dependent: Hedgehog ligand is produced and acts on the same, or neighboring tumor cells, supporting their growth and survival.

C) Type III cancers are paracrine ligand dependent: HH ligand is produced by the tumor cells and responded to by the surrounding stroma, which emits growth signals to sustain the tumor.

D) Reverse paracrine model: stroma promotes tumor survival secreting HH ligand which is received by the tumor cells.

From Rubin and de Sauvage, 2006.

1.3. Medulloblastoma and its molecular classification-based personal therapeutics

Cerebellar development is an extensive process that begins during early embryonic stages and persists more than one year after birth in human. Therefore, the cerebellum is susceptible to acquire various developmental abnormalities that may lead to medulloblastoma, constituting nearly 10% of all pediatric brain tumors (Millard and De Braganca, 2015; Archer et al., 2017). One third of the patients with medulloblastoma is incurable and survivors have a poor quality of life due to the aggressiveness of the broad-spectrum treatments (Bihannic and Ayrault, 2016).

The incidence of medulloblastoma peaks during the first decade of life with a higher incidence noted in children between 3 and 4 years of age and between 8 and 10 years of age. Fewer than 5 percent of cases are associated with the hereditary cancer predisposition syndromes familial adenomatous polyposis (FAP), historically known as Turcot syndrome, or nevoid basal cell carcinoma syndrome (NBCCS), also called Gorlin syndrome, which is characterized by aberrant Hh activity (McNeil et al., 2002).
Historically, age at diagnosis and extent of disease have been most strongly associated with prognosis, with younger patients and those with more advanced disease faring more poorly than older patients and those with limited disease (Chang et al., 1969). More recently, pre-treatment prognosis of medulloblastoma has been refined by histopathologic subclassification into the following variants: large-cell medulloblastoma, anaplastic medulloblastoma, desmoplastic/nodular medulloblastoma, and medulloblastoma with extensive nodularity (MBEN). The latter two variants have been shown to have a significantly superior prognosis as compared to the large cell and anaplastic variants in young children (Louis et al., 2007).

Recent transcriptional profiling studies, derived from microarray data of large numbers of patients with MB, revealed clusters of patients with similar transcriptomes and proteomes involving in the same signal transduction pathways. Therefore, the recent insights into the biology of medulloblastomas have occurred at the molecular level, resulting in their categorization into the four molecular subgroups: Wingless (Wnt), Sonic Hedgehog (SHh), Group 3, and Group 4. Each subgroup is characterized by a unique set of genetics and gene expression as well as demographic and clinical features (**figure 4;** Northcott et al., 2011; Juraschka and Taylor, 2019).

Treatment for medulloblastoma typically includes surgery, craniospinal radiation therapy and adjuvant chemotherapy. Although the 5-year survival rate is high (80% for standard- risk patients,

55%-76% for high-risk patients), outcomes of these highly toxic treatments are suboptimal with significant long-term morbidity, including neurocognitive impairment, endocrine deficiencies and secondary tumors.

The molecular characterization has helped in identifying the driving factors leading to tumorigenesis, but several other mechanisms may play critical roles in the tumorigenic process. One of these is represented by Chromosomal Instability (CIN; Hanahan and Weinberg, 2011), source of genetic variation in either altered chromosome number (aneuploidy) or structure. CIN facilitates the acquisition of mutations conferring aggressive or drug-resistant phenotypes during cancer evolution and can be found in many MBs belonging to the different molecular subtypes.

This recent advance in the field, combined with the development of associated preclinical models for each subgroup, enable the discovery and use of targeted therapy in clinical treatments for each subtype of medulloblastoma.

Development of therapeutics for the canonical SHh signaling pathway has primarily focused on targeting SMO and GLI1 (Rimkus et al., 2016; **figure 5**).

Natural and synthetic antagonists have been developed for both SMO and GLI1 with many having undergone clinical trials with varying degrees of success. SMO inhibition was first characterized through binding studies of cyclopamine, a natural steroidal alkaloid derived from *Veratrum californicum* (Incardona et al., 1998). Although it significantly reduced tumor growth *in vivo*, cyclopamine never reached its therapeutic potential, as it caused many potent side effects, including weight loss, dehydration, and death in mouse models. Derivatives of cyclopamine were developed to overcome solubility and stability issues and showed promise in *in vitro* studies, though *in vivo* evaluation of these compounds has not been conclusive (Fan et al., 2011).

Vismodegib (Erivedge®, Genentech) and Sonidegib (Odomzo®, Novartis) are two Smo-antagonists of the second generation cyclopamine derivats, approved by the Food and Drug Administration (FDA) for treatment of metastatic and/or locally advanced BCC (Pan et al., 2010; Dlugosz et al., 2012). Despite some promising clinical response, treatments with Vismodegib or Sonidegib have resulted in aggressive tumor relapse, due to the development of resistant tumor clones. In particular, Vismodegib resistance is prevalently associated with SMO mutation and to a lesser extent with alterations of downstream Hh pathway components (SuFu and Gli2) or induction of alternative signaling pathways leading to Gli1 activation, such as phosphatidylinositol 3-kinase (PI3K) and atypical protein kinase C ι/λ (aPKC-ι/λ; Sharpe et al., 2015).

All mechanisms that act downstream of SMO are alternative causes of drug-resistance to the treatment of Hh-driven cancers. Thus, targeting downstream HH components is now considered a

more efficient approach and many attempts have been already carried out (Buonamici et al., 2010; Coni et al., 2017).

GLI transcription factors are the terminal effectors of the SHh-SMO signaling pathway and can also be activated independent of SHh and SMO by other important molecular pathways. GLI antagonists, GANTs, were identified at the National Cancer Institute. GANT-58 and GANT-61 were both discovered to inhibit GLI-mediated gene activation, though GANT-61 showed more specificity towards GLI proteins and more effectively reduced GLI1 and GLI2 DNA-binding ability. Although GANT-61 has shown potent inhibition of GLI1 and GLI2 in many cancer cell lines, including rhabdomyosarcoma, osteosarcoma, neuroblastoma, and ovarian cancer, no clinical trials are currently ongoing (Lauth et al., 2007; Srivastava et al., 2014).
Arsenic trioxide (ATO) is an FDA-approved inhibitor of GLI1 and GLI2 transcription factors. It has been approved for treatment of acute promyelocytic leukemia (List et al., 2003). ATO directly binds to GLI1 and GLI2, inhibiting activity and decreasing expression of canonical SHh-GLI genes. Studies have shown that ATO also reduced the viability of pancreatic cancer stem cells and prostate cancer-initiating cells, underlining its effectiveness in killing of tumor epithelial cells and tumor-initiating cells (Bansal et al., 2015). Arsenic trioxide is currently in several clinical trials ranging from Phase I to Phase IV for both solid tumors and hematological malignancies.
Glabrescione (GlaB) is an isoflavone naturally present in the seeds of *Derris glabrescens* (Leguminosae). This small molecule binds the protein Gli at its Zinc Finger domain, inhibiting its interaction with DNA. GlaB has proved to be an effective inhibitor of Hh/Gli tumor growth (Infante et al., 2015). Furthermore, it has been observed that the use of Glab in the anticancer treatment of Glioma could lead to changes in the metabolism of tumor cells such as to favor their death (D'Alessandro et al., 2019). Despite the promising results, GlaB is an insoluble molecule and this limits its use in therapy.

Targeting epigenetic regulators such as histone deacetylases (HDACs) has proven a successful therapeutic option in several malignancies. Intriguingly, HDACs have been shown to modulate the activity of HH/GLI signaling with evidence for both a positive and repressive impact, demanding selective inhibition of HDACs, which enhance oncogenic HH/GLI signaling (Canettieri et al., 2010). When administered to mouse models of SHH-MB, HDACi (i.e. mocetinostat MGCD0103) crosses the blood-brain barrier, represses Hh signaling, inhibits cell proliferation and promotes apoptosis of tumor but not of normal cells (Coni et al., 2017). Anyway, no clinical trials are currently ongoing. Lower doses of epi-drugs are beneficial since they allow to achieve the genetic and epigenetic

“reprogramming” effects in cancer cells and simultaneously cause less toxicity in surrounding healthy tissues. Moreover, matching epigenetic therapies with the individual patient's clinical characteristics, personal needs, goals, or preferences, aimed at improving survival and quality of life, is in line with the principles of personalized medicine (Katarzyna et al., 2019).

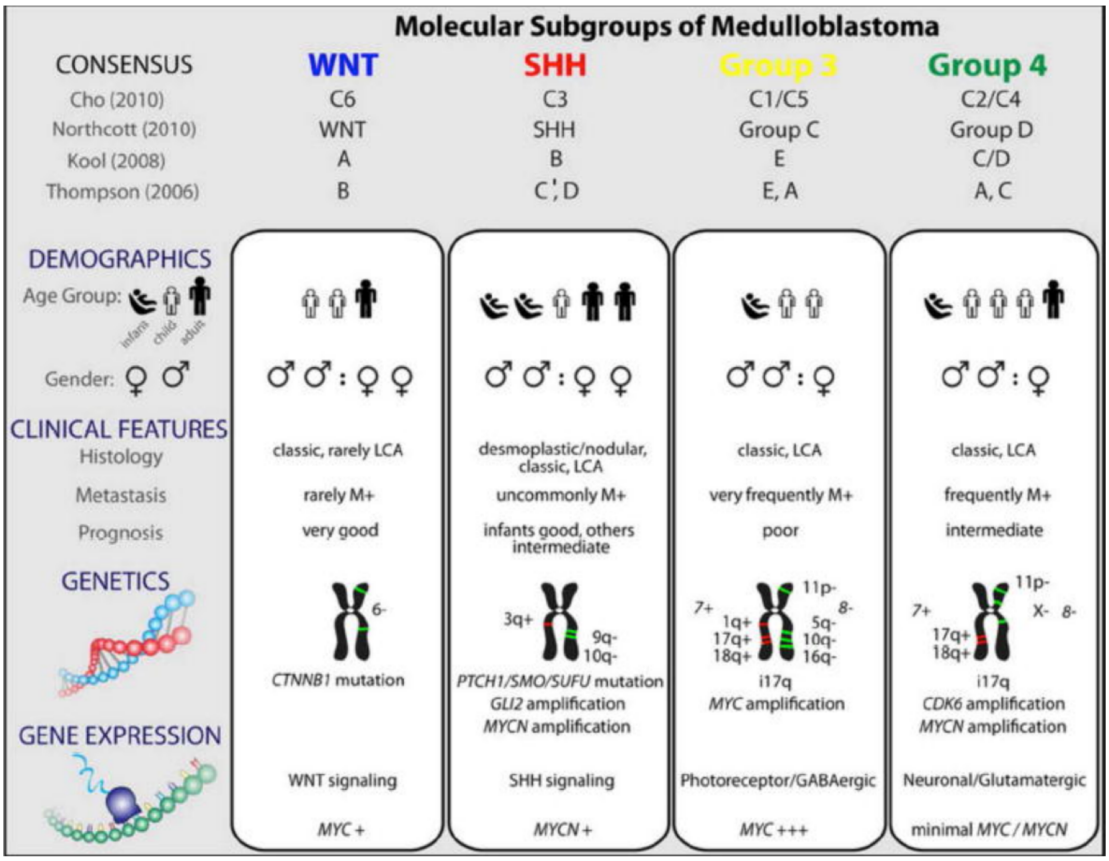

Figure 4. **Comparison of the molecular subgroups of medulloblastoma**

From Taylor et al., 2012.

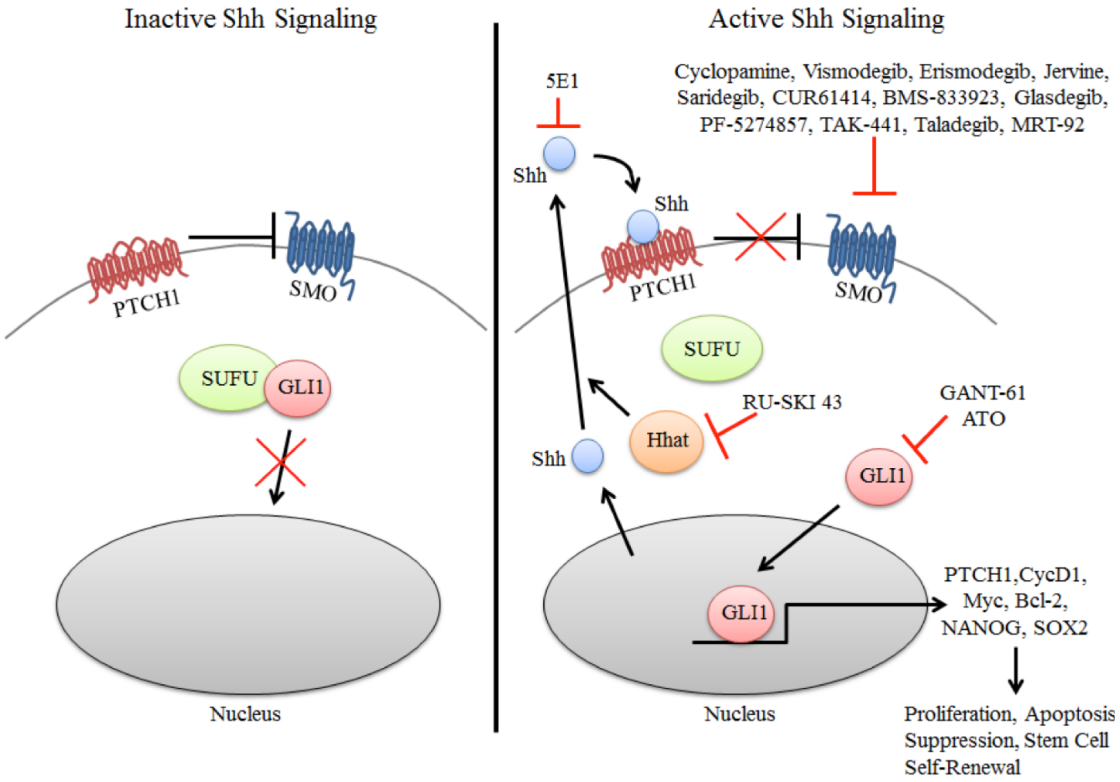

Figure 5. **Inhibition of components of the SHh Pathway in cancer.**

Inhibition of the SHh pathway is primarily directed at inhibition of SMO and GLI1, with many of these compounds in clinical trials for solid cancers.

From Rimkus et al., 2016.

1.4. The KCASH family of proteins

The KCASH family of proteins belongs to the wider family of the KCTD containing proteins (**figure 6**) that share a potassium (K^+) *C*hannel *T*etramerization *D*omain at their N-termini. This domain is also known as Bric-a-brack, Tram-track, Broad complex (BTB) domain, or POZ domain (Liu et al., 2013) and is a highly versatile protein-protein interaction motif of about 100 amino acids that allows homodimerization or heterodimerization.

The 25 described KCTD proteins can be classified into seven groups (named from A to G) based on the amino acid sequences of the potassium tetramerization domains (**figure 6**; Liu et al., 2013) and their ability to bind Cullins (Cul) to form E3-ubiquitine ligase complexes.

Indeed, KCTD proteins may act as adaptors for interactions between one of the known seven Cul ubiquitin ligase and their substrates to facilitate the process of ubiquitination and degradation of the target protein.

The BTB domain is involved in several functions including transcriptional repression (Melnick et al., 2000), cytoskeleton regulation (Kang et al., 2004), tetramerization and gating of ion channels (Minor et al., 2000) and interaction with the Culs proteins to form an E3-ubiquitine ligase complex (Smaldone et al., 2015; Pinkas et al., 2017). Furthermore, the KCTD proteins have been implicated in regulation of different pathways, counting Wnt/β-catenin (Dutta et al., 2010), FGF (Takahashi et al., 2010), GABA (Seddik et al., 2012) and Sonic Hedgehog (De Smaele et al., 2004; Canettieri et al., 2010; De Smaele et al., 2011).

Highlighting KCTD importance, defects in KCTD genes have been associated with several diseases, including medulloblastoma (Mancarelli et al., 2010; De Smaele et al., 2011), breast carcinoma (Faryna et al., 2012), obesity (Yoganathan et al., 2012), and pulmonary inflammation (Koehler et al., 2012).

The KCTD subfamily KCASH (KCASH1, KCASH2 and KCASH3; **figure 7A**) has been involved in negative regulation of the Hh signaling. In fact, the KCASH proteins act in concert to promote the ubiquitination and consequent proteasomal degradation of HDAC1, thereby inhibiting transcriptional activity of Gli1 and Gli2 (De Smaele et al., 2011).

The first identified member of the KCASH family was REN^{KCTD11} (KCASH1).

KCASH1 is localized, as a single-exon locus, to chromosome 17p13.2. Loss of heterozygosity (LOH) on chromosome 17p has been found to be a frequent and specific event in medulloblastoma (Lamont et al., 2004). Allelic deletion on chromosome 17p11.2-pter occurs in up to 50% of MB, with a LOH

sometimes restricted to a common region at 17p13.2–13.3 that might cause the deletion of one or more genes involved in a tumor suppressor pathway. KCASH1 allelic deletion occurs in 39% sporadic human MB but its expression is down-regulated also in diploid tumors (Di Marcotullio et al., 2004; Mancarelli et al., 2010).

KCASH1 expression was shown to promote growth arrest, differentiation, apoptosis and to antagonize Hedgehog signaling in GCPs, suggesting that it was required for restraining GCP expansion at the outer to inner EGL transition. (Argenti et al., 2005).

KCASH1 expression inhibits the growth of MB cells *in vitro* and *in vivo* by antagonizing the Gli-mediated transactivation of Hh target genes (Di Marcotullio et al., 2004).

While searching for additional Hh suppressors in human cancers, two KCASH1 homologues were identified and characterized: KCTD21 (KCASH2) and KCTD6 (KCASH3) (De Smaele et al., 2011). Both transcripts are encoded by bi-exonic genes and map to human chromosomes 11q14.1 (*KCTD21*) and 3p14.3 (*KCTD6*) respectively. KCASH2 and KCASH3 contain a BTB domain sharing a high homology (58% [64/109 aa] and 54% [59/109 aa], respectively) with the KCASH1 BTB motif, whereas the whole sequences present a 42% (111/260 aa) and 32% (77/237 aa) of homology, respectively (**figure 7B**). These genes are conserved throughout most vertebrates (*KCASH1* and *KCASH3* in euteleostoma while *KCASH2* in amniota) and *KCASH3* branched earlier in the evolution than both the other members family (**figure 7A**).

KCASH1, KCASH2 and KCASH3 The KCASHs protein may form, through BTB domain, homo-oligomers or hetero-oligomers with each other, with the exception of KCASH2/KCASH3.

Through their BTB domain, KCASH1 and KCASH2 are able to bind Cul3 to form the active E3-ligase complex. By recruiting Cul3 into a complex with HDAC1, bound by their C-terminal region, the two KCASHs proteins promote the ubiquitination and consequent proteasomal degradation of HDAC1, thereby inhibiting the deacetylation-mediated transcriptional activity of Gli1 and Gli2 (De Smaele et al., 2011). Of note, KCASH3, which is unable to bind directly HDAC1, recruits this deacetylase through KCASH1, exploiting its ability to heterodimerize with it.

Analysis of the expression of KCASH2 and KCASH3 in different mouse tissues indicates that both genes, similarly to KCASH1, are expressed in cerebellum. Moreover, expression of the two genes increases during development, presenting the higher levels in adult cerebellum.

KCASH2 and KCASH3 expression was also significantly reduced in human MB (**figure 7C and 8A**). Indeed, in silico KCASH2 expression analysis on a publicly available database of 763 MB samples (Cavalli et al., 2017) by software R2 (R2: Genomics Analysis and Visualization Platform (http://r2.amc.nl)) confirmed in a wider cohort of tumors that KCASH2 expression levels are significantly lower in SHh-MB compared with MB of the other groups (**figure 8B**).

In addition to still unidentified epigenetic silencing events, *KCASH2* allelic deletion was also observed to contribute to the reduced expression of this gene (**figure 7C**; De Smaele et al., 2011).
The KCASHs inhibitory role on Hh signaling and their reduced expression in primary MB suggest that these proteins could suppress tumor cell growth, displaying an antitumor activity.
KCASH2 shares with the other KCASH family members the N-terminal BTB domain, essential both for homo- or hetero- tetramerization of the KCASH proteins and for binding to Cullin3.
On the other end, KCASH proteins present a divergent C-terminal region, which characterizes the different members, suggesting additional peculiar biological functions for these proteins that warrant further investigations.
Indeed, while only KCASH1 and 2 are able to bind HDAC1, KCASH3 was shown to be able to bind USP21 (Heride et al., 2016).
At present, no further specific function for KCASH2 has been described, although the KCASH2 C-terminal region is highly conserved by evolutionary pressure from fishes (81% conservation) to reptiles (93%), birds (91%), and mammals (mouse 99.6 %; **figure 9**).
Interestingly, other tumor types such as colon cancer, not classified so far as Hh-dependent, may present low KCASH2 levels (this work, see results), suggesting further functions for KCASH2 in these contexts. Of note, chromosome 11q, where *KCASH2* gene is localized, can be lost in several sporadic tumors, including MB (Reardon et al., 2000; Lescop et al., 1999), neuroblastoma (Luttikhuis et al., 2001), leukemia (Stankovic et al., 2014) and prostate cancer (Schleutker et al., 2003).

The KCASH proteins control Hh signaling through action on HDAC1. HDACs are considered to be among the most promising targets in drug development for cancer therapy (Minucci and Pelicci, 2006; Di Marcotullio et al., 2011). While traditional inhibitors of HDACs may present a wide spectrum of action on other signaling pathway, the identification of a mechanism that physiologically represses HDAC function in cerebellum, as the KCASH proteins can do, is relevant to prevent medulloblastoma tumorigenesis. It becomes fundamental, though, to understand the mechanism through which the expression of KCASHs is repressed and what are the factors that may restore or upregulate their physiological levels.

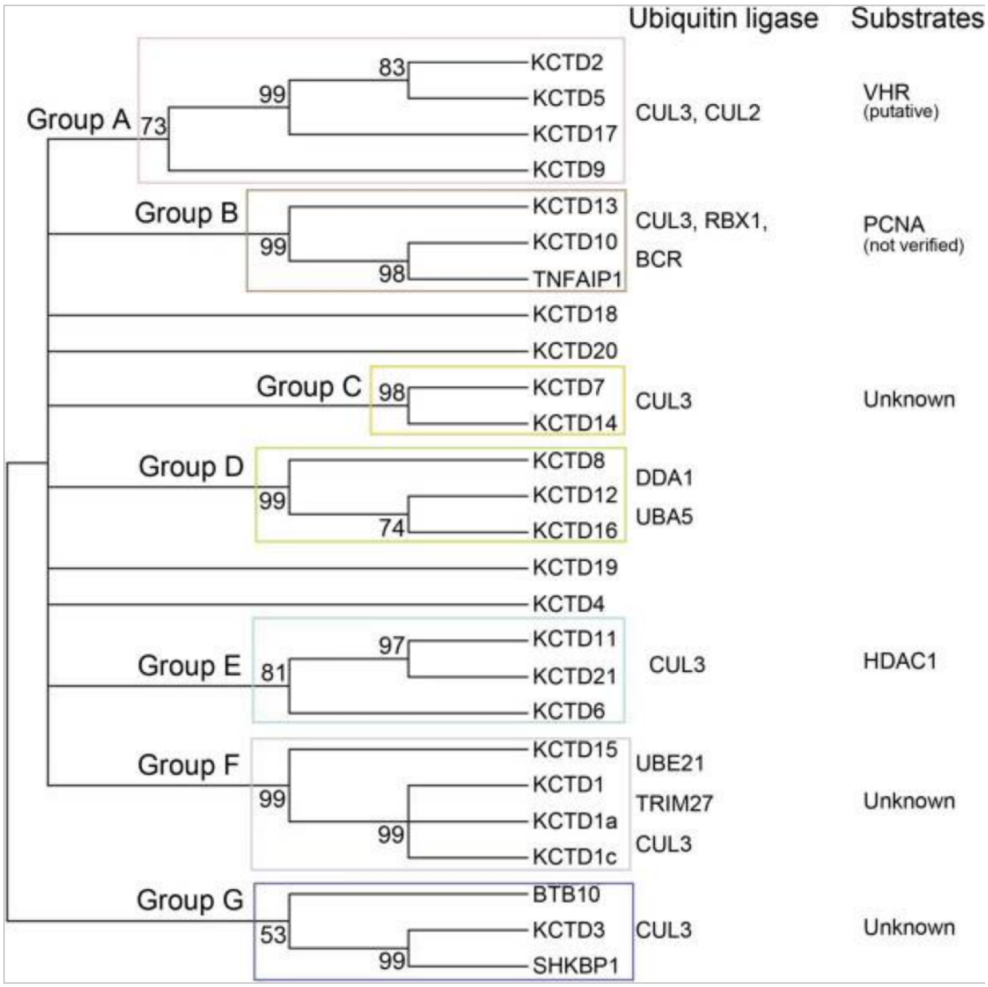

Figure 6. **A paralogues tree built using the entire aminoacidic sequences of the KCTD family proteins**

Right side of the panel: it is specified the E3 ubiquitin ligase associated to the KCTD proteins and their substrate.

From Liu et al., 2013.

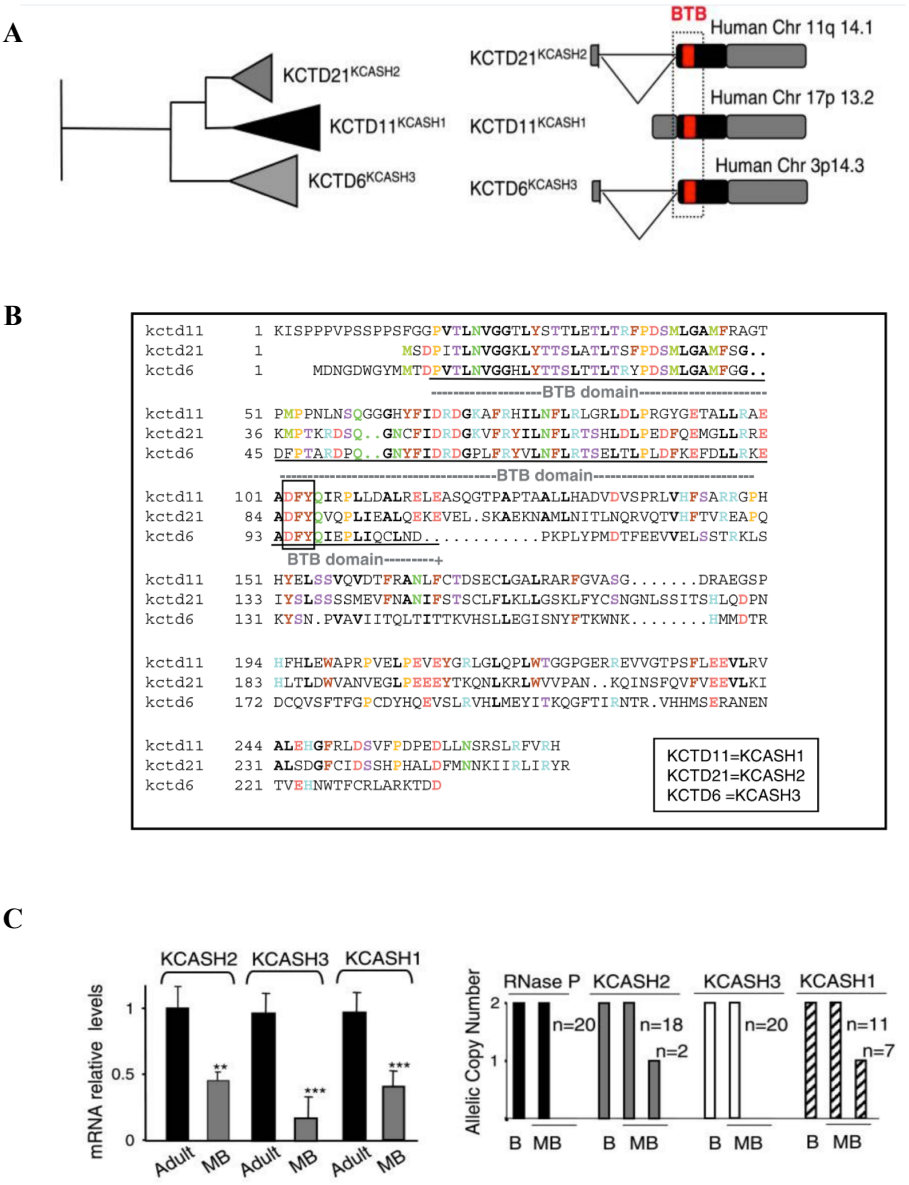

Figure 7. **The KCASH family of proteins**

A) Left panel: phylogenetic tree of KCASH1, KCASH2 and KCASH3; right panel: schematic representation of their human genetic loci and BTB domain indication.

B) Sequence alignment of human KCTD proteins. Matching amino acids are colored. The BTB domain is underlined on the sequences. DFY is included in a black frame.

C) Left panel: KCASHs expression is significantly reduced in human MB. Right panel: allelic deletion of KCASH1 and KCASH2 were observed in MB samples.

From De Smaele et al., 2011.

A

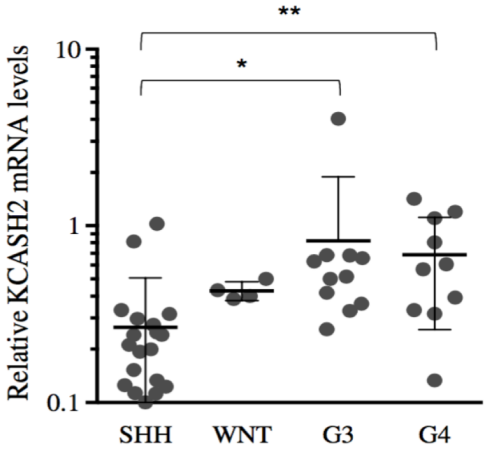

B

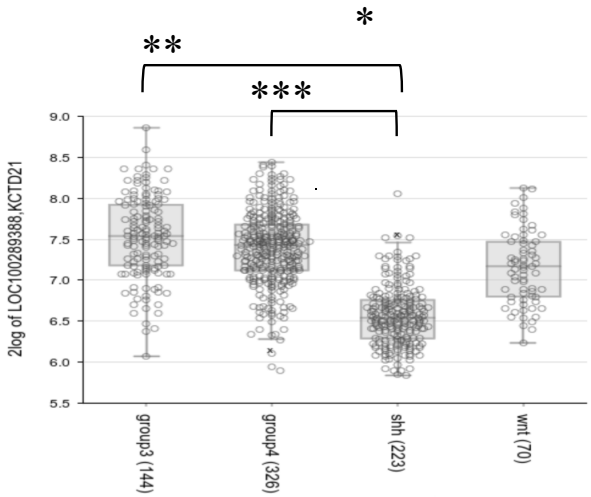

Figure 8. SHH-dependent MBs frequently present KCASH2 reduced expression

A) 47 human sporadic MBs belonging to different molecular groups have been assessed for KCASH2 expression by Q-RT-PCR analysis. The relative mRNA levels were expressed as the ratio of the sample quantity to the mean values of 9 normal cerebella (Ctr). *P<0.05 G3 versus SHH, **P<0.01 G4 versus SHH (Mann-Whitney test).

From Spiombi et al., 2019.

B) Correlation analysis performed on a larger group of samples in publicly available database (Cavalli et al., 2017).

Figure 9. The KCASH2 C-terminal region is highly conserved by evolutionary pressure

Alignment of C-terminal KCASH2 protein sequence through vertebrates. Homology percentage is indicated (CLUSTAL multiple sequence alignment by MUSCLE program).

2. SEARCH FOR NEW KCASH2 INTERACTORS AND MECHANISMS OF KCASH2 MODULATION

In order to better characterize the role and mechanisms of KCASH2 modulation, we have searched, by means of a proteomic approach, for new KCASH2 interactors, in collaboration with the group of Prof. Lucia Di Marcotullio (Dip. Molecular Medicine, Sapienza University) and Prof. Daniele Guardavaccaro (Hubrecht Institute of Utrecht, NL).

The experimental strategy and the mass spectrometry analysis were previously described (Spiombi et al., 2019). Briefly, we transfected HEK293T cells with an expression vector encoding for human *KCASH2* tagged N-terminally with both HA and Flag tags (**figure 10A**), the performed a sequential double co-immunoprecipitation of the cell lysates. The highly pure immunocomplexes were then analyzed by LC-MS/MS analysis and polypeptides represented with a number of peptides ≥3 were selected for further analysis (**figure 10B**).

The most represented interactors were KCTD15 (Potassium Channel Tetramerization Domain Containing 15 protein) and MAD2L1 (Mitotic Arrest Deficient) that present, respectively, 13 and 4 different peptides co-immunoprecipitated with KCASH2.

2.1. New KCASH2 protein interactors: KCTD15

Similarly to KCASH2, KCTD15 is a member of the KCTD family of proteins and contains a conserved N-terminal BTB domain. It belongs to the sixth group of KCTD proteins classified according on amino acids sequence similarities (group F; Liu et al., 2013). Human *KCTD15* gene maps to chromosome 19q13.11 and encodes a 283 aminoacids (31 KDa) protein.

Until today, KCTD15 has not been extensively studied, and informations about its functions are limited.

KCTD15 has been previously associated, by genome-wide association studies (GWAS), to obesity and eating disorders (Waalen, 2014; Gamero-Villaroel et al., 2017) and the significance of this association has been hypothesized to be related with KCTD15 expression in areas of the brain involved into central regulation of food intake and feeding behavior (Thorleifsson et al., 2009; Willer et al., 2009; Williams et al., 2014). Anyway, the mechanisms have not been clarified and KCTD15 association with obesity or BMI is still controversial, since other research groups did not find any significant association, and Baranski et al have demonstrated that the functional genes may not be the

nearest ones (KCTD15), but instead, a nearby cis gene (i.e. CHST8) is the functional target (Baranski et al., 2018).

KCTD15 has also been described to play a role in neural crest (NC) formation. Indeed, in zebrafish, KCTD15 affects NC formation through both the Wnt/β-catenin signaling (essential pathway for NC specification and later differentiation; Dorsky et al., 1998) and AP-2α (transcription factor activating enhancer binding protein 2) modulation. In fact, KCTD15 interacts with AP-2α through its BTB domain and represses its transcriptional activity in zebrafish embryos (Dutta and David, 2010; Zarelli and Dawid, 2013).

The KCTD15 expression in different adult mouse and human tissue, including adult brain and cerebellum (Yue et al., 2019), may suggests a potential interplay with KCASH2 in Hh regulation during cerebellar development and differentiation. On the other side, most of the cerebellar cell types (including cerebellar granule neuron, Purkinje cells, Bergmann Glia, astrocytes) do not derive from NC but from the neural tube, and AP-2α expression has been reported to be limited to developing and adult cerebellar GABAergic interneurons (Purkinje cells; Zainolabidin et al., 2017). Thus, KCTD15 most probably plays different functions in cerebellar context, where KCASH2 acts (De Smaele et al., 2011).

Previous data produced in our laboratory have validated the mass spectrometry data, through co-immunoprecipitation (Co-IP) assays of overexpressed tagged -KCASH2 and KCTD15 proteins (**figure 11A, left panel**). Because of the high homology within the KCASH proteins and their shared functions, it was also evaluated if KCTD15 may interact with the other KCASH proteins, KCASH1 and KCASH3 (**figure 11A, central and right panels**). Our data showed that KCTD15 binding was unique for KCASH2 family member. The KCASH2-KCTD15 interaction did not require the presence of further adaptor proteins and neither of the two proteins needed to undergo posttranslational modifications, since an *in vitro* assay (GST pull-down assay performed with *in vitro* translated KCTD15 and KCASH2-GST fusion protein) did show a direct binding (**figure 11B**).

It was also examined the KCTD15 capability to form homo-oligomers complex through its BTB domain performing co-immunoprecipitation assay (**figure 12A**), after co-expressing full-length KCTD15, the BTB-containing N-terminal half of the protein (BTB- KCTD15) and the C-terminal half lacking the BTB domain (called ΔBTB-KCTD15). Similarly, it was assessed that the BTB domain mediated the KCASH2-KCTD15 interaction, through BTB-KCTD15 and ΔBTB-KCTD15 fragments, following Co-IP assays (**figure 12B**).

Interestingly, it was assessed that the KCTD15 overexpression in HEK293T cells significantly decreased the transcriptional activity of a Gli1-responsive luciferase reporter (**figure 12C**).

These preliminary results demonstrated that KCASH2 and KCTD15 could act together (forming heterodimers) and that KCTD15 somewhat modulates Hh pathway activity, and prompted us to elucidate its mechanism of action, which has been investigated in the work presented in the first section of this thesis.

A

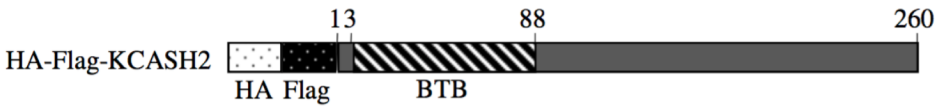

B

Accession number	IDENTIFICATED PROTEINS	KCASH2 number of unique peptides
IPI00896634	BTB/POZ domain-containing protein KCTD21/KCASH2	17
IPI00234793	BTB/POZ domain-containing protein KCTD15	13
IPI00012369	**Mitotic spindle assembly checkpoint protein MAD2A**	4
IPI00438229	Isoform 1 of Transcription intermediary factor 1-beta	4
IPI00218466	Isoform 1 of Protein transport protein Sec61 subunit alpha isoform 1	3
IPI00328354	Isoform 1 of Melanoma-associated antigen D1	3

Figure 10. KCTD15 is the most represented interactor of KCASH2 in the Co-IP assay

A) Schematic representation of the dual tagged KCASH2 vector used for Co-IP assay.

B) List of the most relevant KCASH2 interactors with corresponding numbers of unique peptides obtained from the MS analysis.

From Spiombi et al., 2019.

A

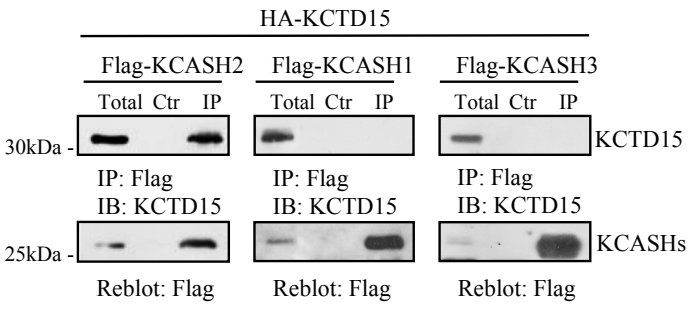

B

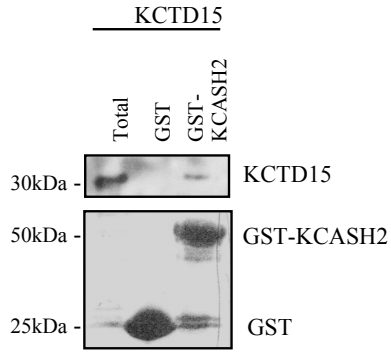

Figure 11. KCTD15 interacts specifically with KCASH2

A) KCTD15 co-immunoprecipitates with KCASH2 but not with KCASH1 and KCASH3.

B) KCASH2 interacts with KCASH15 *in vitro*.

From Spiombi et al., 2019.

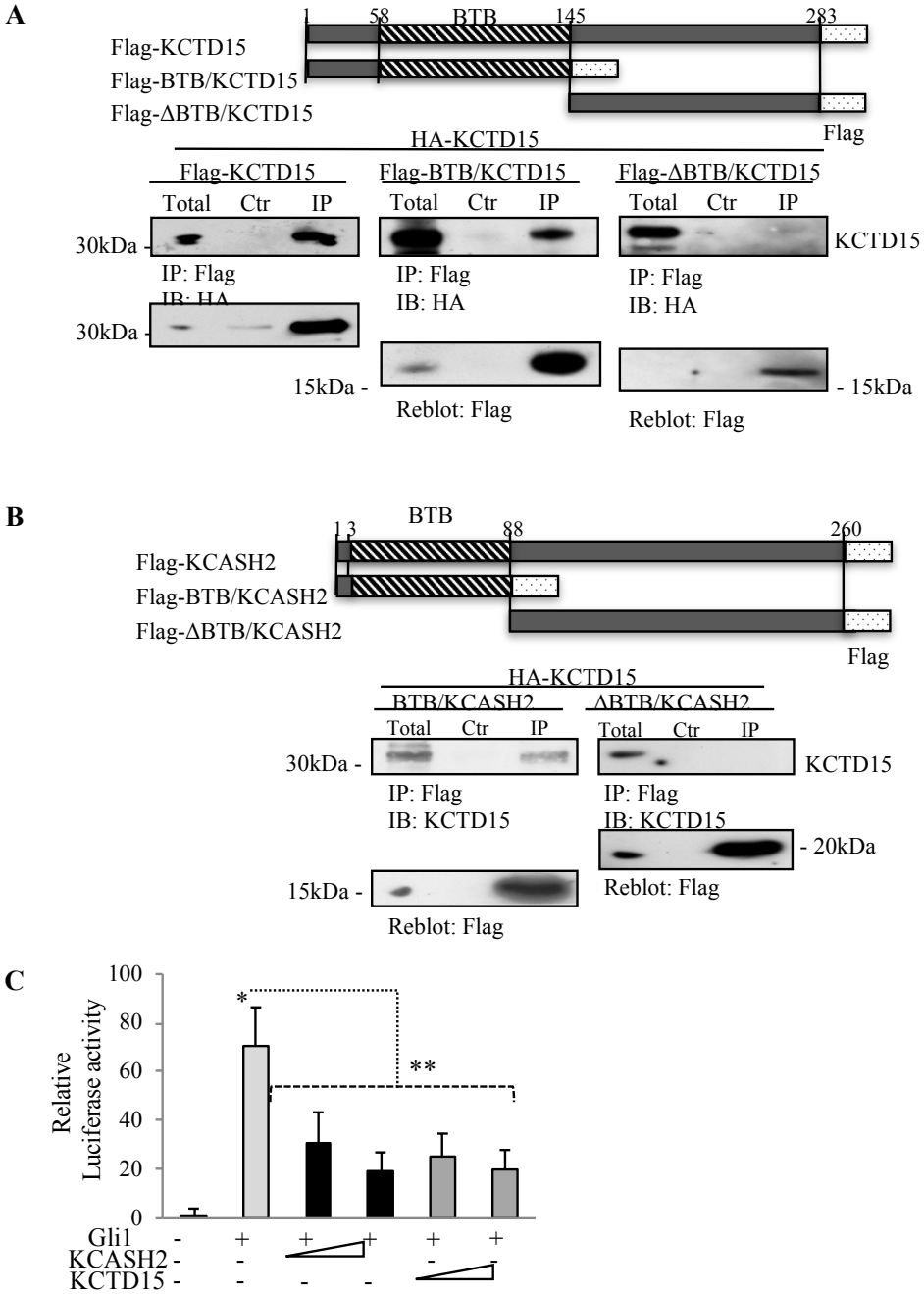

Figure 12. KCTD15 homo-and hetero-oligomerizes via BTB-POZ domain and downregulates Gli1 transcriptional activity

A) KCTD15 forms homo-oligomeric complexes via the BTB-POZ domain.

B) KCTD15 forms hetero-oligomeric complexes with KCASH2 via the BTB-POZ domain.

C) KCTD15 expression reduces Gli1-responsive Luciferase activity.

From Spiombi et al., 2019.

2.2. New KCASH2 protein interactors: MAD2

The second most represented interactor identified by CO-IP and MS was Mitotic Arrest Deficient 2-like1 (MAD2L1 or MAD2).

MAD2 plays a fundamental role in the cell cycle regulation and has been involvement in aneuploidy and tumorigenic processes (see below). For these reasons, investigation of the effects of MAD2-KCASH2 interaction could yield very interesting results.

Preliminary data obtained in our lab had validated the KCASH2-MAD2 interaction. To this purpose, we performed Co-IP assay following overexpression of Flag-KCASH2 in HEK293T cells. Indeed, endogenous MAD2 was able to co-immunoprecipitate with KCASH2, confirming the MS data (**figure 13A**).

Moreover, we verified that MAD2 interaction was specific for KCASH2 (**figure 13B**) and identified by Co-IP assay the C-terminal region of KCASH2 protein as the one involved in MAD2 interaction (**figure 13C**).

The specific binding of MAD2 to KCASH2 and the relevance of MAD2 in the cell cycle control, suggested us to investigate further the KCASH2-MAD2 interaction and its function.

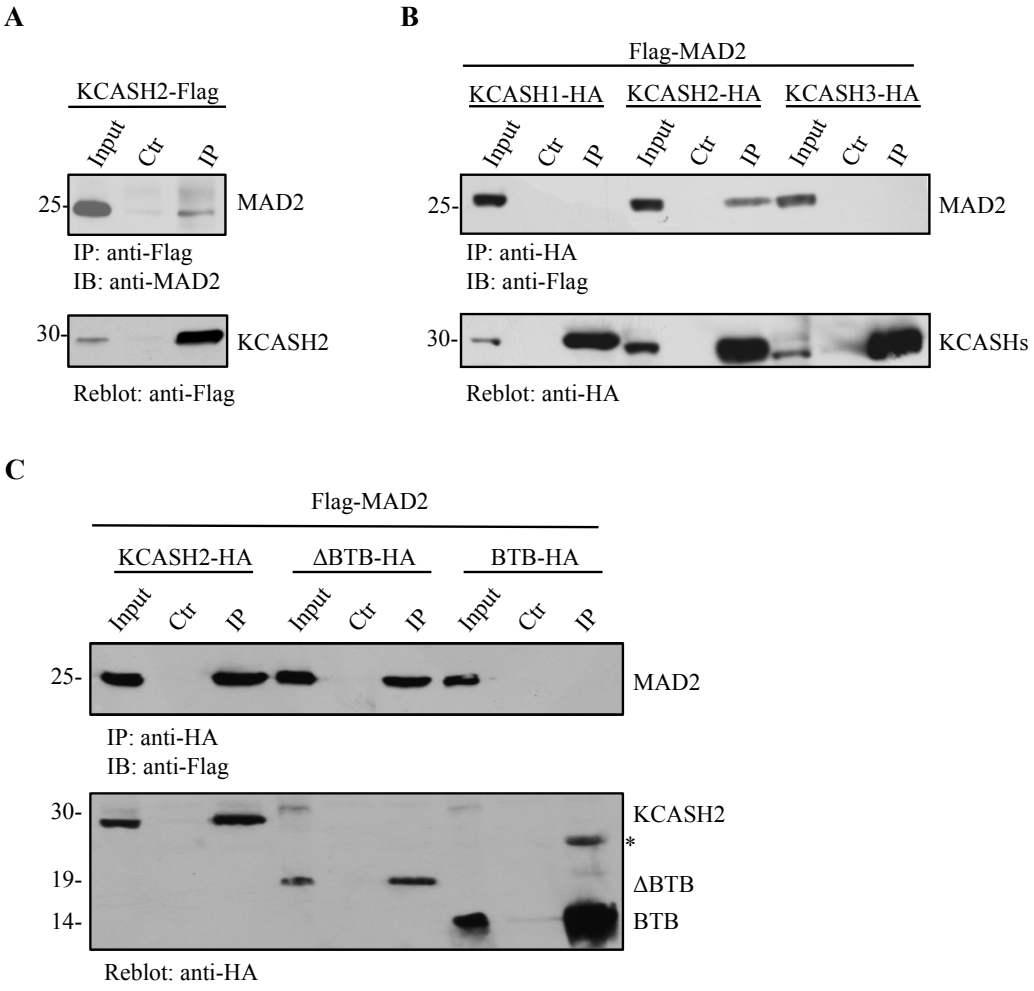

Figure 13. KCASH2 interacts with MAD2 through its C-terminal region

A) Endogenous MAD2 co-immunoprecipitates with KCASH2.

B) MAD2 co-immunoprecipitates only with KCASH2 and not with the other family members. **C)** C-terminal domain of KCASH2 is required for the interaction with MAD2.

Co-IP experiments performed in lysates from HEK293T cells transfected with expression vectors encoding for the indicated tagged proteins and co-immunoprecipitate with anti-Flag agarose beads (A) and anti-HA agarose beads (B, C). Immunoprecipitated samples and a fraction of the total lysate (Input) were loaded and separated on SDS-PAGE gels. Blots were immunoblotted (IB) with anti-MAD2 (A) and anti- Flag (B, C) as indicated. Reblots with anti-Flag and anti-HA antibodies were performed to verify immunoprecipitation.

2.2.1. An overview of MAD2 functions: from cell cycle regulation to tumorigenesis

MAD2 gene was first identified in the yeast *Saccharomyces Cerevisiae* in a screen for genes which, when mutated, would confer sensitivity to anti-microtubule drug benomyl (Li and Murray, 1991). A number of properties of the yeast MAD mutants indicate that they are defective in the negative control over the exit from mitosis in cells with altered chromosome segregation. Many of the proteins found in budding yeast have homologues which are expressed in humans. Indeed, MAD2 is conserved from yeast to mammalian cells, both at a structural and functional level (Glotzer, 1996; Li and Benezra, 1996). In human cells two MAD2 orthologues have been identified: MAD2L1 (also known as MAD2) and MAD2L2 (also known as Rev7).

The essential goal of a correct mitosis is the equal distribution of sister chromatids into daughter cells, event that requires exquisite kinetics and regulation (Walczak and Heald, 2008).
The mitotic (M) phase (**figure 14**) can be subdivided in mitosis (nuclear division) and cytokinesis (cytoplasmic division).
The morphological changes required for nuclear division have traditionally been used to define the different stages throughout mitosis (Perez-de Castro et al., 2007):

- At prophase, chromatin condenses into chromosomes and the nuclear envelope breaks down (NEBD).
- During prometaphase, a massive reorganization of the cytoskeleton results in the generation of the bipolar spindle where chromosomes are attached.
- At metaphase, chromosomes are bound to the plus ends of the microtubules through their kinetochores are aligned at the metaphase plate in the center of the mitotic spindle.
- The segregation of the two sets of chromosomes occurs during anaphase after loss of the sister chromatid cohesion.
- Finally, in telophase, chromosomes decondense and the two new nuclei are formed after reconstruction of the nuclear envelope.

Once the two new nuclei are separated, the cell undergoes cytokinesis to divide the cytoplasm and separate the two daughter cells (Somers and Saint, 2003).

To ensure that only healthy cells proliferate, several mechanisms of control (checkpoints) have been developed. These processes, on one hand, may induce cell-cycle arrest in response to detection of defects that may have arisen during DNA replication or in other steps leading to mitosis (Kulukian et al., 2011), on the other one, may trigger events (e.g. apoptosis, mitotic catastrophe, senescence) to

prevent the propagation of severely damaged or high-risk cells (Dominguez-Brauer et al., 2015). In particular:

- The G1/S checkpoint restricts cells with damaged DNA from entering S phase until the damage is removed or it triggers cell death or senescence.
- The intra-S checkpoint delays the firing of replication origins or slows down DNA replication during S phase in order to minimize replication errors.
- The G2/M checkpoint preserves genomic integrity through regulating proper timing of the metaphase-to-anaphase transition and thus it minimizes chromosome mis-segregation.
- The post-mitotic checkpoints prevent daughter cells originated by abnormal mitosis from entering the next interphase.

All these checkpoints are essential to reduce genomic instability during cell-cycle progression (Tipton et al., 2013).

MAD2 protein is a central regulator of the mitotic G2/M checkpoint machinery.
During the M phase, multiple proteins assemble in distinct structures: the centrosome and the kinetochore/centromere, which direct the process of cell division (Zheng et al., 2014; **Figure 15**).
The centrosomes are the microtubule organizing centers (MTOCs), which participate in the organization and orientation of the mitotic spindle apparatus, and thus direct the alignment of chromosomes and the segregation of sister chromatids during cell division (Perez-de Castro et al., 2007).
Centromeres, specialized chromatin domains on the chromosome, serve as spindle connection points and direct chromosome segregation (Black and Bassett, 2008). Upon the centromeres is assembled the kinetochore, a specialized protein complex which connects to microtubule-based fibers that extend from the opposite poles of the mitotic spindle and allows the attachment of the chromosomes to the spindle, to ensure accurate chromosome segregation.
Alteration of the centrosome or disorganization of the kinetochore/centromere complex are catastrophic for cells and can lead to cell death or tumorigenetic processes.

The G2/M checkpoint halts the process of cell division and imposes a mitotic arrest when the chromosome–microtubule attachment is perturbed (Musacchio and Salmon, 2007).
During the G2/M phase, accurate kinetochore attachment to the spindle is tightly monitored by a checkpoint signal termed the Spindle Assembly Checkpoint (SAC; Musacchio and Salmon, 2007). In presence of unattached kinetochores, SAC activates the G2/M checkpoint, inhibiting mitosis,

halting progression to anaphase until all chromosomes are aligned on the metaphase plate and every kinetochore is properly attached to the spindle.

MAD2 is a key component of the SAC, and together with MAD1, BubR1, the BUB (budding uninhibited by benzimidazole) proteins BUB1 and BUB3, forms the Mitotic Checkpoint Complex (MCC) which inhibits CDC20, an essential regulator of cell division (Musacchio and Salmon, 2007) (**figure 16**). CDC20 is able to activate a E3 ubiquitin ligase called Anaphase-Promoting Complex/Cyclosome (APC/C), that in turn ubiquitylates Securin and Cyclin B1 and promotes anaphase onset. Securin is an inhibitor of Separase, a protease that cleaves a Cohesin subunit allowing sister chromatid separation, while Cyclin B1 is an activator of CDK1, the major mitotic kinase (Lischetti and Nilsson, 2005).

SAC is assembled on unattached kinetochore where all SAC components are recruited, forming a fully assembled MCC. The MCC in turn inhibits CDC20, leading to inhibition of the APC/C. Once all kinetochores are correctly attached to microtubules, the MCC disassembles and the APC/C–CDC20 complex becomes active and triggers anaphase entry (Howell et al., 2004; Shah et al., 2004).

A second control feedback mechanism of cell division, generally referred to as error correction, prevents the stabilization of kinetochore–microtubule attachments until they come under tension (Li and Nicklas, 1995). Improper kinetochore–microtubule attachments (**figure 17**) such as merotelic or syntelic attachments are distinguished from proper attachments (amphitelic attachment or biorientation) and corrected because they are not under full tension.

Among these erroneous attachments, merotelic attachment, a type of mis-attachment in which a single kinetochore binds microtubules from two spindle poles rather than just one, can represent a particular threat for dividing cells. The merotelic kinetochore orientation occurs frequently in mitosis and it is considered a major cause of CIN, as it is not detected by the SAC because the kinetochore is attached to microtubules and under tension exerted by pulling force from both spindle poles that stabilizes the attachment (Cimini, 2008). Uncorrected merotelic attachment gives rise to lagging chromosomes, which can be a cause of both numerical and structural chromosome abnormalities as well as formation of micronuclei (Tanaka et al., 2016).

The molecular basis of stabilization or destabilization of improper attachments is being actively investigated. The first proteins to be clearly implicated in this process are the Aurora B and MPS1 kinases. The catalytic activity of MPS1 is implicated both in error correction and in the spindle checkpoint. On one hand, MPS1 is a checkpoint component required for the recruitment of the MAD1–MAD2 complex to unattached kinetochores. On the other hand, MPS1 is implicated in biorientation and in error correction: it inhibits AURORA B activity thus the error correction and the

spindle checkpoint mechanisms may respond to a single upstream sensor designed to detect lack of attachment and reduced or missing tension (Santaguida et al., 2010). MPS1 may contribute to biorientation and error correction phosphorylating the CENP-E proteins, required for chromosome congression (Espeut et al., 2008).

For proper mitotic chromosome segregation, sister kinetochores on a replicated chromosome pair have to attach to microtubules from opposite spindle poles (amphitelic attachment or bi-orientation) (**figure 17**). As kinetochores can attach to microtubules only after NEBD in cells that undergo open mitosis, elaborate mechanisms exist to ensure the establishment of bi-orientation for all the sister kinetochores at every mitosis. Failure in this process leads to chromosome mis-segregation that results in abnormal numbers of chromosomes, known as aneuploidy (Kuniyasu et al., 2019). An Aurora B gradient and SAC play a role in the correction of erroneous attachment (monotelic, syntelic or merotelic attachment): the first one destabilizes them, the second one halts mitotic progression, allowing time for error correction.

Mitotic chromosomes must undergo several modifications before sister chromatid segregation can occur in anaphase. Firstly, the chromosomes must condense; then, the topoisomerase II enzyme must decatenate the two DNA molecules; finally, cohesion complexes must be removed at the metaphase-anaphase transition to allow for sister chromatid separation and segregation.

Defects in any of these processes generate chromosomes whose chromatids cannot separate from each other and produce a typical cellular phenotype, which is the presence of anaphase chromosome bridges (**Figure 18**; Pampalona et al., 2016). Anaphase lagging chromosomes are identified as single, kinetochore-positive chromosomes that lag between the two masses of segregating chromosomes during anaphase. Lagging chromosomes are commonly caused by merotelic attachments. By contrast, pathological chromosome bridges completely span the segregating masses of chromosomes during anaphase. Pathological bridges are caused by condensation and cohesion defects, or by dicentric chromosomes being pulled to opposite poles. When they do eventually break, one daughter cell can end up with either a gain or a loss of chromosomal material (Ganem and Pellman, 2012). Micronuclei (MN) can originate during anaphase from lagging acentric chromosome or chromatid fragments caused by misrepair of DNA breaks or unrepaired DNA breaks. Dissegregation of whole chromosomes at anaphase may also lead to MN formation as a result of hypomethylation of repeat sequences in centromeric and pericentromeric DNA, defects in kinetochore proteins or assembly, dysfunctional spindle and defective anaphase checkpoint genes (Fenech et al., 2011).

In cancer cells, the depletion of molecules involved in end-on attachment show chromosome misalignment and increased chromosome mis-segregation (Maiato et al., 2017; Almeida et al., 2018).

Interestingly, in MAD2-depleted cells anaphase bridge enumeration showed a three-fold higher percentage compared with scramble controls (Prencipe et al., 2009).

Upon the completion of spindle attachment, the microtubule-kinetochore interaction is thought to silence SAC signal, and the amount of MAD2 bound to the kinetochores diminishes while the free fraction of the protein increases. The dissociation of MAD2 from CDC20 coincides with the formation of a complex with the protein $p31^{comet}$, one the putative SAC silencer. $p31^{comet}$ binds to the CDC20-bound conformation of MAD2, changing MAD2 conformation and releasing MAD2 from the complex (**figure 19**; Mapelli et al., 2006; Habu and Matsumoto, 2013).
Indeed, binding of MAD2 to CDC20 involves a conformational change of MAD2 (Luo et al., 2000; Sironi et al., 2002). MAD2 protein has a HORMA domain (Rosenberg and Corbett, 2015) which consists of two functionally distinct regions: the core, comprising the first ∼150 aa, and the C-terminal "safety belt" region depicted in **figure 19**. The safety belt region can pack against the HORMA domain core in two different conformations to produce the so-called "open" or "closed" states. This change enables either MAD1 or CDC20 to interact with MAD2 to form the "liganded" MAD2 (Sironi et al., 2002). The major MAD1 function is to recruit MAD2 to unattached kinetochores, where MAD2 molecules are converted from open (O-MAD2) to closed (C-MAD2) conformation. This conformational change is a critical signal amplification mechanism for the mitotic checkpoint (Mapelli and Musacchio, 2007; Musacchio, 2015).

Although MAD2 plays a fundamental role in cell cycle regulation, the mechanisms regulating MAD2 protein levels during the cell cycle are still unclear. Indeed, MAD2 regulation has been described primarily only in terms of transcriptional control, with studies demonstrating that MAD2 is a transcriptional target of E2F, BRCA1, Myc, and REST (Hernando et al., 2004; Menssen et al., 2007; Guardavaccaro et al., 2008).
Among the wide range of post translational modifications (PTMs), it is known that MAD2 undergoes phosphorylation to change conformation and, therefore, participate to SAC and mitotic checkpoint control (Strumillo and Beltrao, 2015). Other PTMs of MAD2 are have not yet been described.
On the other side, ubiquitination is an event which plays a role in MCC disassembly: in fact, ubiquitylation of CDC20 (Reddy et al., 2007) and BubR1 (Sitry-Shevah et al., 2018) is required for the dissociation of MCC from APC/C. Moreover, USP44-mediated de-ubiquitination stabilizes the CDC20-MAD2 complex by removing ubiquitin conjugates from CDC20 (Nilsson et al., 2008; Ge et al., 2009).

The E3-ubiquitine ligase SMURF2 (SMAD Specific E3 Ubiquitin Protein Ligase 2) has been demonstrated to be involved in MAD2 control, increasing its protein stability, although the mechanism of action was not clarified. To this end, the authors hypothesized two different models (**Figure 20;** Osmundson et al. 2008).

The first one, named the direct model, hypothesizes that E3 ligase activity of SMURF2 would mediate the attachment of mono-ubiquitin or non-Lys48 linked (non-degradative) ubiquitin chains (e.g. Lys63 linkage) on MAD2 stabilizing the protein.

In the second model, the indirect one, SMURF2 catalyzes the ubiquitin-dependent degradation of an unidentified E3 ligase (or its critical cofactor) that promotes constitutive MAD2 polyubiquitination. In this way, SMURF2 activity would antagonize the action of this unknown E3 ligase, thereby allowing for stability of MAD2.

Up to date, the two models have not been further studied and validated.

Over the years, MCC has become widely recognized as a specialized signal transduction pathway that contributes to the fidelity of chromosome segregation. Nevertheless, several questions persist with regard to basic features and working mechanisms of the MCC.

For example, it is not clear when exactly the MCC begins to be assembled during the cell cycle. Sudakin and colleagues (2001) showed that MCC (BUBR1:BUB3:MAD2:CDC20) exists in both interphase and mitotic cells. Many research groups reported that BUBR1 and BUB3 form a cell cycle independent complex, but more CDC20 and MAD2 associate with BUBR1:BUB3 during mitosis (Hardwick et al., 2000; Fraschini et al., 2001; Chen et al., 2002; Tipton et al., 2011). MCC-like protein complexes have been reported in either interphase cells (Mossaid and Fahrenkrog, 2015) or in the absence of kinetochores (Poddar et al., 2005; Malureanu et al., 2009). In either situation there must be a fraction of endogenous MAD2 existing in C-conformation due to the interconversion between the two MAD2 conformers (Fava et al., 2011), therefore a low level of MCC still forms. This housekeeping MCC pool sets the timer for mitosis progression.

The formation of the MCC in interphase is dependent on the MAD1–MAD2 complex and its association with NPC, the nuclear pore complex embedded in the nuclear envelope (NE), thereby spanning the inner nuclear membrane (INM) and the outer nuclear membrane (ONM; Mossaid and Fahrenkrog, 2015). Indeed, multiple NPC components were shown to be critical for faithful cell division and implicated in the regulation of different steps of the mitotic process (Rodriguez-Bravo et al., 2014). In this context, the NPC acts as a scaffold for MCC signaling and the MAD1 depletion displaced the MAD1–MAD2 complex from NPCs, which abolished the formation of the interphasic MCC. The combined MCCs allow for the delay of anaphase onset and lead to a more sensitive and

stronger SAC. Intracellular level of MAD2 is also subjected to regulation by p53 and Rb/E2F pathway (Michel et al., 2001). However, in many cancer cell lines with compromised Rb/E2F and/or p53 pathway (e.g. HeLa cells), the level of total MAD2 protein is constant throughout the cell cycle (Schvartzman et al., 2011).

The disruption of cell cycle control mechanisms is a recurrent theme in tumorigenesis. A weakened SAC may allow cells to enter anaphase in the presence of unattached or misaligned chromosome. Indeed, uncontrolled progression through mitosis can result in the mis-segregation of whole chromosomes and production of progeny cells with an abnormal chromosome content, which is referred to as aneuploidy. In multicellular organisms, chromosomal gain or loss is largely lethal (Lindsley et al., 1972; Hodgkin, 2005). In humans, all monosomies and most trisomies cause embryonic lethality (Hassold and Hunt, 2001), the only exception is chromosome 21 trisomy, compatible with survival into childhood. The range of adverse effects due to an unbalanced karyotype is wide: metabolic alterations (Williams et al., 2008), proliferation defects (Thompson and Compton, 2010; Santaguida et al., 2015), genome instability (Ohashi et al., 2015), proteotoxic stress (Santaguida and Amon, 2015).

Defects in control machineries lead to cell death in most cases but they might also be a trigger for oncogenic transformation. Indeed, in somatic tissues only 2% of cells has an aneuploid karyotype, indicating that aneuploidy has detrimental consequences on cellular fitness (Knouse et al., 2014). Tumor initiation and progression are multistep processes associated with multiple genetic and epigenetic alterations (Hanahan and Weinberg, 2011). Since T. Boveri observed abnormal chromosome complements in tumor cells at the beginning of the twentieth century, the role of chromosome instability (CIN) in tumor initiation and progression has been a central issue in cancer biology (Boveri, 1902). Given the potential link between aneuploidy and tumorigenesis, it is critical to understand how abnormal karyotypes affect cellular physiology but, even now, several questions and controversies still remain.

Many experiments over the past decade have provided evidence for changes in the levels of spindle checkpoint components in cancer cells, although there can be a lot of variation between cells and/or samples and, above all, it can be difficult to establish if changes in SAC proteins promote tumorigenesis or are simply the result of cancer development.

The most compelling answer to this question comes from works in genetically engineered mice (Schuyler et al., 2012). MAD1 or MAD2 levels have been manipulated in several experimental models. In cell lines and in animal models, partial loss of MAD2 function leads to a high rate of aneuploidy and polyploidy; MAD2 heterozygous animals develop papillary lung adenocarcinomas

with very long latencies (Michel et al., 2001). Similar tumor predisposition or acceleration occurs in animal models in which other components of the MCC are partially inactivated and the animals exposed to chemical tumor promoters or other oncogenic stimuli (Baker et al., 2004; Babu et al., 2003). Complete loss of MAD2 or other mitotic checkpoint components, on the other hand, leads to early embryonic lethality and associated chromosome mis-segregation events (Wang et al., 2004). In mouse model MAD2 overexpressing, tetracycline-inducible, the hyperactive mitotic checkpoint leads to a highly penetrant induction of a wide range of tumors, including lung adenomas, hepatomas and hepatocellular carcinomas, lymphomas and fibrosarcomas (Sotillo et al., 2007).
Although the mechanism by which a MAD2 overexpression leads to cell cycle defects and contributes to CIN and, in the long run, to tumorigenesis has not yet been explored, *in vitro* and *in vivo* models show that hyperactive mitotic checkpoint plays a random role in onset and progression of cancer. In all the animal model listed, chromosome instability, due to both a MAD2 depletion and overexpression, contributes to the transformation process (Sotillo et al., 2007).

However, the relationship between aneuploidy and cancer is still complex and much debated.
There are several evidences suggesting that aneuploidy can exert an antitumorigenic or a pro-tumorigenic effect (Simonetti et al., 2019; **Figure 21**). Aneuploidy is generally disadvantageous for cells: changes in chromosome copy number result in transcriptomic alterations and gene-dosage effects at the proteomic level (Ried et al., 2012), that mean an imbalance in the cellular protein composition, proteotoxic stress, altered redox anabolic homeostasis (Gorrini et al., 2013; Valind et al., 2013). Indeed, aneuploidy has negative effect on the fitness of malignant cells. All observations indicating that single-chromosome aneuploidy is not sufficient *per se* to induce malignant transformation, but rather has antitumorigenic properties, are as extensively reviewed by Simonetti G. and colleagues (2019). Nevertheless, definitive conclusion cannot be drawn from correlations between diminished mitotic checkpoint signaling and tumorigenesis, since each of these mitotic checkpoint contributors is also present throughout interphase and is known to participate in cellular functions other than chromosome segregation (Weaver et al., 2006). MAD2, for example, is bound to the nuclear envelope and nuclear pores and has been implicated both in the DNA replication checkpoint (Sugimoto et al., 2004) and in promoting chromosomal rearrangements in yeast (Myung et al., 2004).
Overall, evidence obtained in nonmalignant cells and cancer models indicates that aneuploidy, which is detrimental *per se*, can be beneficial and even favor the development and selection of aggressive malignant clones by enabling cells to modulate independent pathways simultaneously and to explore a wide phenotypic landscape.

Despite the detrimental effect of chromosome number alterations on cellular fitness, aneuploidy is one of the hallmarks of cancer. According to the Mitelman Database, about 90% of solid tumors and 50% of hematological neoplasms are aneuploid. Aneuploidy confers an evolutionary flexibility by favoring genome and chromosome instability, cellular adaptation, stem cell-like properties and immune escape. These properties represent the driving force of aneuploid cancers, especially under conditions of stress and pharmacological pressure, and are currently under investigation as potential therapeutic targets (Simonetti et al., 2019). Indeed, aneuploidy and genomic instability are features that distinguish cancer cells from normal cells and represent tumor-specific vulnerabilities that could be exploited. Many anti-tumor drugs currently used in the clinic inhibit the cell cycle by altering the mitotic spindle (Wood et al., 2001). The idea is that these drugs, by reducing microtubule dynamics, keep the SAC in an active state, and that sustained SAC activation is often followed by cell death (Jordan et al., 2004). At present, MTAs (Microtubule-targeting agents) are the most important antimitotic drugs used in the clinic. However, there is an urgent need for the discovery of new strategies to more effectively target heterogenic tumor cell populations with fewer toxic side effects. Mitotic regulators therefore offer a wide range of opportunities for drug design and the induction of tumor cell-specific death. An approach based on inhibition of mitotic checkpoints could drive genomic instability and induce cell-cycle arrest and death of cancer cells, targeting genomically unstable cancer cells while sparing non-malignant ones (Dominguez-Brauer et al., 2015).

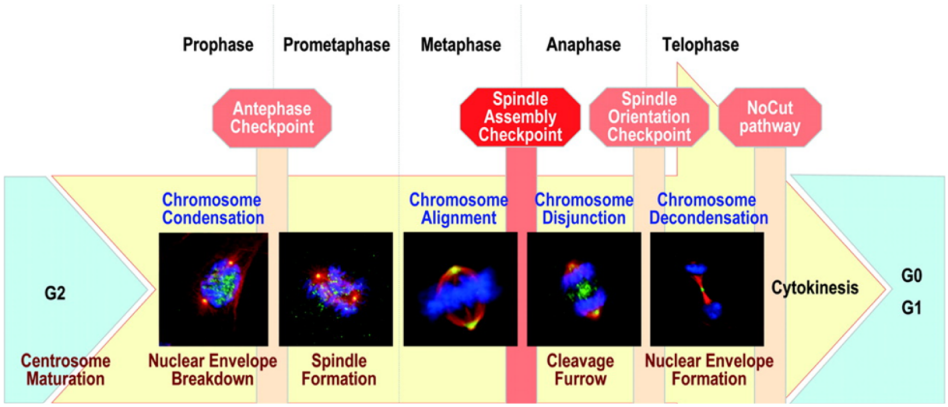

Figure 14. A cellular and molecular view of mitosis

Major changes in chromosome and spindle structure as well as the mitotic checkpoints that regulate transition through the different stages of mitosis are indicated. Pictures represent NIH-3T3 cells at different stages during mitosis. DNA is stained with 4′,6-diamino-2-phenylindole (blue); microtubules (red) and PLK1 (green) are detected using anti-α-tubulin or anti-PLK1-specific antibodies.

From Perez-de Castro et al., 2007.

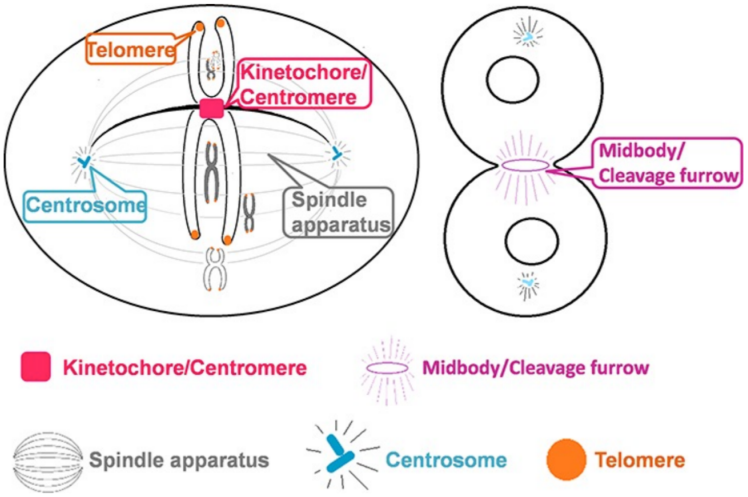

Figure 15. Mitotic structures that direct the process of cell division

Schematic diagram of the different subcellular positions including midbody/cleavage furrow/bud neck/phragmoplast, centrosome/spindle pole body, kinetochore/centromere, telomere and spindle apparatus in eukaryotic cells.

From Huang et al., 2014.

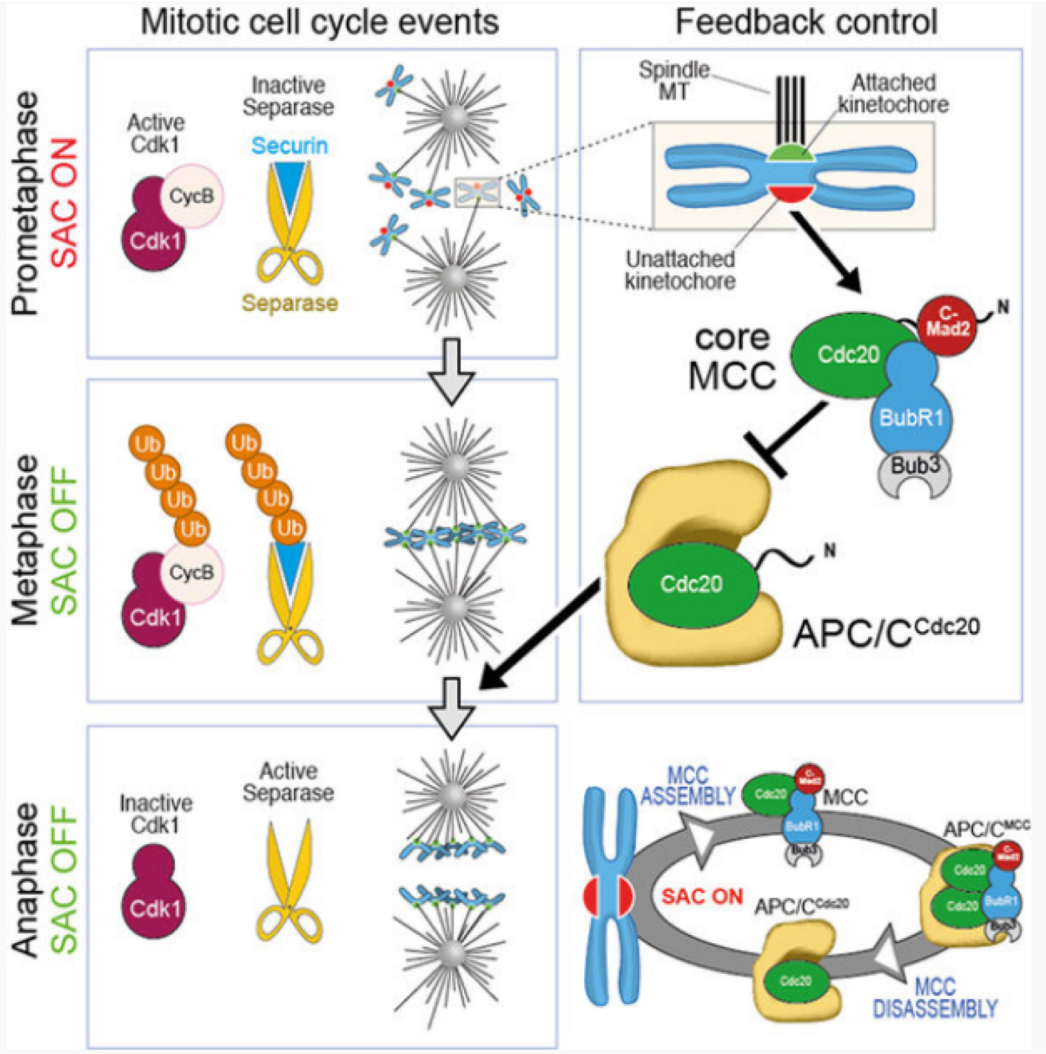

Figure 16. Kinetochore-microtubule attachment and SAC

During mitotic progression, unattached kinetochores try to capture microtubules, while emitting a signal that ultimately results in the assembly of the MCC. MCC inhibits the anaphase promoting complex/cyclosome (APC/C), preventing it from targeting Cyclin B and Securin for degradation. Subsequent destruction of these substrates upon SAC satisfaction allows mitotic exit via CDK1 inactivation and activation of Separase. During mitotic arrest, MCC is continuously produced and disrupted, thus ensuring responsiveness.

From Musacchio, 2005.

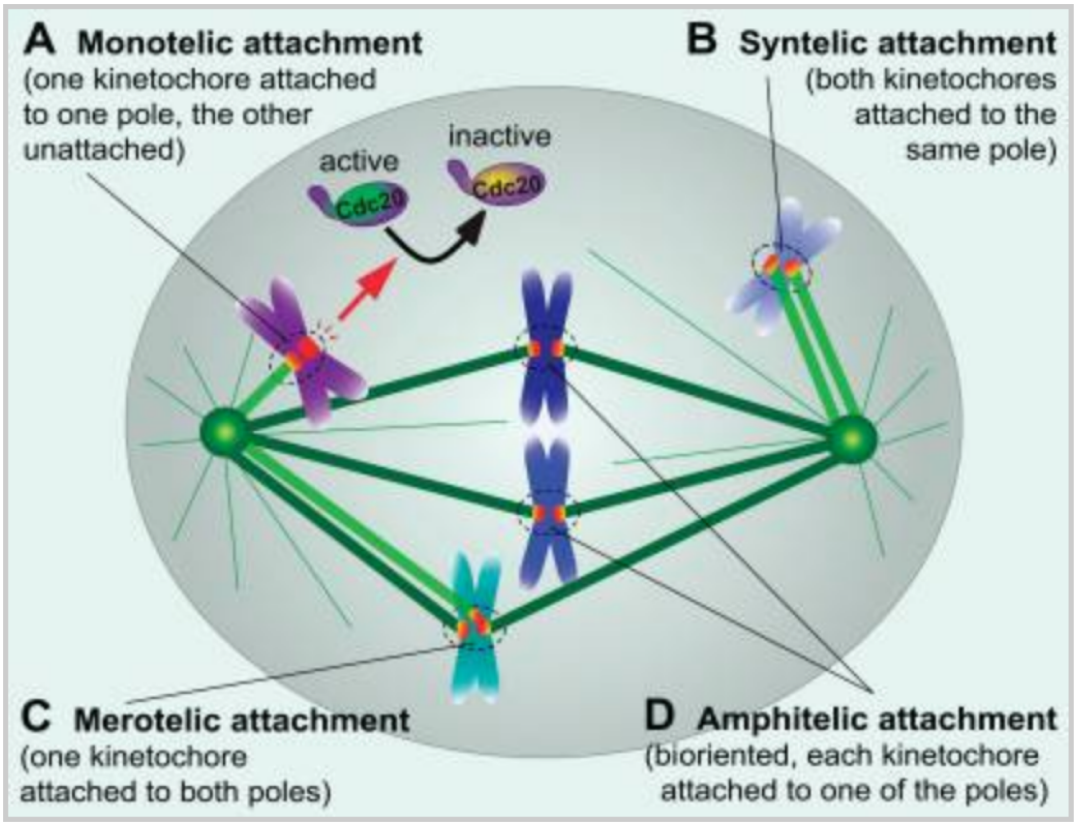

Figure 17. Microtubule–kinetochore attachments

Four types of kinetochore–microtubule attachments are highlighted. (A) Monotelic attachment: unattached kinetochores produce the mitotic checkpoint inhibitor that delays advance to anaphase. (B) Syntelic attachment (C) Merotelic attachment (D) Bioriented attachment (also known as amphitelic).

From Lan and Cleveland, 2010

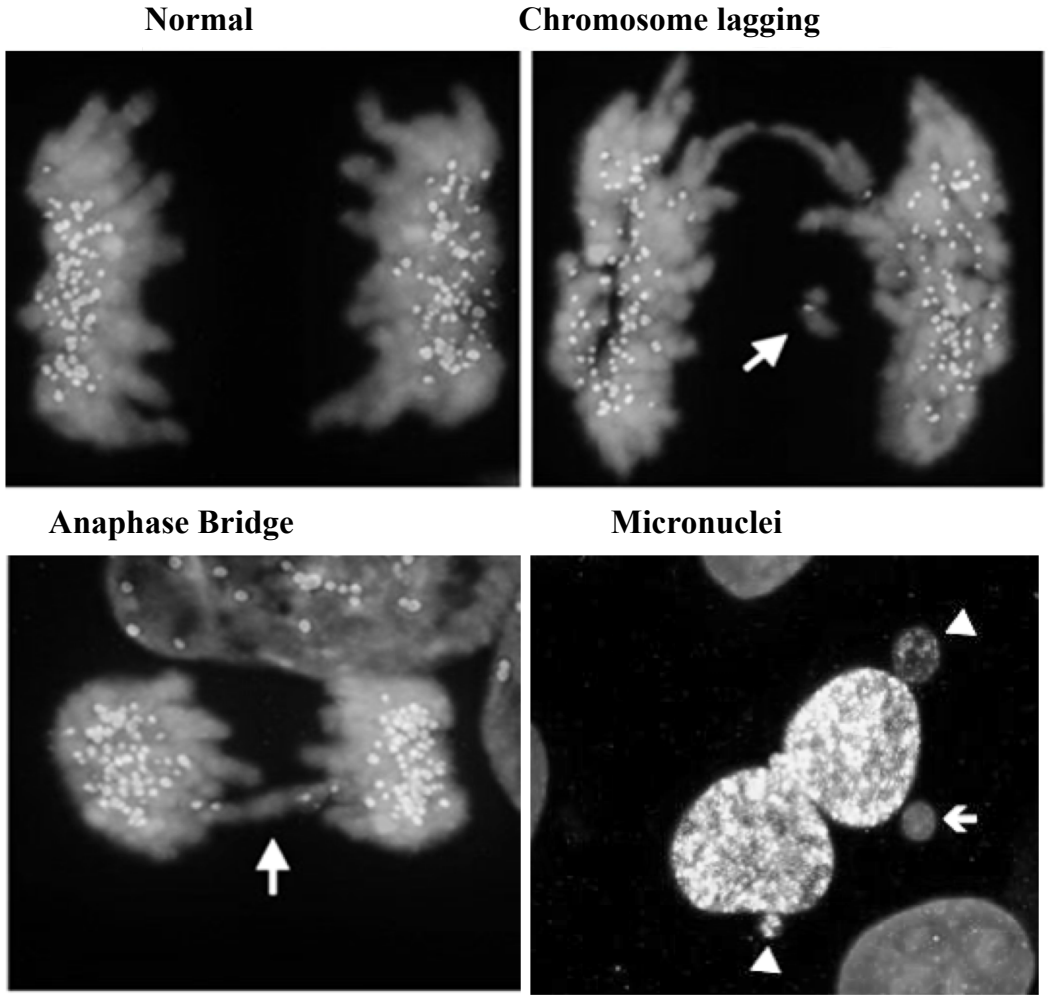

Figure 18. Mitotic defects

Lagging chromosomes are identified as single, kinetochore-positive chromosomes that lag between the two masses of segregating chromosomes during anaphase. By contrast, anaphase chromosome bridges completely span the segregating masses of chromosomes during anaphase. Micronuclei can originate during anaphase from lagging acentric chromosome or chromatid fragments caused by misrepair of DNA breaks.

Modified from Ganem and Pellman, 2012.

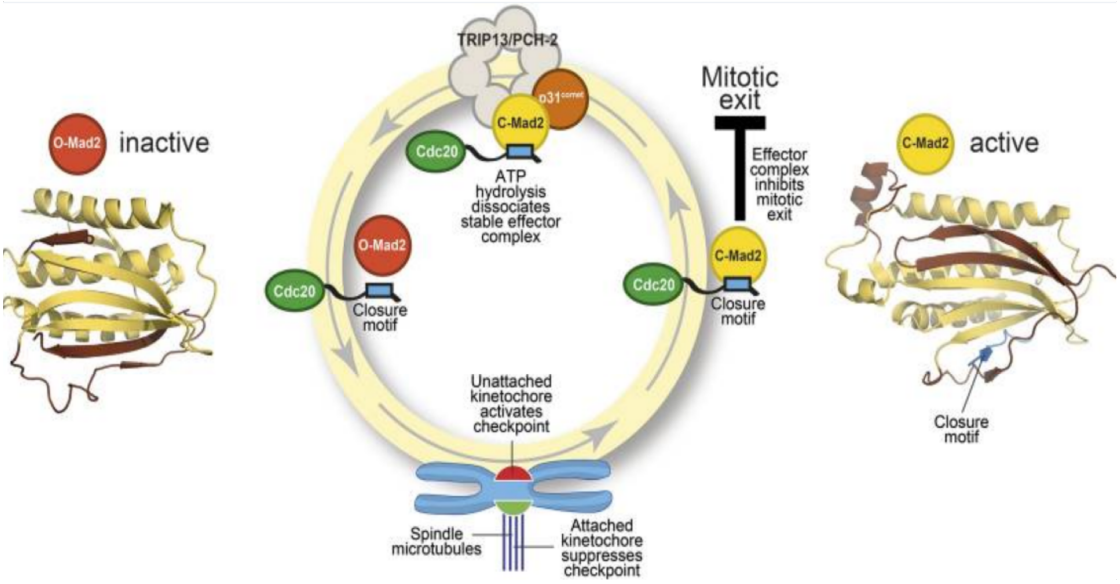

Figure 19. The MAD2 cycle

The MAD2 protein exists in an 'inactive' open form (left) and an 'active' closed form (right). The structural elements highlighted in pale yellow have the same relative positions in the two states; the elements highlighted in brown have different relative positions. The open form (red) is converted to the closed form (bright yellow) by a closure motif (blue rectangle) within a CDC20 protein. Formation of the effector complex (containing closed MAD2 and CDC20) suppresses the chromosomes separation. The $p31^{comet}$ proteins acts as a bridge to allow an enzyme called TRIP13/PCH-2 to dissociate this effector complex, which is very stable. From Musacchio, 2015.

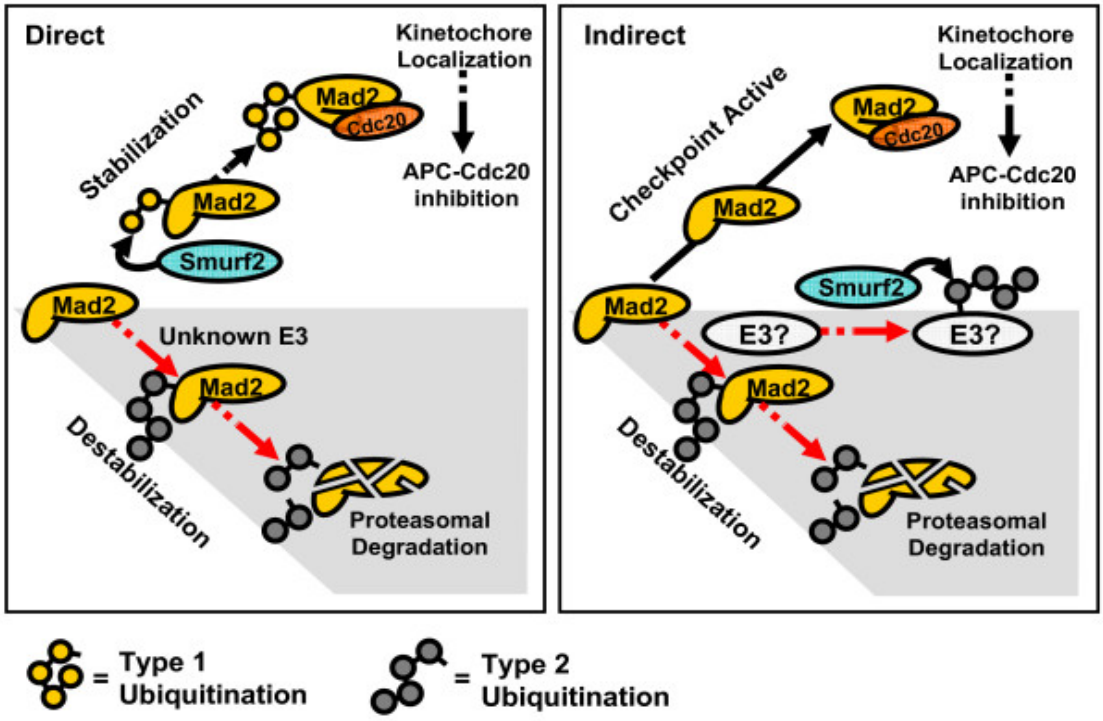

Figure 20. Putative models depicting the role of Smurf2 in MAD2 stabilization

Osmundson et al. (2009) demonstrated that the HECT E3 ligase SMURF2 acts as a suppressor of ubiquitin-dependent degradation of MAD2. Thus, they elaborated two models to explain the effect of SMURF2 on MAD2:

- according to the "direct" model (left panel), SMURF2 enhances MAD2 stability through post-translational modifications;
- according to the "indirect" model (right panel), SMURF2 catalyzes the ubiquitin-dependent degradation of at the time unidentified E3 ligase (or its critical cofactor) that promotes polyubiquitination of MAD2.

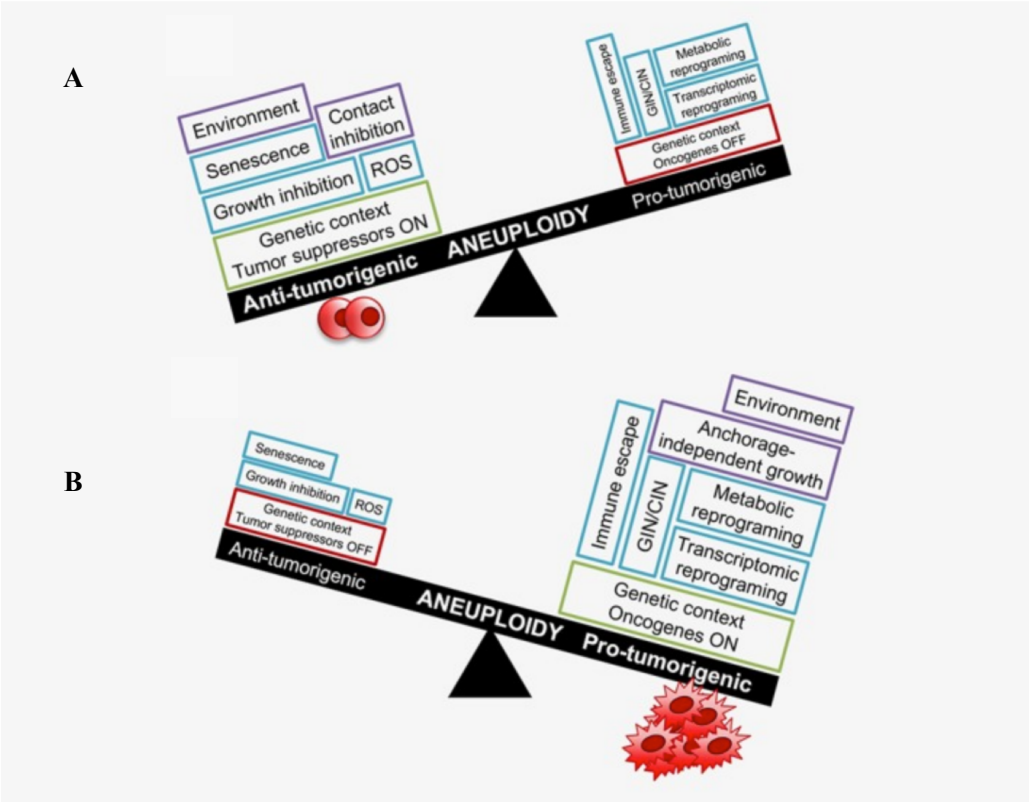

Figure 21. The complex relationship between aneuploidy and cancer

A) Aneuploidy-related growth and contact inhibition, ROS production, cell senescence can cooperate with environmental conditions and tumor suppressor activity to inhibit malignant transformation (round shaped cells represent nontransformed cells).

B) When prosurvival and protumorigenic events induced by aneuploidy (anchorage-independent growth, transcriptional and metabolic reprogramming, GIN, CIN, immune escape) synergize with activation of oncogenes and favorable environmental conditions, cells carrying an aberrant chromosome number undergo malignant transformation (irregular shaped cells represent malignant cells).

From Simonetti et al., 2019.

AIM OF THE STUDY

The Hh pathway is involved in fundamental processes during embryogenesis and in adult life, including cell proliferation, differentiation and morphogenesis, stem cell maintenance and regeneration (Lee et al., 2016). Modulation of the Hh signaling is critical for proper cerebellar development and aberrant Hh activity is responsible for a large fraction of all human MB, the most common solid tumor in childhood (Rossi et al., 2008).

KCASH2^{KCTD21} belongs to the protein KCASH family and shares with the other two family members (KCASH1-3) structural and functional features. Indeed, members of KCASH family act as negative regulators of Hh signaling, inhibiting Gli transcription factors activity.
The presence of three members with common functions, belonging to the same family, suggests a redundancy of the system that makes the Hh regulation more solid and fine-tuned.
KCASH proteins possess a well conserved N-terminal BTB domain but an heterogenous C-terminus, suggesting the presence of peculiar functions or different mechanisms of individual KCASHs functional regulation. In particular, KCASH2 C-terminal region is highly conserved by evolutionary pressure, underlying undiscovered important biological functions.

The aim of this thesis is to shed light on the so far unknown functions performed by KCASH2 and to understand the regulatory mechanisms involved in KCASH2 mRNA and protein modulation.
To achieve this goal, we have investigated KCASH2, researching, at first, protein interactors, whose binding was not shared with other family members.

The first putative KCASH2 protein interactor, KCTD15, was identified in our laboratory through mass spectrometry approaches. This interaction was preliminarily validated and was identified the region involved in hetero-oligomerization of the two proteins. Moreover, it was assessed that KCTD15 negatively controls the transcriptional activity of Gli1 (the main effector of Hh signaling), although the KCTD15 involvement in MB tumorigenesis and the molecular mechanisms underlying the negative regulation of Hh pathway mediated by KCTD15 were not yet known.
The first goal of this thesis was the understanding of the biological meaning of KCASH2-KCTD15 interaction in SHh-MB context, understanding how KCTD15 could be a novel player in the complex network of regulatory proteins which modulate Hh pathway.

This, on one hand, could increase the current knowledge of Hh signaling modulation, on the other hand, suggest novel potential therapeutically approaches aimed to modulate downstream the pathway in Hh-dependent tumors.

The second identified KCASH2 protein interactor was the core spindle checkpoint protein MAD2. MAD2 is a particularly interesting interactor, since it is essential for the function of the spindle assembly checkpoint (SAC). In particular, MAD2 protein levels have been found either aberrantly elevated or reduced in a wide range of tumors, underlying that its fine-tuned regulation is necessary to the correct segregation of chromosomes, thus preventing aneuploidy.
In the second part of this thesis we aimed to better characterize the KCASH2-MAD2 interaction, and the functional role of the latter during cell cycle, trying to understand the mechanism that regulate MAD2 stability, its degradation mechanisms as well as the events by which both hyper and hypo-expression of MAD2 may lead to tumorigenesis.

In the final part of the thesis, we focused on KCASH2 transcriptional regulation, with the purpose to study the KCASH2 proximal promoter, identifying putative transcription factors involved in its physiological or pathological modulation.

Overall, the work presented here aims to draw a more complete picture of the complex biological role of KCASH2, unveiling additional functions and novel mechanism of regulation of its expression, both at protein and mRNA level.

RESULTS

FIRST SECTION:

KCTD15 inhibits the Hedgehog pathway in Medulloblastoma cells by increasing protein levels of the oncosuppressor KCASH2

1. KCTD15 expression is downregulated in SHh-dependent MB

Our preliminary data have hinted for a KCTD15 role in Hh signaling, since KCTD15 expression was able to decrease the transcriptional activity of a Gli1- responsive luciferase reporter.

To verify a potential correlation between KCTD15 expression and Hh expression, we have investigated KCTD15 expression levels in a group of 47 human sporadic MB samples and 9 cerebellar controls. Interestingly, in a relevant subset of the SHh subgroup (5/19, 26.3 % of the samples) there was a marked reduction of KCTD15 mRNA levels (**figure 22A**), supporting a role for KCTD15 in Hh context.

Furthermore, by software R2 (R2: Genomics Analysis and Visualization Platform (http://r2.amc.nl)), we could not find a correlation between expression levels of KCTD15 and KCASH2 in this SHh-MB context (**figure 22B**), indicating that KCTD15 is not acting on KCASH2 transcription.

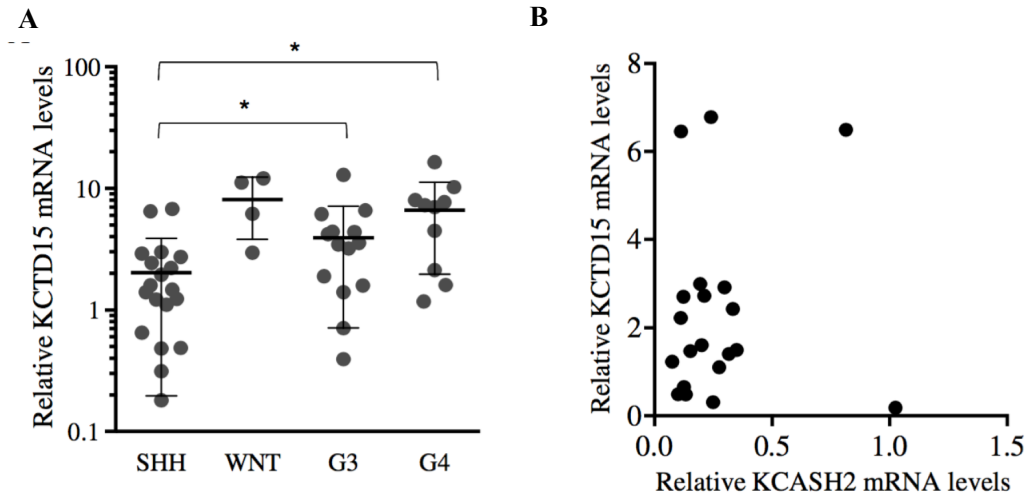

Figure 22. SHh-dependent MBs frequently present KCTD15 reduced expression.

A) 47 human sporadic MBs belonging to different molecular groups have been assessed for KCTD15 expression by Q-RT-PCR analysis. The relative mRNA levels were expressed as the ratio of the sample quantity to the mean values of 9 normal cerebella (Ctr). *P<0.05 G3 versus SHH, **P<0.01 G4 versus SHH (Mann-Whitney test).

B) No significant correlation was observed (r: 0,1; p= 0.69) between KCASH2 and KCTD15 expression analysis in SHH human MB.

2. KCTD15 downregulates HDCA1 protein levels but does not bind neither Cul3 nor HDAC1

To further investigate KCTD15 working mechanism and its interplay with KCASH2, we evaluated if KCTD15 overexpression acted on Gli1, affecting the levels of HDAC1 and paralleling or contributing, in this way, to the well-known KCASH2 mechanism of action. We co-transfected HEK293T cells with vectors encoding for Flag-KCTD15 and HA-KCASH2 and, by Western-Blot analysis, we observed a significant reduction of HDAC1 protein, following KCTD15 overexpression (**figure 23A**).

Moreover, since a HDAC1 protein decrease leads to a higher Gli1 acetylation, we monitored the levels of Gli1 acetylation following KCTD15 overexpression, performing an experiment similar to the one performed in Canettieri et al. (2010) and Coni et al. (2017). The KCTD15 overexpression is responsible not only of lower HDAC1 protein expression, but also of the decrease in its activity, since acetylated-Gli1 protein levels are notably higher than in the control cells (**figure 23B**). Next, we wondered if the KCTD15 activity on HDAC1 was mediated by the formation of a complex recruiting Cul3 and HDAC1, as KCASH2 acts, or by a different mechanism. Through co-expressing vector encoding for tagged-protein in HEK293T following Co-IP assays, we observed that neither of the two proteins (Cul3 in **figure 23C** and HDAC1 in **figure 23D**) was able to co-immunoprecipitate with KCTD15. Indeed, Cul3 recognition is not a universal property among KCTD proteins. The KCTD15 inability to bind Cul3 has already been predicted using bacterial system in which recombinant proteins were expressed (Smaldone et al., 2015). Although KCASH2 and KCTD15 share a relatively high homology at the BTB domain sequence, the N-terminal portion of the two proteins diverge for their capability to bind Cul3, probably due to their involvement in independent activities that require or not Cul3 functions, leading to its loss.

These data, taken together, suggest an indirect mechanism of action for KCTD15 on the Hh pathway, and led us to verify if KCTD15 acts mediating for an effect on KCASH2.

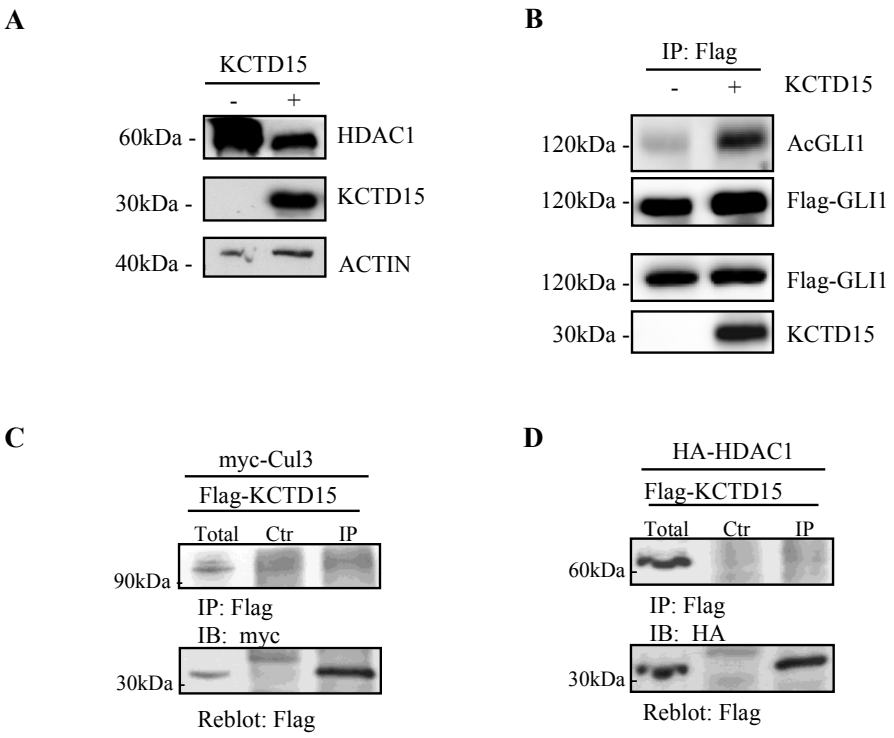

Figure 23. KCTD15 reduces HDAC1 protein levels but does not interact with Cul3 and HDAC1.

A) KCTD15 expression reduces HDAC1 protein levels. HEK293T were co-transfected with HDAC1-HA vector, plus empty or Flag-KCTD15 vectors and protein lysates were analyzed by WB.

B) HEK293T were co-transfected with Flag-GLI1 vector plus empty or KCTD15. IP was performed with anti-Flag conjugated agarose beads. Blots were IB with anti- acetylated lysine (K518) antibody and reblotted with anti-Flag antibody (upper panel). Total lysates were analysed by Western Blot using anti-KCTD15 and anti-Flag antibodies (lower panel).

C-D) KCTD15 is not able to interact with Cul3 (C) and HDAC1 (D). Co-IP experiments are performed in lysates from HEK293T cells transfected with expression vectors encoding for the indicated proteins.

3. KCTD15 increases KCASH2 protein stability, increasing its effect on Gli1

Since KCTD15 overexpression is responsible of a HDAC1 protein levels reduction, paralleling the KCASH2 activity, we hypothesized a KCASH2 upstream mechanism in which KCTD15 expression affected KCASH2 protein levels, increasing its activity or stability.

We overexpressed increasing amounts of KCTD15 and we evaluated the effect on KCASH2 protein levels. We performed this experiment co-transfecting three different KCASH2 concentration (125ng, 250ng, 500ng) and valuating, for each condition, the dose-dependent KCTD15 contribution on KCASH2 protein levels. Anyhow, overexpressed KCTD15 increases the KCASH2 protein levels in HEK293T cells dose-dependent (**figure 24A**).

We confirmed the obtained data valuating the endogenous KCASH2 protein levels, following KCTD15 overexpression (**figure 24B**), leading to the hypothesis that KCTD15 activity on Hh pathway is an effect of the increase of KCASH2 protein in the cells.

We tested this hypothesis by performing a Gli-responsive luciferase reporter assay in which we co-transfected different amounts of KCTD15 alone or together with a fixed amount of KCASH2 expressing vector. As shown in **figure 25A**, KCTD15 increases the inhibition of GliRE-luciferase activity in KCASH2 co-transfected cells in a dose-dependent manner. Compared to the KCASH2 effect on Gli1 activity reduction in presence of only endogenous KCTD15, the overexpression of the latter leads to a major decrease of Gli1RE-luciferase activity. Furthermore, KCTD15 alone has an inhibitory effect that can be related to stabilization of the endogenous KCASH2.

To verify if the KCTD15 has a physiologically relevant function, we monitored the effect of the depletion of endogenous KCTD15 in HEK293T cells on a Gli-RE luciferase assay (**figure 25B**). As expected, siRNA- mediated depletion of endogenous KCTD15 abrogated its stabilizing effect on KCASH2, resulting in an increment of the baseline of Gli1 transcriptional levels. Moreover, in condition of KCTD15 depletion, the KCASH2 activity on Gli1 is reduced compared to control (siCTR), indicating that KCTD15 ability to inhibit Gli1 activity depends on the presence of KCASH2.

Next, we confirmed this observation silencing the KCASH2 expression, transducing HEK293T with lentivirus expressing control and KCASH2 shRNA (**figure 26A**). In sh-KCASH2 cells, the KCTD15 overexpression has no suppressive effect on Gli1RE-luciferase activity (**figure 26B**).

All together, these data indicate that KCTD15 participates to Hh signaling regulation, increasing KCASH2 protein levels and, indirectly, affecting Gli1 transcriptional activity.

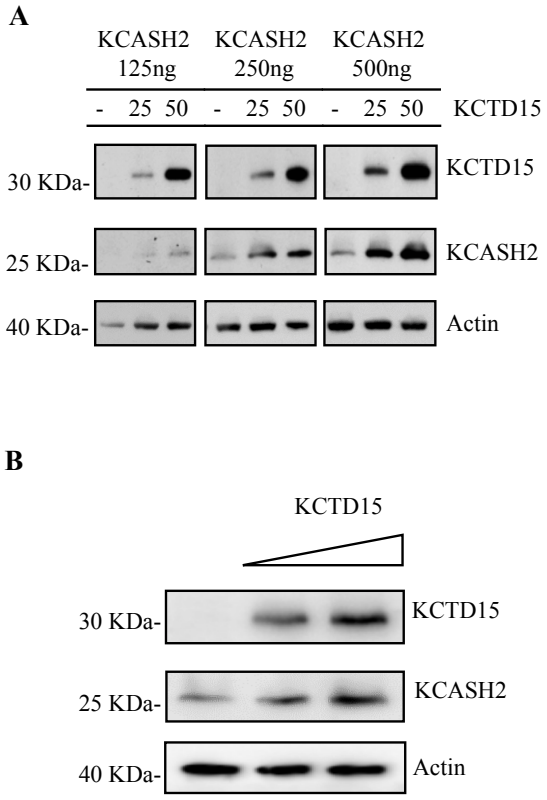

Figure 24. KCTD15 increases endogenous and exogenous KCASH2 protein levels

A) HEK293T cells were transfected with different amounts of Flag tagged KCTD15 and KCASH2 (as indicated), then analyzed by WB with anti-Flag antibody. Actin protein is shown as a normalizer.

B) HEK293T cells were transfected with increasing amount of KCTD15-Flag and endogenous KCASH2 was detected by anti- KCASH2 antibody. Actin was used as a loading control.

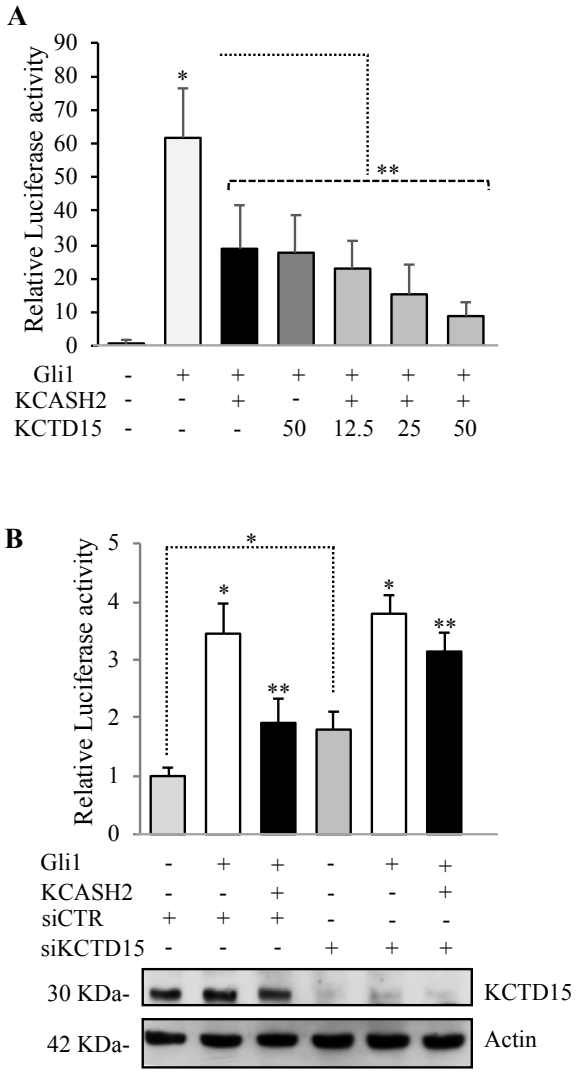

Figure 25. KCTD15 enhances its inhibitory activity on Gli1.

A) KCTD15 increases the inhibition of GliRE- luciferase activity in KCASH2 co-transfected cells. HEK293T cells were transfected with 12× GliRE-Luc and pRL-TK Renilla (as a normalizer) plus variable amounts of the indicated vectors. *p<0.05 versus control. **p<0.05 versus Gli1.

B) Depletion of endogenous KCTD15 reduces KCASH2 inhibitory activity on Gli1. Relative luciferase activity was measured in HEK293T cells transfected with scrambled siRNA (siCtr) or with KCTD15 siRNA (siKCTD15) followed by 12× GliRE-Luc and pRL-TK Renilla plus the indicated vectors. Bottom panel shows KCTD15 protein levels. Actin was used as loading control. *p<0.05 versus control. **p<0.05 versus Gli1 transfected.

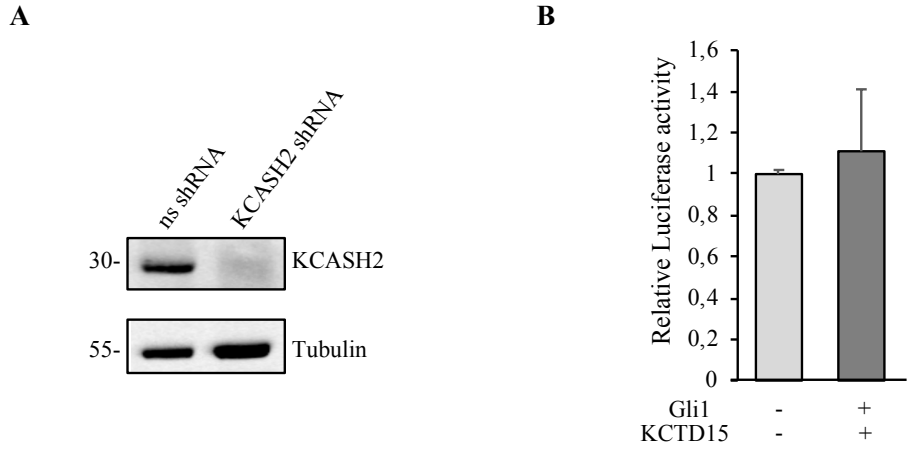

Figure 26. KCTD15 is not able to decrease GliRE luciferase activity in KCASH2 knock-down HEK293T.

A) Generation of KCASH2 knock down HEK293T cells. Western blot analysis of KCASH2 protein expression in lentiviral control and KCASH2 shRNA-transduced HEK293T cells. Alpha-tubulin is shown as loading control.

B) KCTD15 is not able to decrease GliRE luciferase activity in KCASH2 knock- down HEK293T. Cells were transfected with 12× GliRE-Luc, Gli1, KCTD15. pRL-TK Renilla was cotransfected as a normalizer.

4. KCTD15 expression reduces Hh-dependent medulloblastoma cells proliferation

We verify the KCTD15 effect on KCASH2 protein stability in DAOY cells, a widely used human primary SHh-dependent medulloblastoma cell line. The KCTD15 overexpression lead to an increase of endogenous KCASH2 protein levels (**figure 27A**). Accordingly, it is responsible also of a Hh signaling activity reduction (**figure 27B**). We monitored the mRNA levels of Gli1 and Hh target genes, such as N-myc and Cyclin D2, observing a strong reduction of their expression. Indeed, KCTD15 is able to interact with the Hh inhibitor KCASH2, stabilizing the protein and enhancing its inhibitory effect in MB cells.

We aimed to investigate the KCTD15 role in Hh-dependent proliferation to assess its role in tumor context. We performed colony assay on control and KCTD15 overexpressing DAOY and we demonstrated a strong reduction of the absolute colonies number (**figure 28A-B**), indicating that KCTD15 overexpression impairs MB cell proliferation. We analyzed also the size distribution of colonies, through the ImageJ plugins "colony-counter" (version 1.49v, Java 1.8.0_45, Wayen Rasband, U.S. National Institutes of Health, Bethesda, MD, USA). Interestingly, not only the absolute number of the colonies was reduced by 40%, but also the size distribution of the colonies was affected (**figure 28C**). Indeed, we observed a marked reduction in the percentages of the medium (from 19% to 12%) and large (from 1 to 0.5%) colonies in KCTD15 transfected cells. This suggests that the overexpression of KCTD15 leads to both a reduced Hh-dependent stemness of MB cells (which is indicated by a reduced number of colonies) but also a reduction of self-renewal ability, the proliferative potential of the cells, which leads to smaller size of colonies. This is consistent with Hedgehog (Hh) pathway function in development and tumorigenesis, processes sustained by stem cells (Po et al., 2010). Indeed, Gli1 suppression inhibits cell proliferation, attenuates cell stemness and increases apoptosis in Hh-dependent tumor models (Teglund and Toftgård, 2010; Po et al., 2017).

To confirm the anti-proliferative effect of KCTD15 on DAOY cells, we performed an EdU incorporation assay to detect and quantify cell proliferation *in vivo*. We overexpressed KCTD15 in DAOY cells and analyzed the percentage of EdU positivity, calculating number of EdU positive cells over total cells, counterstained with Hoechst 33342 (**figure 29A**). As expected, the KCTD15 overexpression leads to a reduced EdU positivity percentage (**figure 29B**). We obtained concordant data using a cell metabolism/proliferation assay (MTT assay). To this end, we transfected DAOY cells with KCTD15 empty or vector and measured absorbance. The KCTD15 overexpressing cells present lower cell metabolic activity, indicating lower cell proliferation (**figure 29C**).

Finally, we evaluated if the decreased proliferation was associated with an increased apoptotic rate in KCTD15 overexpressing cells. For this purpose, we detected apoptosis through DNS assay

(Differential Nuclear Staining) in KCTD15 overexpressing DAOY cells (**figure 30A**). Through this assay (Forrester, 1999), double staining with both Hoechst 33342 and PI dyes allows recognition of the late apoptotic cells nuclei, which contain several fragmented pink bodies, from live and early apoptotic cells. For this reason, late apoptotic cells were the only ones measured in the analysis, probably underestimating the number of cells that undergo apoptosis. Indeed, KCTD15 overexpression ended up in a slight but significant increase (from 2.5% to 5%) in apoptotic cell death in DAOY overexpressing KCTD15. This data was confirmed by Western Blot analysis for cleaved Caspase 3 (**figure 30B**).

Here we report the identification of KCTD15 as a novel player in the complex network of regulatory proteins which modulate Hh pathway. Indeed, KCTD15 is able to interact with the Hh negative modulator KCASH2, stabilizing the protein and enhancing its inhibitory effect in MB cells. Moreover, KCTD15 overexpression in MB cell line DAOY induces Hh signaling suppression and reduction of cell proliferation, partially explained with an increment of apoptosis.

Data presented here have been published (Spiombi*, Angrisani* et al., *Oncogenesis,* 2019).

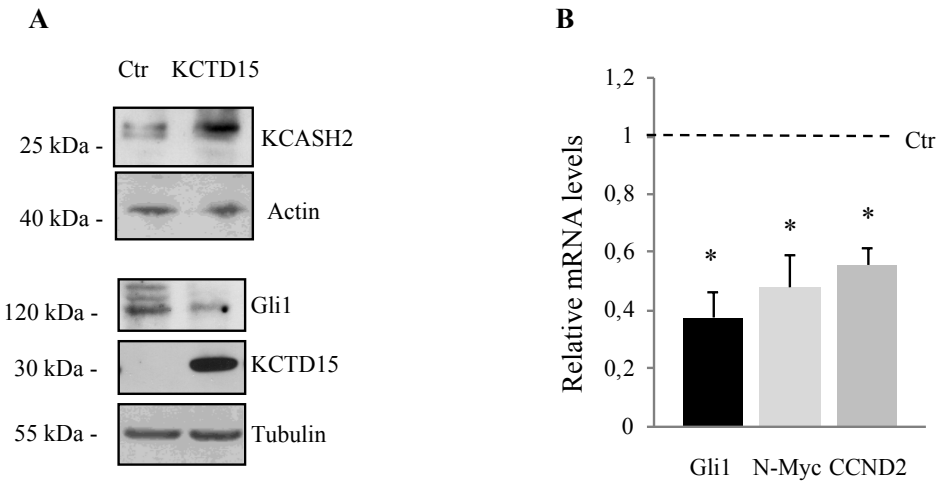

Figure 27. KCTD15 expression increases KCASH2 protein levels in medulloblastoma cells
A) KCASH2 protein levels are increased in DAOY cells expressing KCTD15 while Gli1 protein is reduced. DAOY cells were transfected with KCTD15-Flag and protein lysates were immunoblotted with anti-KCASH2 antibody (upper panels) or anti-Gli1, anti-Flag antibodies (lower panels). Anti-Actin and anti- Tubulin antibodies were used as loading controls.
B) Hh pathway activity is downregulated in KCTD15- transfected MB cells. Q-RT-PCR analysis of endogenous Hh targets mRNA levels are normalized to the control (Ctr). *$p<0.05$ versus Ctr.

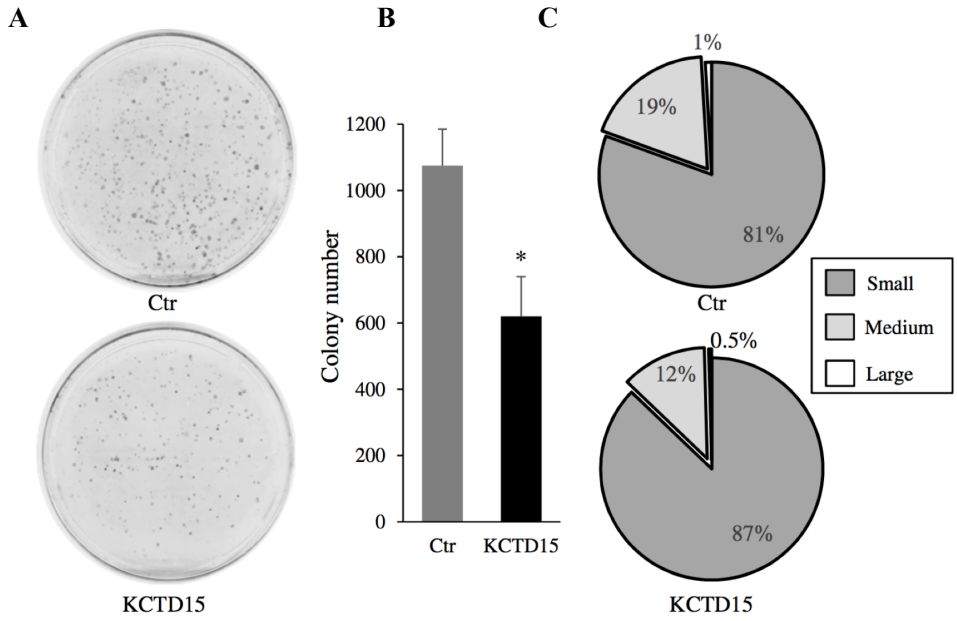

Figure 28. KCTD15 expression reduces Hh-dependent medulloblastoma cells proliferation

A-C) DAOY cells overexpressing KCTD15 were assayed for their capability to form colonies. Representative images were shown from three independent experiments (A) and number of colonies (B) are shown in correlation with the empty vector (Ctr). C Percentage of small, medium and large size colonies is indicated in DAOY Ctr cells (upper panel) and DAOY transfected with KCTD15 (lower panel).

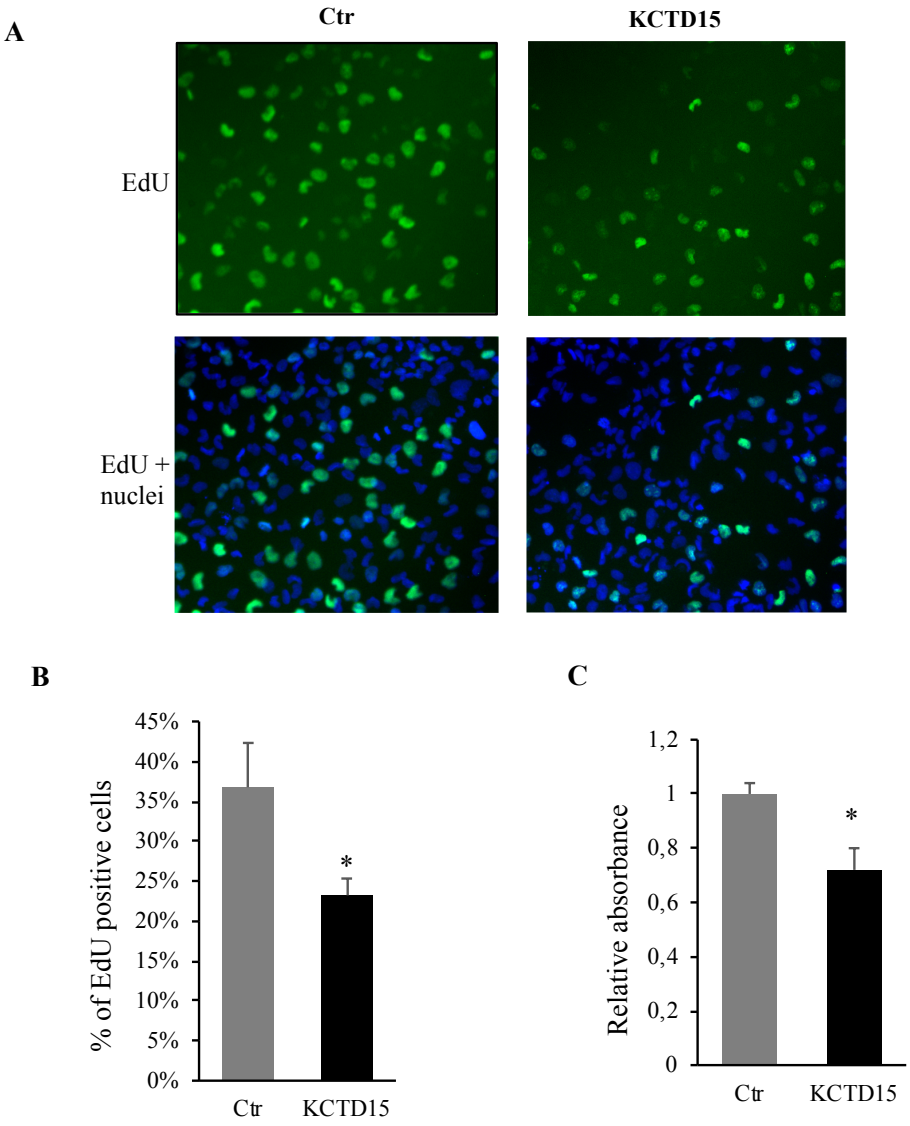

Figure 29. KCTD15 expression reduces Hh-dependent medulloblastoma cells proliferation

A-B) DAOY cells were transfected with indicated vectors for 24 hours. Following 6 h incubation with EdU, the cells were fixed and stained with Click-iT kit. Number of EdU positive cells were calculated over total cells and expressed as percentage vs total cells. a Dividing cells incorporate EdU (shown in green). Cells' nuclei are counterstained with Hoechst (in blue). b Results are expressed as the mean ± SD of three independent experiments (*P<0.05, Student's t-test).

C) MTT assay on DAOY cells transfected with empty or KCTD15 vectors and analyzed after 24 hours. Results are expressed as the mean ± SD of five independent experiments, each performed in triplicate (*P<0.05, Student's t-test).

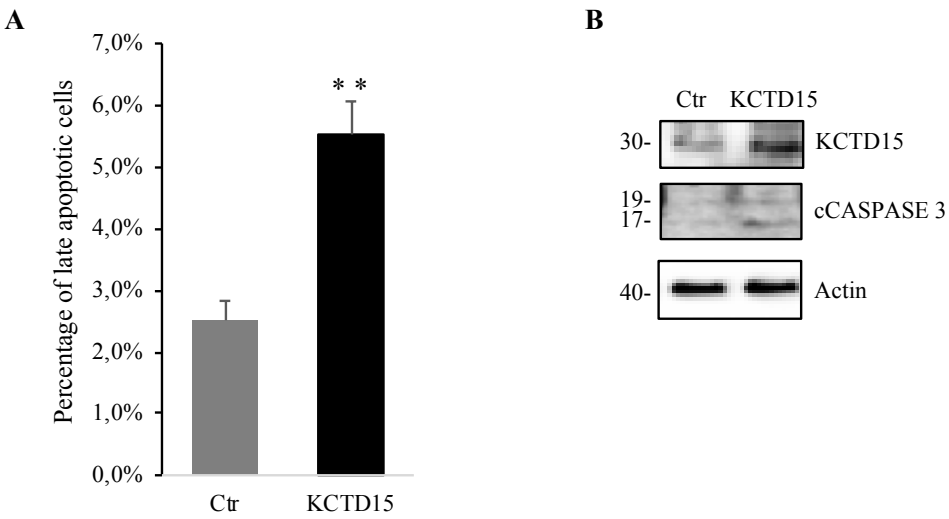

Figure 30. Overexpression of KCTD15 increases apoptosis in DAOY cells.

A) DAOY cells were transfected with KCTD15 or empty vector (Ctr). The percentage of late apoptotic cells that incorporated both PI and Hoechst dyes was measured using the ImageJ software. Results are expressed as the mean ± SD of five independent experiments (**P<0.01 calculated by a Student's t-test).

B) WB analysis of cleaved Caspase 3 protein in DAOY cells transfected as above. Actin is shown as loading control.

5. Discussion

We have identified KCTD15 as a novel player in the complex network of regulatory proteins that inhibits the Hh pathway, describing the first mechanism that modulate tumor suppressor KCASH2 protein stability and as a consequence, protein levels.

KCTD15 has been previously observed in vertebrate neural crest during development, in which KCTD15 has been demonstrated to negatively regulate the transcription factor TFAP2A, a target of WNT signaling by binding to it, changing its conformation and precluding transcriptional activation (Zarelli and Dawid, 2013). Anyway, it has also been noted that expression pattern of TFAP2 and KCTD15 are not largely overlapping and therefore KCTD15 necessarily plays other roles in different tissues.
KCTD15 expression has been reported in adult cerebellum (Willer et al., 2009). Interestingly, most of the cerebellar cell types (including cerebellar granule neuron, Purkinje cells, Bergmann Glia, astrocytes) do not derive from neural crest but from the neural tube, and TFAP2A expression has been reported to be limited to developing and adult cerebellar GABAergic interneurons (Purkinje cells). Thus, KCTD15 most probably plays different functions in cerebellar context, one of whom is the modulation of KCASH2 in Hh- responsive cells (i.e. cerebellar granule cells).

KCASH2 is able to induce Hh pathway downregulation through recruitment, ubiquitination and degradation of HDAC1, in turn allowing hyperacetylation and inhibition of transcriptional activity of Gli1, the main target and effector of the Hh pathway.
Here, we observed that the KCTD15 overexpression also leads to HDAC1 protein levels decrease, producing an aberrant Gli1 activity and repression of its transcriptional activity. Anyway, KCTD15 is not able to bind neither HDAC1 or Cul3, underlining its involvement with mechanisms different from that elicited by KCASH2 on Hh signaling regulation.

KCTD15 protein has been previously grouped together with KCTD1 in a clade of the KCTD family which has been recently attributed at non-protein degradation functions. In fact, in purified bacterial systems it was observed that KCTD15 is not able to interact with Cul3 and thus does not appear to be able to directly ubiquitinate and degrade its protein interactors (Smaldone et al., 2015).
Indeed, in our context, KCTD15 regulates Hh signaling through binding to KCASH2 which leads to an increase of KCASH2 protein stability and its enhanced inhibitory effect in MB cells, reducing tumor cell proliferation.

A deeper study of the crystallographic structure of the two proteins, and specifically of their BTB domains, could be useful to identify the exact aminoacids involved in the interaction. The interaction between KCTD15 and KCASH2 could be hypothesized to be due to a conformational change of the oligomer, which may protect it from faster protein turn-over.

Loss or reduction of KCTD15 expression in cerebellum may lead to a reduced KCASH2 stability and to an incomplete turn-off of the Hh pathway, with a consequent increased proliferation of GCPs, delayed differentiation and tumorigenesis.
KCASH2 expression is significantly reduced in human MB, as we observed in both RT-qPCR analyses performed on sporadic human MB tissues and in online public database of a larger cohort of MB tissues. Interestingly, we have discovered that KCTD15 expression is reduced in a percentage of human sporadic MB which present Hh hyperactivation (SHh MB). Indeed, our results indicate that only a subpopulation of SHh medulloblastoma expresses significantly low KCTD15 mRNA levels. It is possible that a certain number of MB may express mutated forms of KCTD15 or have downstream alterations in KCASH2 (loss of expression, mutations) or Hh pathway components that render not necessary KCTD15 suppression. This may be due in part to the fact that KCTD15 is not a direct modulator of the Hh pathway but acts through the modulation of one inhibitor that is KCASH2, adding complexity and background noise to the analysis.
It has also to be noted that among the other subgroups, only 2/14 samples in Group 3 (which overall presents higher KCTD15 expression) presented a KCTD15 reduction. However, Group 3 of MB is highly heterogeneous and presents a significantly higher KCTD15 expression than SHh group. Moreover, since the expression of KCASH2 does not appear to be relevant in Group 3 (Cavalli et al., 2017), the possibility that KCTD15 plays a role in Group 3 MB would be most likely through a completely different molecular mechanism that is not currently the goal of the work.

The new role identified for KCTD15 suggests novel potential therapeutic approaches for modulating the Hh pathway in Hh dependent tumors. Up to date there are no available strategies to positively regulate KCTD15 expression in cancer, though further studies on its transcriptional modulation may uncover potential pharmacological modulators. A future strategy may be to use bioinformatic, proteomic and biochemical approaches to identify KCTD15/KCASH2 critical binding sites and generate small peptides or small molecules that may mimic KCTD15, binding and stabilizing KCASH2.

SECOND SECTION:

The tumor suppressor KCASH2 negatively modulates the mitotic checkpoint protein MAD2, delaying the mitotic exit

1. KCASH2 overexpression reduces MAD2 protein levels

Once verified that KCASH2 indeed interacts with MAD2 through its C-terminal region, we investigated the biological effect of this interaction.

For this purpose, we co-transfected HEK293T cells with Flag-MAD2 and Flag-KCASH2 vectors. By Western Blot analysis, we observed a consistent reduction of both exogenous and endogenous MAD2 protein levels (**figure 31A**), suggesting a role for KCASH2 in the MAD2 degradation. To confirm this observation, we analyzed the effects of KCASH2 depletion on MAD2 stability, transducing HEK293T cells with lentivirus expressing control and KCASH2 shRNA. Coherently with a negative role of KCASH2 on MAD2, in shKCASH2 cells, MAD2 expression was higher than in control cells (shRNA; **figure 31B**).

Moreover, we investigated if KCASH C-terminal region was responsible not only for the interaction with MAD2, but also for the KCASH2-mediated effect on MAD2. To this end, we co-transfected in HEK293T Flag-MAD2 vector together with full-length KCASH2, the BTB or the ΔBTB fragments. Of note, overexpression of either KCASH2 protein portions alone did not affect MAD2 protein levels, while this effect is visible in presence of the full-length KCASH2 (**figure 31C**). These data indicate that the presence of entire KCASH2 protein is essential to elicit its function on MAD2 protein stability, suggesting that the BTB-domain plays a role not in KCASH2-MAD2 interaction, but in the biological effect which follows it.

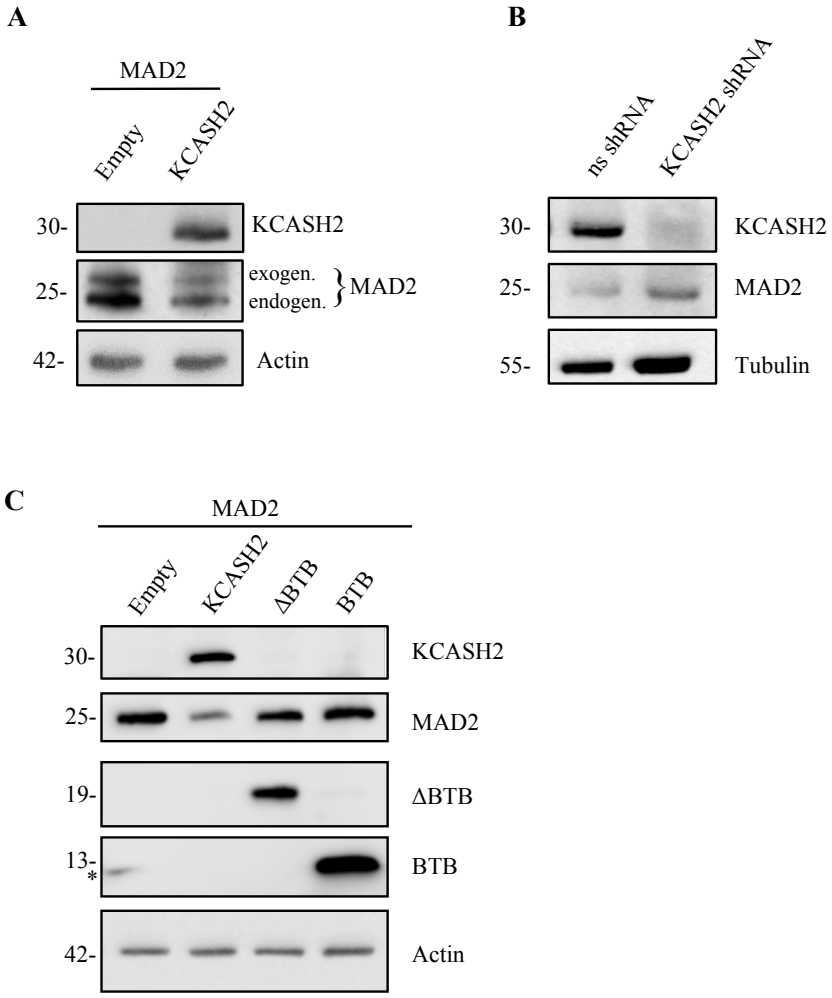

Figure 31. Full-length KCASH2 leads to MAD2 protein levels decrement.

A) Overexpression of KCASH2 in HEK293T cells leads to a significative reduction of both exogenous and endogenous MAD2 compared to control. Actin is shown as loading control.

B) HEK293T cell line transduced with shKCASH2 shows higher level of MAD2 protein compared to control (ns shRNA). Tubulin was used as loading control.

C) full-length KCASH2 is required for MAD2 downregulation. HEK293T cells were transfected with Flag-MAD2 together with either an empty vector, KCASH2-Flag, ΔBTB-KCASH2-Flag and BTB- KCASH2-Flag fragments. Actin was used as loading control.

2. KCASH2-Cul3 complex leads MAD2 to ubiquitination and degradation

As previously described, the BTB-domain of the KCTD proteins is involved in protein-protein interaction and may facilitate successful ubiquitination of substrates protein, complexing with one of the different Culs proteins (Liu et al., 2013).

Indeed, our group have demonstrated that KCASH2 may drive degradation of HDAC1 acting as an adaptor between Cul3 (through BTB domain, generating the E3-Ubiquitine Ligase complex) and HDAC1 (which is bound through the C terminal fragment; De Smaele et al., 2011).

We hypothesize therefore a similar mechanism in which KCASH2 acts 1) as a scaffold for interaction with MAD2 and 2) as E3-ubiquitine ligase, by binding to Cul3, leading to MAD2 ubiquitination and degradation.

To test this hypothesis, we performed a ubiquitination assay in HEK293T cells co-transfected with Flag-MAD2, HA-ΔBTB, HA-KCASH2, HA-Ub expression vectors. We observed that MAD2 ubiquitination levels increase only when full-length KCASH2 is overexpressed, while this effect is absent (as expected) in the presence of the protein lacking the BTB domain (**figure 32A**).

We also verified if KCASH2 was bound to Cul3 to form a E3-ubiquitine ligase complex. To this end, we co-transfected HEK293T with vectors encoding MYC-Cul3, Flag-MAD2 and HA-KCASH2. Following Co-IP assay, we demonstrated that MAD2 is able to bind Cul3 only in presence of KCASH2 (**figure 32B**).

MAD2 ubiquitination, in turn, leads to its proteasome-dependent degradation, since the use of a proteasome inhibitor (MG132) brings to a significant accumulation of the protein (**figure 32C**).

According to these data, we propose a model in which KCASH2 acts as a scaffold, binding Cul3 with its BTB domain and MAD2 with its ΔBTB. This event leads to formation of the Cul3-KCASH2-MAD2 complex, which is responsible of MAD2 ubiquitination and degradation with a mechanism that parallels the one already described for HDAC1 (De Smaele et al., 2011).

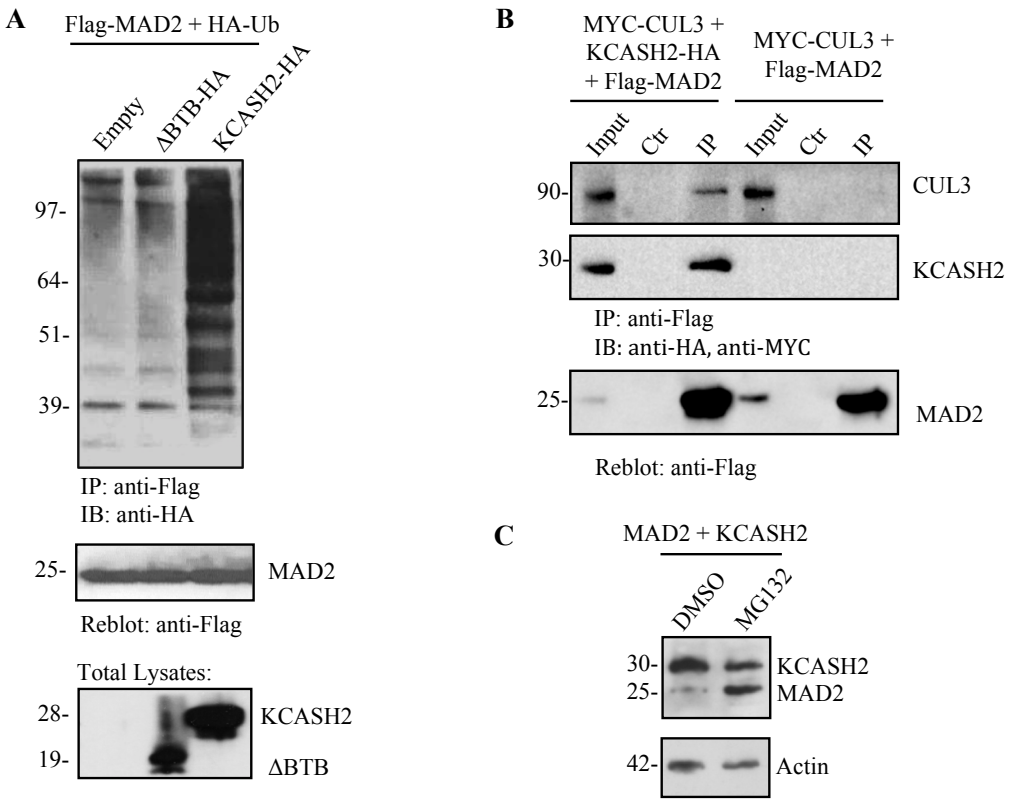

Figure 32. KCASH2-Cul3 is the E3 ubiquitin ligase complex responsible for MAD2 ubiquitination and proteasomal degradation.

A) KCASH2 promotes MAD2 poly-ubiquitination. HEK293T cells were transfected with HA-Ub and Flag-MAD2 both alone and with HA-KCASH2 or ΔBTB-KCASH2. Cell lysates were immunoprecipitated with anti-Flag agarose beads and immunoblotted with anti-HA. The blot was reblotted with an anti- Flag antibody. Bottom, KCASH2 and ΔBTB-KCASH2 total protein levels were revealed with an anti-HA antibody.

B) CUL3 co-immunoprecipitates with MAD2 only in presence of KCASH2. Co-IP experiment performed in lysates from HEK293T cells transfected with expression vectors encoding for the indicated tagged proteins and immunoprecipitated with anti-Flag agarose beads. IP samples and a fraction of the total lysate (Input) were loaded and separated on SDS-PAGE gels. Blots were immunoblotted (IB) with anti-MYC and anti-HA; reblots with anti-Flag.

C) MAD2 protein levels accumulate when the 26S proteasome is inhibited. Cell lysates from MG132-treated HEK293T cells, transfected with Flag-MAD2 and KCASH2-Flag, were loaded and separated on SDS-PAGE gel. MAD2 levels, revealed with anti-Flag antibody, were compared with the control (DMSO-treated) and normalized to β-actin.

3. KCASH2 acts on MAD2 closed conformation

MAD2 function in checkpoint signaling is intimately linked to conformational changes of the protein, which make possible binding with protein partners. Indeed, MAD2 adopts two conformations, an inactive open state (O-MAD2) and an active closed state (C-MAD2). After SAC activation, MAD2 assumes the closed conformation upon binding to MAD1 at the kinetochore (Lischetti and Nilsson, 2005).

Specific mutations that limit dimerization and structurally constrain MAD2 protein to a specific conformation have been described: MAD2L13A, MAD2 mutant locked in its closed conformation, and MAD2V193N, mutant locked in its open conformation (Mapelli et al., 2006; Mapelli et al., 2007; Kruse et al., 2014); MAD2R133A, monomeric form of MAD2 which cannot self-dimerize (Shandilya et al., 2015).

To investigate which conformation of MAD2 is required for interaction with KCASH2, we cloned the above indicated MAD2 mutants and expressed them by transfection in HEK293T cells. Subsequently, we assessed the KCASH2 capability to bind the mutants through Co-IP assay, observing that KCASH2 preferentially interacts with MAD2L13A, the closed conformation of MAD2 (**figure 33A**).

Moreover, we proved that overexpression of KCASH2 leads to a significant downregulation of MAD2 and C-MAD2, but not of the O-MAD2 levels (**figure 33B**).

We verified also that KCASH2 is able to bind the MAD2 mutant MAD2R133A, the closed form that exists exclusively as a monomer (**figure 33C**).

This observation suggests that KCASH2 may bind the C-MAD2 conformer and does not compete with either MAD1 or CDC20 binding.

Indeed, KCASH2 may play a role in modulation of MAD2 in its closed form, when it is active in MCC assembly or disassembly. According to these data, KCASH2 could act not as a MAD2 homeostatic protein levels regulator, but it could participate to the metaphase-anaphase transition checkpoint, fine-tuning the closed-MAD2 protein levels available for MCC assembly, or turning-off the SAC after having absolved its role.

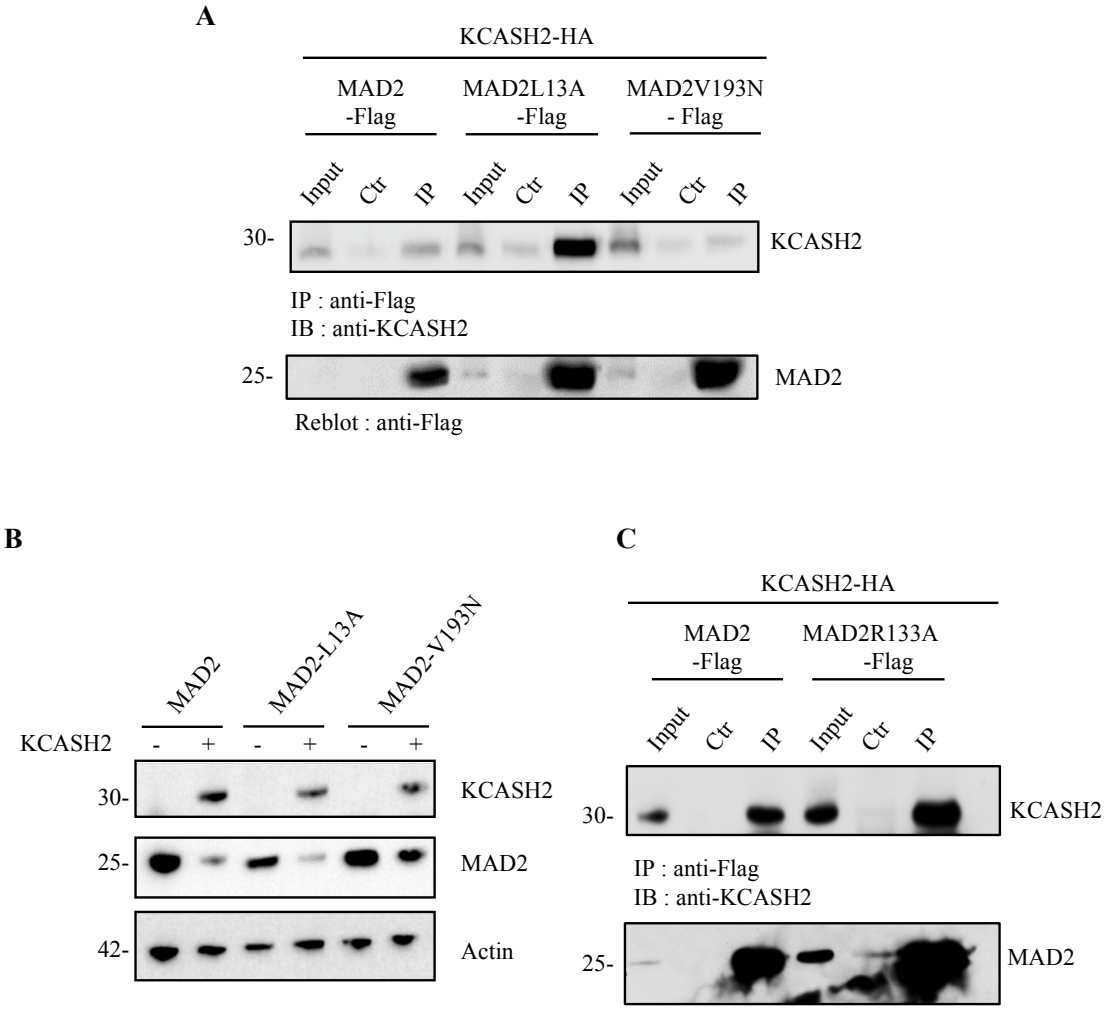

Figure 33. KCASH2 interacts with and modulates MAD2 closed conformation

A) KCASH2 interacts with the closed conformation of MAD2 (MAD2L13A mutant). Co-IP experiment performed in lysates from HEK293T cells transfected with expression vectors encoding for the indicated proteins and immunoprecipitated with anti-Flag agarose beads. Immunoprecipitated samples and a fraction of the total lysate were loaded and separated on SDS- PAGE gels. Blots were immunoblotted with anti-KCASH2 and Reblot with anti-Flag.

B) KCASH2 effect on MAD2 closed conformation. HEK293T cells were transfected with vectors encoding for the flag-tagged MAD2 wt, MAD2-L13A (C- MAD2), MAD2-V193N (O-MAD2) either alone or in presence of KCASH2-Flag. Total lysates were loaded and separated on SDS-PAGE gel and the blot was immunoblotted with anti-Flag and anti-βactin for normalization.

C) KCASH2 interacts with the conformation of MAD2 (MAD2R133A mutant), enable to dimerize. Co-IP experiment was performed as described above (figure 33A).

4. KCASH2 counteracts SMURF2-mediated MAD2 stabilization

The execution of the mitotic program with high fidelity is dependent upon precise spatiotemporal regulation of posttranslational protein modifications. Anyway, so far, no PTMs able to modulate MAD2 protein levels have been described. Osmundson and colleagues (2009) suggested that SMURF2, a HECT family E3 ligase, was involved into the stability of MAD2 and, in turn, into the function of the spindle checkpoint. However, they did not elucidate the molecular mechanism underlying the SMURF2-mediated MAD2 stability, proposing the two models previously described (see 1.2.2.1. paragraph).

Since we identified the E3-ubiquitine ligase complex involved into MAD2 degradation, we aimed to test the hypothesis that KCASH2 could represent the ubiquitin ligase targeted by SMURF2-mediated degradation. We co-transfected HEK293T cells with Flag-MAD2 and Flag-KCASH2 in presence or absence of SMURF2-myc and performed a Co-IP assay. SMURF2 is able to co-immunoprecipitate with MAD2 only in absence of KCASH2, suggesting that KCASH2 interferes the MAD2-SMURF2 binding (**figure 34A**). Moreover, we co-transfected both SMURF2 and KCASH2 in presence of MAD2 in HEK293T cells to investigate if one of the two protein has a dominant activity on the other one (**figure 34B**). In this context, SMURF2 did not increase MAD2 levels and therefore did not affect significantly KCASH2 protein levels, accordingly aminoacidic KCASH2 sequence lacks the "PPxY" motif necessary for the recognition by SMURF2 (**Figure 34C**).

These results indicate that, although KCASH2 is not a target of the ubiquitin Ligase Smurf2 and KCASH2 overexpression has a dominant effect on SMURF2.

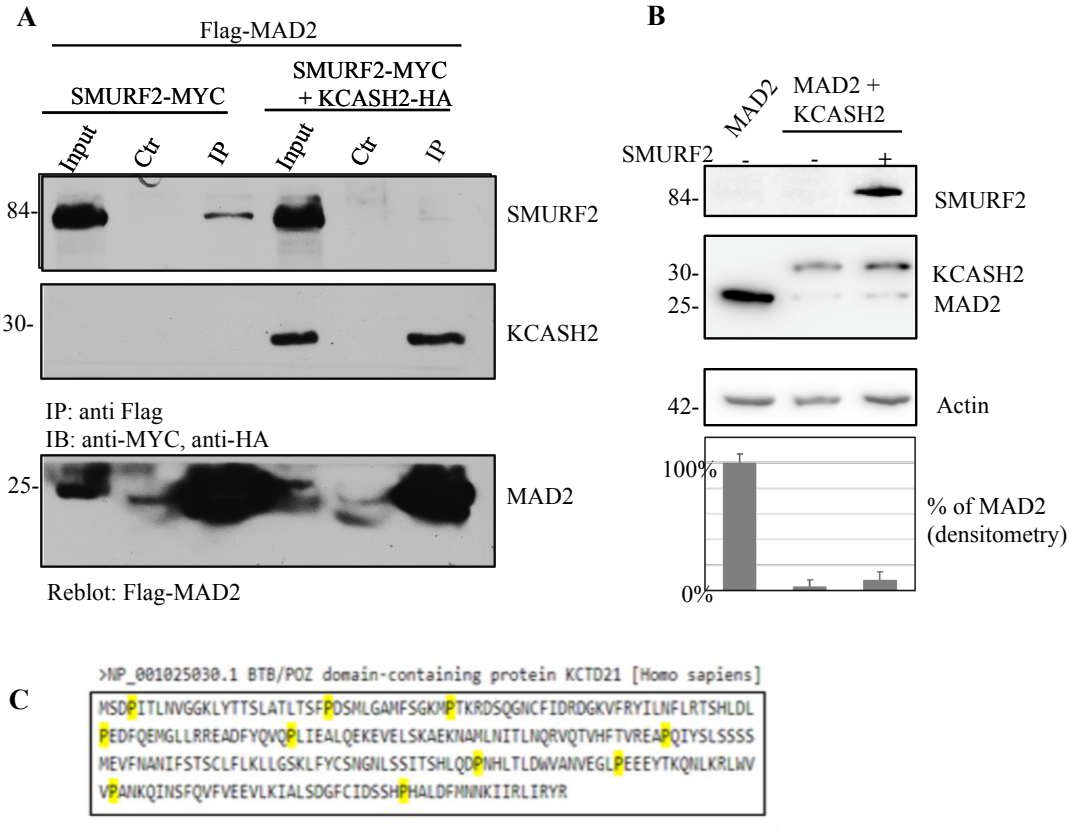

Figure 34. KCASH2 counteracts SMURF2-mediated MAD2 stabilization

A) SMURF2, in presence of KCASH2, is no longer able to bind MAD2. Co-IP experiment performed in lysates from HEK293T cells transfected with vectors encoding for the indicated proteins and immunoprecipitated with anti-Flag agarose beads. IP samples and a fraction of the total lysate were separated on SDS- PAGE gels. Blots were immunoblotted (IB) with anti-MYC and anti-HA and reblotted with anti-Flag.

B) SMURF2 does not downregulate KCASH2 and, thus, does not repristinate MAD2 protein levels. HEK293T cells were transfected with vectors encoding for the indicated proteins. Total lysates were separated on SDS-PAGE gels and the proteins were revealed with anti- tag antibodies and anti-βactin for the normalization. Bottom, densitometry of MAD2 protein levels realized with ImageJ.

C) KCASH2 aminoacidic sequence (from Pubmed) lacks the the "PPxY" motif necessary for the recognition by SMURF2.

5. KCASH2 overexpression causes a delayed metaphase-anaphase transition

The spindle checkpoint ensures accurate chromosome segregation by controlling cell cycle progression in response to aberrant microtubule-kinetochore attachment. Drastic changes in MAD2 levels may lead to an altered spindle checkpoint that causes chromosome instability and aneuploidy, frequently associated with tumorigenesis. Since MAD2 controls the metaphase-anaphase transition and we demonstrated that KCASH2 is involved in negative C-MAD2 regulation, we wondered if the KCASH2 overexpression may trigger to a significant alteration of cell cycle.

To this purpose, we have chosen as cell line model to perform our experiments the human colorectal cancer cell line HCT116. HCT116 is a model frequently used for cell cycle studies and characterized by a pseudodiploid karyotype (polyploidy=6,8%). We transduced HCT116 cells with lentivirus expressing KCASH2-GFP or GFP alone (**figure 35A**) and treated them with nocodazole, a microtubule de-polymerization agent, which arrests cells in mitosis. Mitotic cells were collected by mechanical shake off, seeded again in fresh medium and harvested at different time points. Nuclear DNA content was analyzed by propidium staining and flow cytometry analysis.
Interestingly, a higher percentage of KCASH2 overexpressing cells was arrested in G2/M phase compared to the control cells, indicating a delay in the G2/M-G1 transition (**figure 35B**).
This delay in metaphase-anaphase transition we confirmed by an accumulation of Cyclin B1 protein in KCASH2 overexpressing cells (**figure 35C**) while Cyclin A was not modulated (**figure 35D**). Indeed, cyclin B1 protein is a good marker for the identification of G2/M transition: its levels oscillate during cell cycle progression, accumulating during G2 and mitosis and suddenly disappearing just before the onset of anaphase.

These results were unexpected. Several research groups have demonstrated that MAD2 depletion not only prevents cells from arresting in response to the presence of misoriented chromosome, but also accelerates mitosis dramatically in cells in which chromosome segregation is proceeding normally. MAD2-depleted cells show accelerated transit through prometaphase and premature sister chromatid separation, fail to form metaphases, and exit mitosis soon after nuclear envelope breakdown (Howell et al., 2004; Michel et al., 2004).

To further confirm on our data, we decided to evaluate the cell cycle progression in an hTERT RPE-1 cell line (hTERT-immortalized retinal pigment epithelial cell line), another model largely used for cell cycle studies. We transduced hTERT RPE-1 cells with lentivirus expressing KCASH2-GFP or

GFP alone and synchronized with RO-3306, reversibly arresting proliferating human cells at the late G2 phase. We used RO-3306, a selective cyclin-dependent kinase 1 (CDK1) inhibitor, to sincronize cells in late G2 phase, before the entry in mitosis. RO-3306 arrested cells are able to enter mitosis rapidly after RO-3306 washout (Matson and Stukenberg, 2011).
In our experiments, we collected the cells at different time-points following removal of RO-3306 inhibitor, stained DNA with PI, and assessed by FACS analysis the cell cycle status was. Again, a significantly high percentage of KCASH2 overexpressing cells delay the mitotic exit and accumulate in G2/M (**figure 36**).

Since FACS analysis are based on DNA content, it cannot discriminate G2 phase from M: to overcome this limitation, in collaboration with Prof. Stefano Santaguida (Dep. of Experimental Oncology, IEO, Milan), we performed time-lapse cell imaging experiments and monitored the duration of the mitosis in the cells.
To this end, we generated HCT116 stably expressing mCherry-H2B (to monitor chromosome segregation) and transduced them with lentiviral expressing KCASH2-GFP or GFP alone. Cells were synchronized at the G1/S transition, by thymidine treatment, and analyzed by live cell microscopy for 24 hours, collecting images every 5 minutes. The mitotic time was counted as time taken from NEBD to DNA decondensation. We observed that duration of KCASH2 overexpressing cells mitoses was significantly longer than that of control cells (2 folds, **figure 37**). In particular, KCASH2 overexpressing cells spend more time in prometaphase/metaphase than control cells, as observed by longer chromosome condensation.

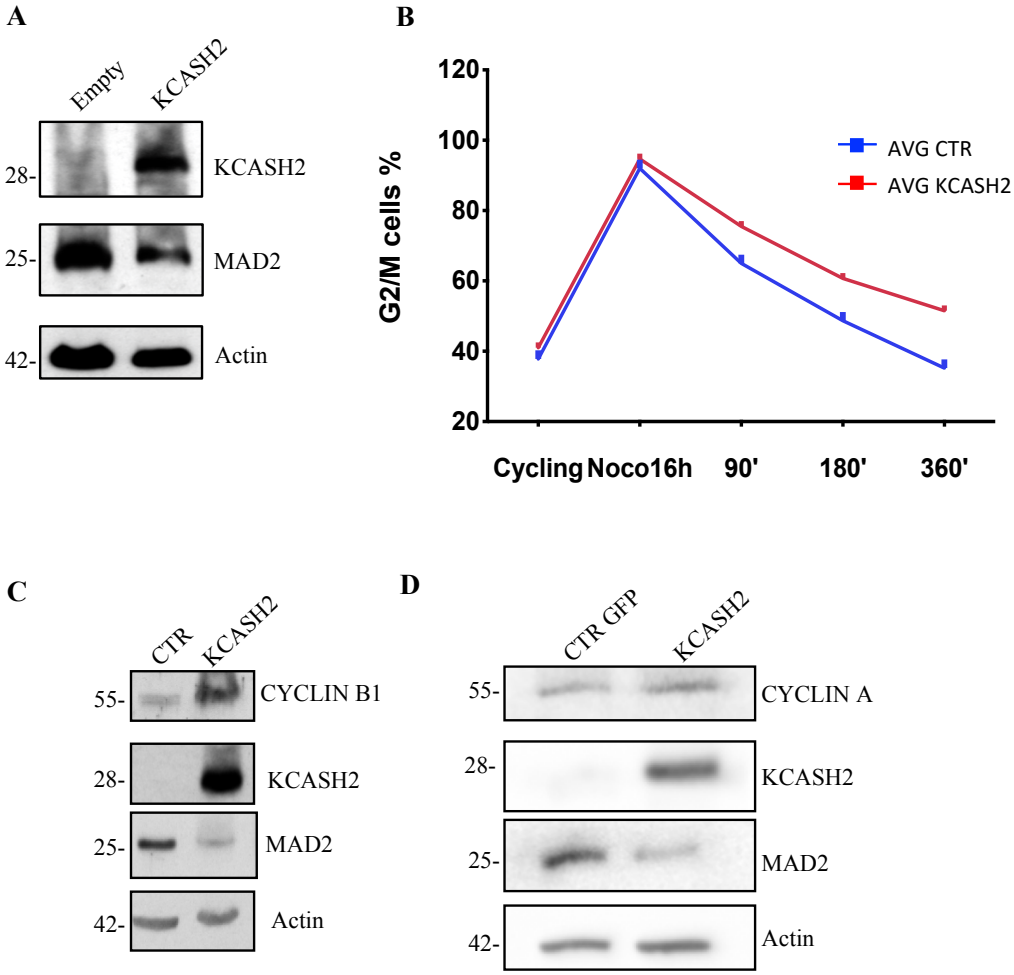

Figure 35. KCASH2 overexpression causes a delayed metaphase-anaphase transition

A) Western blot analysis of KCASH2 protein expression in lentiviral control and KCASH2 GFP-transduced HCT116 cells. Actin is shown as loading control.

B) KCASH2 overexpressing cells presented a significantly delay in the G2/M-G1 transition compared to control cells. HCT116 cells expressing KCASH2-GFP or GFP alone were blocked with nocodazole in G2/M phase. Mitotic cells were collected by mechanical shake off, seeded again and harvested at different time points.

C-D) Cyclin B1 protein accumulates in KCASH2 overexpressing cells (C), while Cyclin A is not modulated (D). HCT116 GFP/KCASH2-GFP total lysates were separated on SDS-PAGE gels and the proteins were revealed with anti- specific antibodies. Anti-βactin is shown loading control.

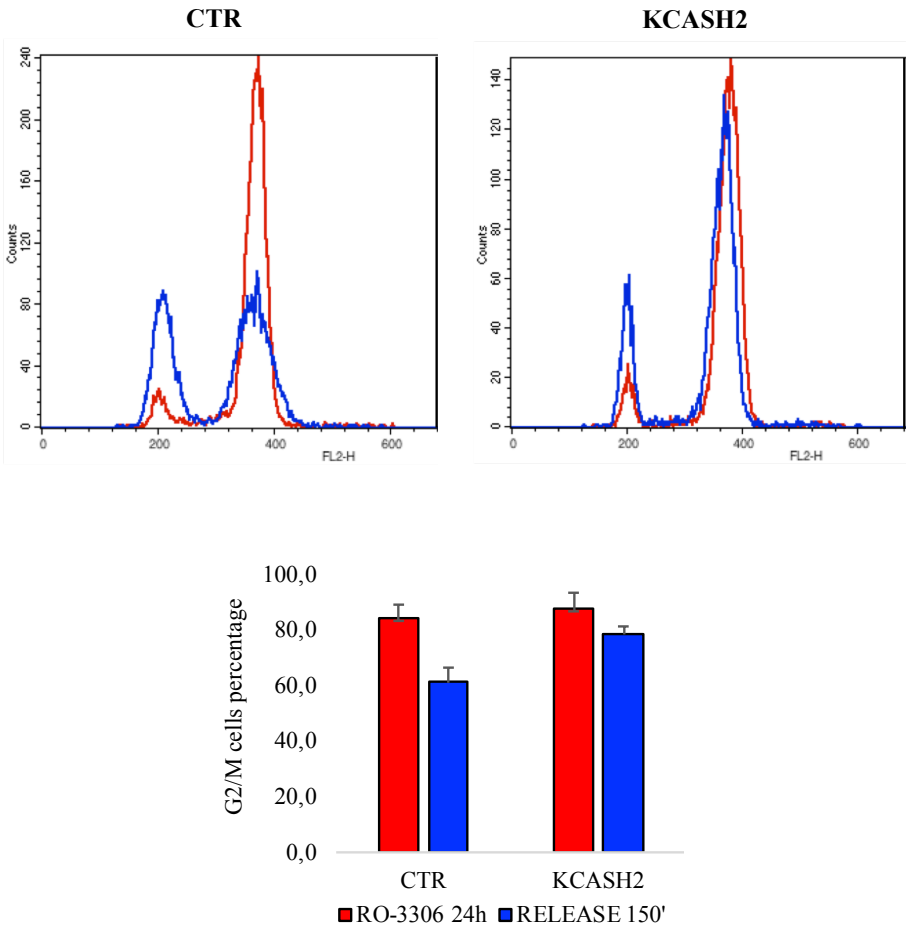

Figure 36. KCASH2 overexpression blocks cells in G2/M phase

Transduced hTERT immortalized RPE-1 cells with lentivirus expressing KCASH2-GFP or GFP alone were treated with the CDK1 inhibitor (RO-3306) for 24 hours to enrich for G2 cells. Cells were then released in fresh medium at different time points and analyzed.

Up panel: FACS analysis. It is represented a single time point (150') of released control and KCASH2-overexpressing cells. Down panel: The histogram reports G2/M cells percentage.

In red: cells collected following 24hours of RO3306 treatment and analyzed. In blue: cells were released for 150' from RO3306 block, collected and analyzed.

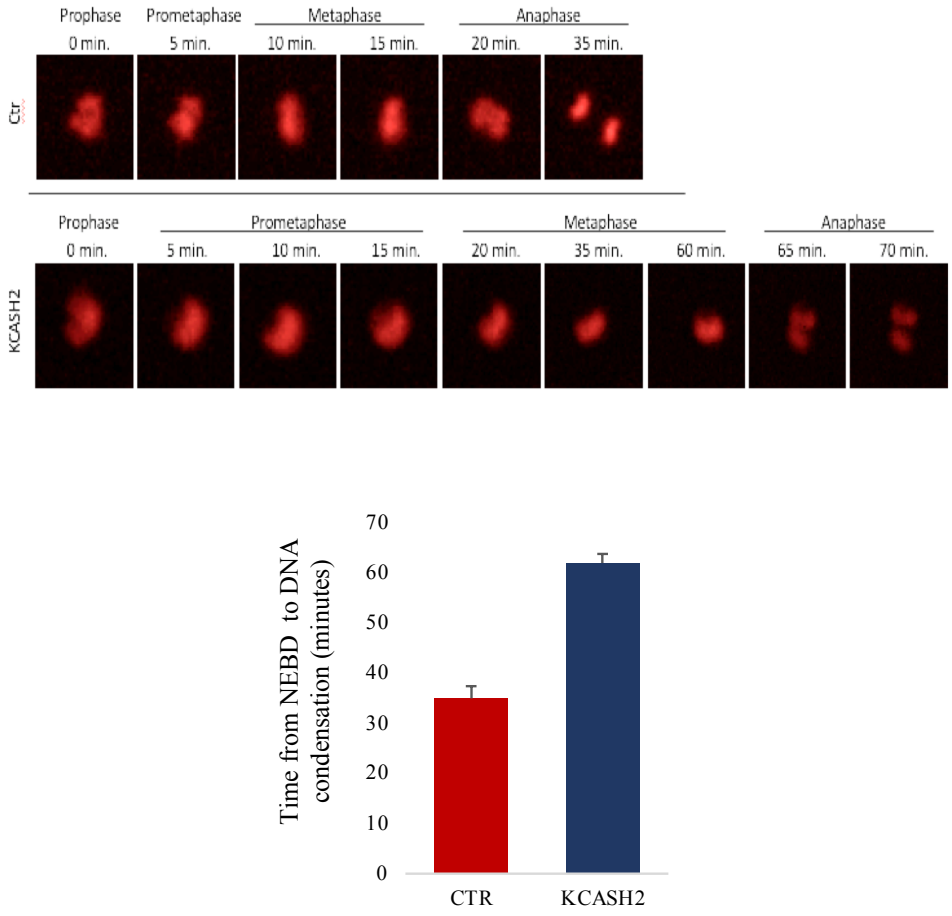

Figure 37. KCASH2 overexpressing cells have prolonged metaphase compared to control cells

HCT116 cells stably expressing mCherry-H2B and KCASH2-GFP or GFP were synchronized at the G1/S transition by thymidine treatment and monitored by time-lapse video microscopy as they transited through mitosis. Down panel: the histogram reports the time in mitosis (measured as the time from NEDB to DNA condensation) spent by control and KCASH2 overexpressing cells.

6. Checkpoint ablation restores normal mitotic time in KCASH2-overexpressing cells

Once assessed that KCASH2 overexpression affects the normal cell cycle progression, causing a longer metaphase-anaphase transition, we aimed to verify that KCASH2 effect depends on its role on MAD2 degradation.

To demonstrate the checkpoint dependency on KCASH2-mediated mitotic exit delay, we used Reversine. It is a potent ATP-competitive inhibitor of human MPS1, which interfering with the recruitment of checkpoint proteins to unattached kinetochores, overrides mitotic arrest (Santaguida et al., 2010; Hiruma et al., 2016).

We performed again time-lapse cell imaging experiments in HCT116 m-CherryH2B- GFP/KCASH2-GFP, following thymidine synchronization and release in fresh medium adding reversine. As expected (**figure 38**), the mitotic time of control cells decreased, given the loss of checkpoint–mediated mitotic arrest (Santaguida et al., 2010; Lan and Cleveland, 2010). Most importantly, KCASH2-overexpressing cells behave like control cells, showing shorter division times, demonstrating that loss of the checkpoint overrides the effects of KCASH2, which must depend on the checkpoint.

Further experiments confirmed this data in the hTERT RPE-1 model: synchronized cells in late G2 phase with RO-3306 were release in fresh medium in the presence of reversine. Again, we observed, by FACS analysis, that the G2/M cell percentage in KCASH2-overexpressing cells becomes similar to that of control cells (**figure 39**).

Taken together, these results indicate that the mitotic delay mediated by KCASH2 is checkpoint-dependent, and so, most likely, MAD2-dependent.

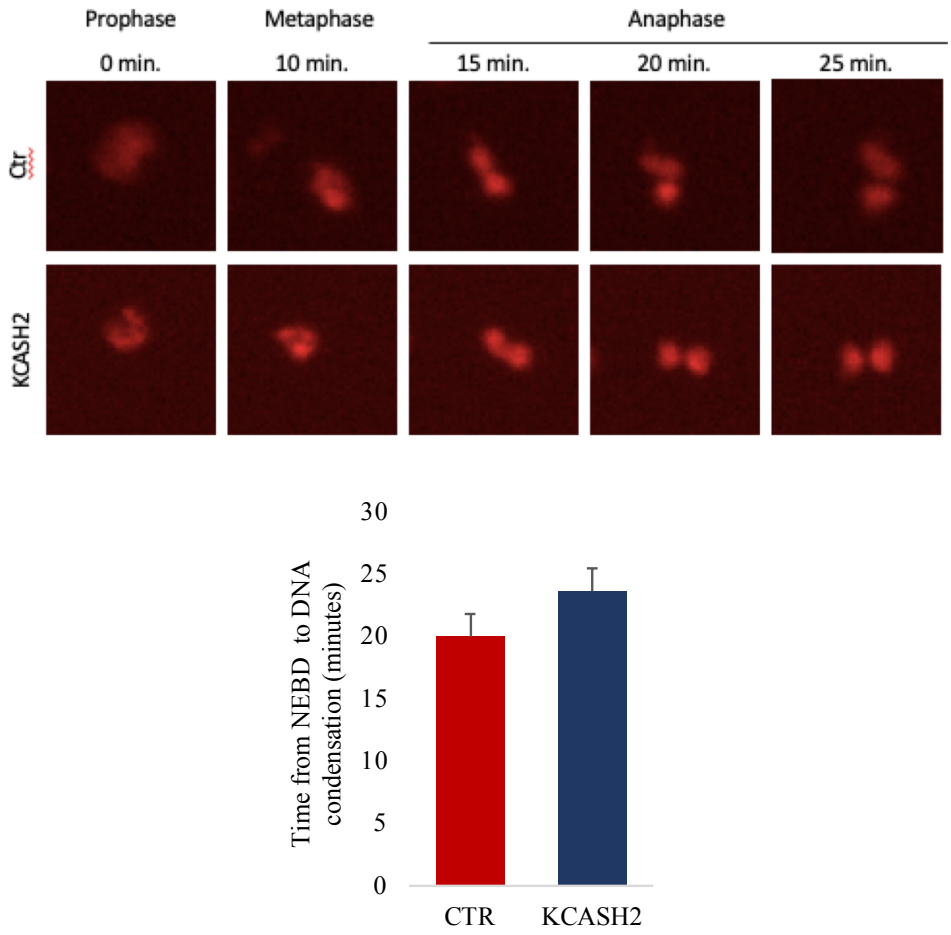

Figure 38. Checkpoint ablation restores normal mitotic time in KCASH2-overexpressing cells

HCT116 cells stably expressing mCherry-H2B and KCASH2-GFP or GFP were synchronized at the G1/S transition by thymidine treatment, released in reversine and monitored by time-lapse video microscopy as they transited through mitosis. Down panel: the histogram reports the time in mitosis (measured as the time from NEDB to DNA condensation) spent by control and KCASH2 overexpressing cells.

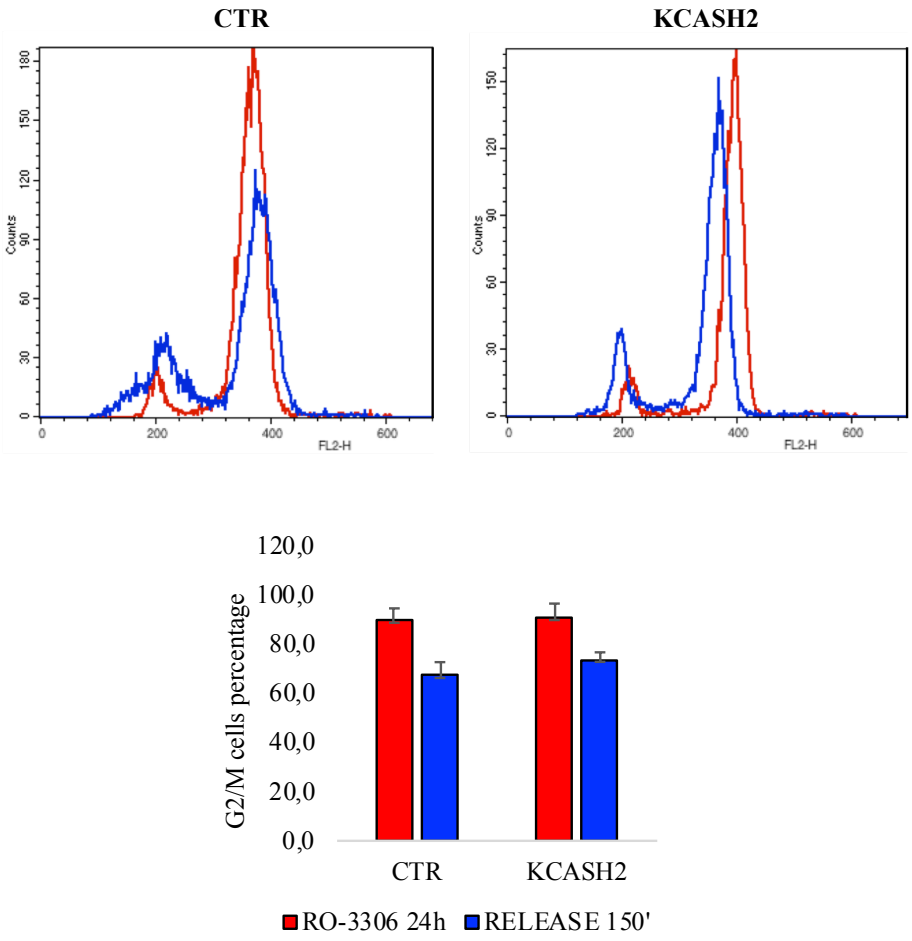

Figure 39. The mitotic delay due to KCASH2 overexpression is checkpoint-dependent

Transduced hTERT immortalized RPE-1 cells with lentivirus expressing KCASH2-GFP or GFP alone were treated with RO-3306 for 24 hours to enrich for G2 cells population. Cells were then released in fresh medium adding reversine at different time points and analyzed.

Up panel: FACS analysis. It was represented a single time point (150') of released control and KCASH2-overexpressing cells. Down panel: The histogram reports G2/M cells percentage.

In red: cells collected following 24hours of RO3306 treatment and analyzed. In blue: cells released in medium adding reversine for 150' from RO3306 block, collected and analyzed.

7. KCASH2 overexpression alters cell cycle inducing mitotic defects

We finally addressed whether delayed metaphase exit and low MAD2 protein levels compromise mitotic fidelity in KCASH2-overexpressing cells, generating chromosomal aberration such as anaphase bridge, micronuclei and chromosome lagging defects.
Live cell microscopy was performed in HCT116 m-CherryH2B- GFP/KCASH2-GFP, following thymidine synchronization and release in fresh medium. Interestingly, KCASH2-overexpressing cells showed a two-fold higher percentage of all three mitotic defects, compared to control cells (**figure 40**).

All together, our data suggested that KCASH2 overexpression, affecting MAD2 protein levels, alters SAC formation during cell cycle, promoting mitotic defects that may give rise to chromosomal aberration and aneuploidy.
Highlighting the potential biological relevance of KCASH2 in this context, it is notable that cancer cell lines expressing either abnormally low and abnormally high levels of MAD2 display a defective mitotic checkpoint concomitant with CIN (Percy et al., 2000; Sotillo et al., 2007).

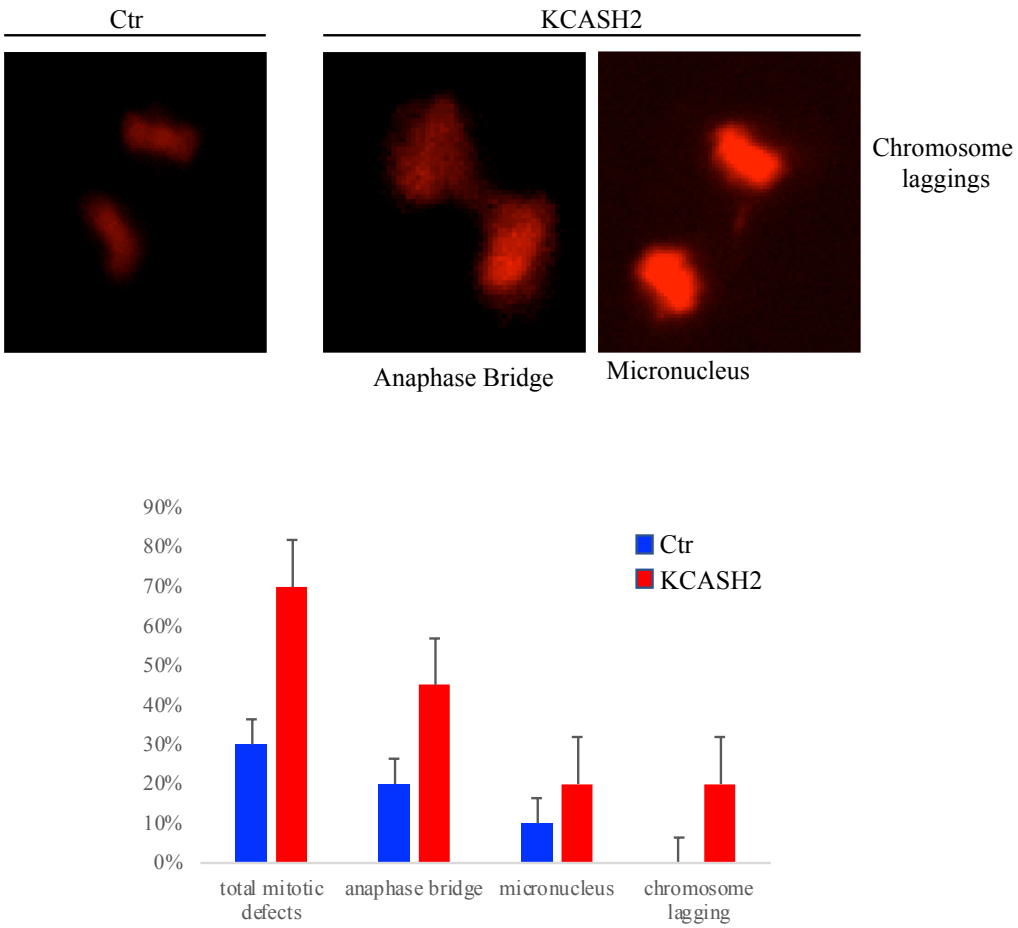

Figure 40. The delay due to KCASH2 overexpression is checkpoint-dependent

Transduced HCT116 cells stably expressing mCherry-H2B and KCASH2-GFP or GFP were synchronized at the G1/S transition by thymidine treatment and monitored by time-lapse video microscopy as they transited through mitosis. Cells were filmed every 10 min for 24 hours to capture mitotic mis-segregation events, shown in upper panel. Down panel: mitotic defects cell percentage. In red control cells, in blue KCASH2-overexpressing cells.

8. Discussion

In order to search for new KCASH2 putative protein interactors, through MS analysis, we have identified MAD2, a core spindle checkpoint protein.
MAD2 has been demonstrated to act in a dynamic complex with other proteins as a molecular switch that monitors proper chromosome attachment to spindle microtubules during cell division, and the correct function of MAD2 and the spindle assembly checkpoint (SAC) are essential for faithful replicative cell division, the prevention of chromosomal abnormalities and the development of cancer. Anyway, the mechanisms regulating MAD2 degradation were not known.

We have demonstrated here the role of KCASH2 in the first E3-ubiquitine ligase complex involved in MAD2 protein stability regulation.
So far, only non-canonical roles for ubiquitination in MAD2 regulation have been described: USP44 or SMURF2 mediate the PTM, increasing MAD2 protein stability (Nilsson et al., 2008; Ge et al., 2009; Osmundson et al., 2009). Our findings unveil the presence of both degradative and non-degradative ubiquitination events that regulates mitotic progression.
Although our results demonstrate unequivocally that KCASH2 may modulate MAD2 levels, the explanation of the biological effects of KCASH2 overexpression and MAD2 degradation on cell cycle and spindle checkpoint is more complex.
Indeed, we have verified the consequences of KCASH2 expression (and MAD2 degradation) in cell cycle progression, monitoring mitotic cells by time-lapse microscopy and FACS analysis, and we observed a high percentage of KCASH2-overexpressing cells that delayed the mitotic exit, stalling in metaphase and completing the process of cell division in a very long time compared control cells.
This result may appear controversial, since other groups have previously demonstrated that MAD2 depletion not only prevents cells from arresting in response to the presence of misoriented chromosome, but also accelerates mitosis dramatically in cells in which chromosome segregation is proceeding normally (Howell et al., 2004; Michel et al., 2004).
It could be hypothesized that KCASH2 modulate mitosis through a not yet identified mechanism, independent of the SAC and of MAD2 regulation. On the other side, ablating the mitotic checkpoint with reversine, we have verified that the delay in mitotic exit mediated by KCASH2 overexpression is reversed, was due to MAD2 protein degradation and not to other side effects. Ablating checkpoint formation with reversine, implying that KCASH2 action is through a modulation of the checkpoint, most likely due to the effect on MAD2 protein. Moreover, KCASH2 overexpression alters cell cycle inducing mitotic defects, such as chromosome lagging, micronuclei, anaphase bridges.

Furthermore, recently a research group has described a role of PTEN in regulating chromosome segregation to prevent genomic instability via positive regulation of MAD2. PTEN knockdown resulted in MAD2 degradation, inducing cell cycle arrest and abnormal chromosome segregation, which manifested as the formation of anaphase bridges, lagging chromosomes and premature chromatid separation (Sun et al., 2019). Although the authors did not explore the mechanism underlying the regulation of MAD2 degradation mediated by PTEN, they observed that low MAD2 protein levels could be associated with a delayed mitotic exit.

Similarly, Das and colleagues (2014) showed the effect of Withaferin A (WA) on cell cycle regulation of colorectal cancer cell lines HCT116 and SW480 and its effect on cell fate. Treatment of these cells with this compound caused the G2/M arrest in both the cell lines, blocking SAC function by proteasomal degradation of MAD2 and CDC20.

It is probably that the effect on cell cycle due to KCASH2 overexpression, as PTEN knockdown, could be different from a *MAD2* gene depletion that impairs the SAC maintaining at all regulation levels. Perhaps KCASH2 acts on MAD2 at a particular stage of cell cycle and MCC formation or disassembly, limiting availability of C-MAD2 protein during SAC activation or when the latter is already satisfied.

Interestingly, KCASH2 preferentially binds and downregulates the closed and active conformation (C-MAD2). This observation allows us to hypothesize a KCASH2 involvement during MCC assembly or disassembly, probably when MAD2 is not implicated in binding with other checkpoint proteins, since KCASH2 still interacts with the mutant MAD2R133A, enable to dimerize with other SAC components. It could be possible that KCASH2 acts on C-MAD2 when it is necessary to disassemble MCC and convert the closed form into the open one, regulating MAD2 during the SAC to catalyze the conversion of the active conformer of MAD2 back to inactive conformer, an energetically costly process. It could be more efficient for the cell to simply bypass this thermodynamic problem through rapid ubiquitin-dependent degradation of the inhibitory MAD2 conformer once the spindle checkpoint has been satisfied, allowing for swift and decisive anaphase onset.

Moreover, Schibler and colleagues (2016) have demonstrated that the only closed MAD2 conformation is capable of binding methylated H3K4 and this interaction regulates resolution of the SAC by limiting closed MAD2 availability for CDC20 inhibition, paralleling $p31^{comet}$ mechanism in SAC silencing. This mechanism could flank with our model in which KCASH2 is able to bind and negatively regulate the C-MAD2 conformation, acting a surveillance mechanism through balance between the conformational MAD2 state and the cellular conditions as checkpoint status. In this way, KCASH2 could cooperate with $p31^{Comet}$ that, together with TRIP13, promotes MCC disassembling:

the ubiquitin-dependent degradation of the inhibitory MAD2 conformer, once the spindle checkpoint has been satisfied, could be the most efficient mechanism for the cell to bypass this thermodynamic problem, allowing for swift and decisive anaphase onset.

Although there are several evidences that MAD2-depleted cells override mitotic arrest, our data described a different outcome on cell cycle progression in cells in which KCASH2 overexpression leads to a MAD2 degradation. The MAD2 levels are crucial during MCC assembly and SAC functions: an unbalance of its levels impairs genome stability and leads to aneuploidy, hallmark of several tumor types.

Several cancer cell lines expressing low or high levels of MAD2 display a defective mitotic checkpoint concomitant with aneuploidy and then CIN (Sotillo et al., 2007; Percy et al., 2000).

In future work, we plan to verify if the observed mitotic defects and prolonged time division due to KCASH2 overexpressing are correlated with aberrant chromosome copy numbers, through single cell sequencing approach, definitely demonstrating that KCASH2 overexpression leads to aneuploidy and genomic instability.

Furthermore, we are performing Co-IP assays to investigate if KCASH2 interferes or promotes the MAD2 binding with the other mitotic checkpoint proteins during different cell cycle stages, since MCC-like protein complexes have been reported in either interphase cells or in the absence of kinetochores. In fact, in either situation there is a fraction of endogenous MAD2 existing in C-conformation due to the interconversion between the two MAD2 conformers (Fava L.L. et al., 2011), therefore a low level of MCC still forms.

Moreover, we plan to better characterize the exact moment and localization of KCASH2-MAD2 interaction during SAC activation and MCC formation. For this purpose, we have tested any available commercial antibody and we also have generated our own antibody against KCASH2, but we have verified that none of them can be used for immunofluorescence experiments.

Therefore, we are performing a knock-in experiment in order to generate an endogenous-tagged *KCASH2* gene, in HCT116 and hTERT RPE-1 cell lines, using the genome editing technique CRISPR-CAS9. This would allow us to study the co-localization throughout the cell cycle of the two endogenous proteins and assess their interaction on centrosome or the kinetochore/centromere structure to define space-temporally the KCASH2 involvement on cell cycle regulation, through its control over the MAD2 protein stability.

On and off switching of the mitotic checkpoint must be fast and definitive because either a weak checkpoint or an asynchronous metaphase-to-anaphase transition leads to irreversible mis-segregation of one or more chromosomes. Indeed, tumorigenesis is frequently associated with genetic

and epigenetic alterations of key cell cycle modulators, targeting entry into cell cycle, G1/S transition and G2/M checkpoint control. Chromosomal instability and aneuploidy are a widespread feature of human cancers: approximately 90% of solid tumors harbor whole chromosome gains and/or losses (Gordon et al., 2012), including non-small-cell lung cancers (NSCLCs), breast tumors, colorectal tumors and prostate tumors deviate from a diploid karyotype (Sansregret and Swanton, 2017).

DNA ploidy is also a prognostic factor in medulloblastoma patients, affecting the tumor severity and clinical outcome. Aneuploidy is driven by alterations in mitotic spindle formation: SAC genes are deregulated at mRNA and protein level in a large number of tumors (Joglekar A.P., 2016), suggesting potential alterations of epigenetic, transcriptional and post-transcriptional regulation. In particular, MAD2 protein levels have been found either aberrantly elevated or reduced in a wide range of tumors, underlying that its fine-tuned regulation is necessary to the correct segregation of chromosomes, thus preventing aneuploidy.

We have several indications that KCASH2 overexpression, affecting the MAD2 protein levels, may lead to aneuploidy.

The research of the last decade is focused on clarifying if aneuploidy is a pro-tumorigenic event, as universally considered since T. Boveri suggested that an abnormal chromosome number causes tumorigenesis, or rather it is a cancer consequence. It is known that cancer cells almost invariably display a combination of numerical (aneuploidy) and structural aberrations (translocations, deletions), as well as the aneuploidy has been well documented to be detrimental to overall organismal development and cell fitness in virtually every species studied. However, the relationship between aneuploidy and cancer is complex and much debated. Studies on yeast strains, murine and human cells have shown that aneuploidy is generally disadvantageous for cells and there are ample evidences of the negative effect of aneuploidy on the fitness of nonmalignant cells, starting with the necessity of aneuploid cells to modulate their metabolic and transcriptional programs to improve their fitness (Simonetti et al., 2019). However, the genetic determinants of the pro-tumorigenic or antitumorigenic effects of aneuploidy and their interplay with the biology of the origin cell remain unclear.

Increasing KCASH2 expression or KASH2 protein levels could be a therapeutic approach since aneuploidy can create vulnerability to specific conditions. The discovery of a mechanism able to modulate MAD2 protein levels or conformation and, indirectly, SAC checkpoint functionality and cell cycle progression may have important implications both in therapeutic interventions directed to the reconstitution of a normal SAC function and in that approaches aiming to increase chromosomal instability to a level not sustainable by tumor cells, leading to their elimination.

THIRD SECTION: Study of the transcriptional regulation of KCASH2

1. Analysis of proximal KCASH2 promoter

Loss of *KCASH2* expression is a crucial event in SHh-dependent MB tumorigenesis. After the identification of KCTD15 as a modulator of KCASH2 protein levels, we aimed to elucidate the *KCASH2* transcriptional regulation, identifying mechanisms and factors that could modulate *KCASH2* expression.

To this end, we started our study analyzing the proximal *KCASH2* promoter sequence, through Genomatix software. We have analized a 974 bp region Human of *KCASH2* promoter that ends 100 bp downstream to the transcription start site (TSS) (**figure 41**). Using the Clustal Multiple Software, we have compared the human and mouse promoter sequences: the high homology (~80%), especially near the TSS, suggests a conserved regulation mechanism that allows *KCASH2* to carry out its functions (**figure 41**).

To study *in vitro* the basal transcriptional activity of the proximal KCASH2 promoter, and the effects on it of expression/suppression of different transcription factors, we cloned the human sequence of *KCASH2* proximal promoter into a luciferase vector (pGL4.10 [luc2]), upstream the report.
To better understand the regulation of *KCASH2* promoter, we used as cellular models different cell lines: immortalized non-tumor HEK293T, SHh-dependent MB DAOY cells, colorectal cancer HCT116. The latest have been chosen since analysis of public available datasets highlights a lower *KCASH2* expression in colon cancer tumor samples compared to normal tissues (R2 software; dataset from Smith et al., 2010; **figure 42**).
We have co-transfected the luciferase construct together with a renilla constitutive reporter (for normalization purposes) in the different cell lines and evaluated the basal activity of the *KCASH2* promoter through luciferase assays (**figure 43**). Compared to the control (the promoterless luciferase reporter pGL4.10 [luc2]), *KCASH2* promoter shows a basal activity in all cell line, recording the highest value in HEK293T cells (22,6 folds the promoterless reporter) and lower values in HCT116 (3,82 folds) and DAOY (11,8 folds) tumor cells. These data confirmed the hypothesis that KCASH2 undergoes negative transcriptional modulation or epigenetic events that are responsible for its low expression in tumor cells.

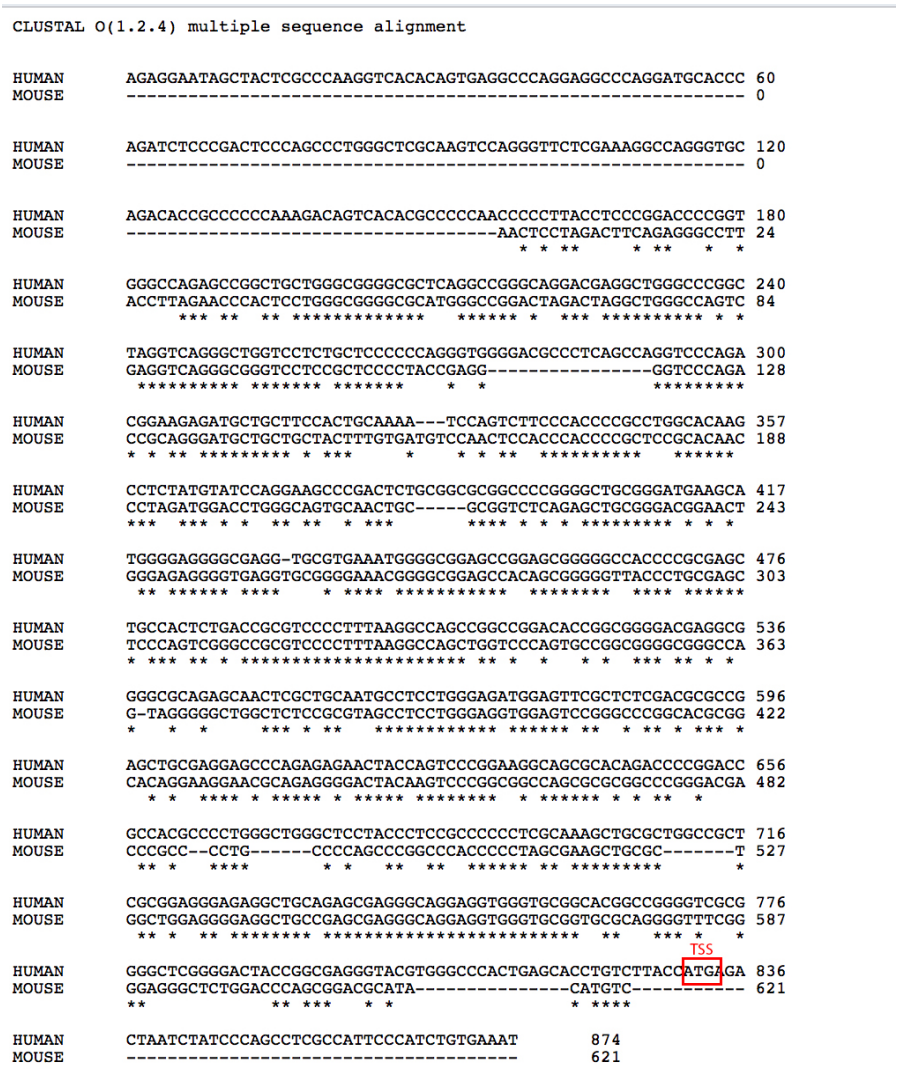

Figure 41. The KCASH2 proximal promoter sequence

Alignment of sequences of KCASH2 human and murine proximal promoter. *conserved site; TSS is highlighted in red. (CLUSTAL multiple sequence alignment by MUSCLE program).

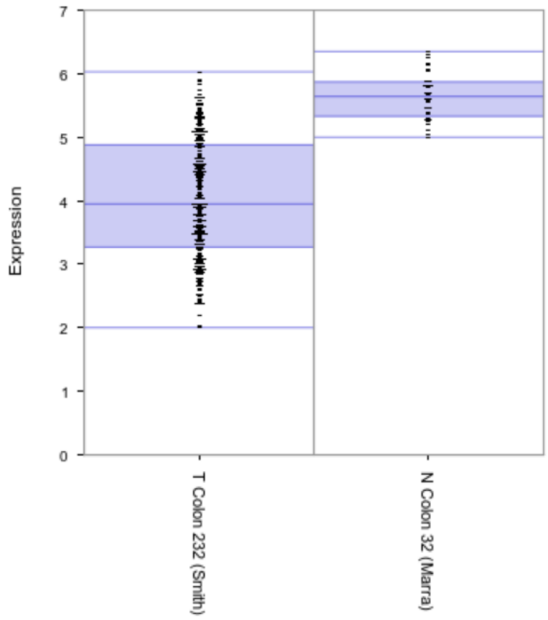

Figure 42. Colorectal cancers present KCASH2 reduced expression

Correlation analysis performed on a larger group of samples in publicly available database (R2 software; Smith et al., 2010)

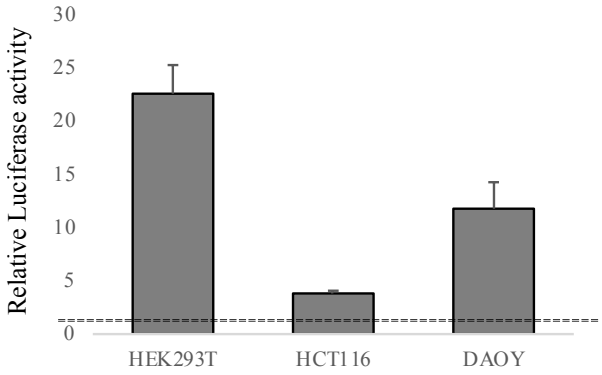

Figure 43. The basal KCASH2 proximal promoter activity in different cell lines

HEK293T, HCT116 and DAOY cells were co-transfected with promoKCASH2pGL4.10[luc] and pRL-TK Renilla (as a normalizer). *$p<0.05$ versus control.

2. SP1: the putative transcription factor involved in *KCASH2* regulation. Who is it?

To identify putative transcription factors involved in *KCASH2* transcriptional control, we have compared online databases, extrapolated from tumor cell lines of MB, neuroblastoma, leukemia and non-small-cell lung cancers, using Genomatix software. We have identified about 200 putative binding sites for TFs and selected the ones with both a 100% match in the target core sequence and a published validation by ChIP-Seq analysis. One of the most significant TF was SP1, for which we identified seven putative binding sites on the proximal promoter of *KCASH2* indicating a plausible SP1 contribution to our gene regulation (**figure 44**).
Furthermore, six of the seven sites were strongly conserved between the human and murine *KCASH2* proximal promoter (**figure 45;** analysis through Clustal Multiple software): in particular, the second and fifth ones, referred as Sp1-B and Sp1-E, 639bp and 394bp upstream of the TSS, respectively) presented a 100% conservation.

The proximal *KCASH2* promoter is a TATA- and CAAT- less promoter. Recent estimates indicate that the majority of mammalian genes (~80%) lacks a TATA box, including most housekeeping gene (López-Maury et al., 2008).
The absence of TATA and CAAT sequences allows us to hypothesize a promoter regulation driven by GC dinucleotides. Indeed, promoters that lack of TATA/CAAT consensus sequences are often characterized by a high GC content, with one or multiple GC box elements that may represent binding sites for the cellular transcription factor SP1.
The transcription factor Specificity Protein 1 (SP1) was identified as a basal transcription factor, required for the transcription of a large number of housekeeping genes, recruiting the general transcription machinery in the TATA box absence. SP1 was the founding member of the SP transcription factor family, the members of which contain C2H2-type zinc fingers and resemble the larger family of Kruppel-like factors (Black et al., 2001). SP factors may be classified into two groups: SP 1-4 and SP 5-9. While the first group factors preferentially bind GC boxes, the second one recognizes CACCC boxes (**figure 46**). SP1-4 have similar N-terminal transactivation domain characterized by glutamine-rich regions which have adjacent serine/threonine-rich regions. The DNA-binding domains include three highly homologous C2H2-type zinc fingers, which preferentially bind to the same GC consensus site. In contrast to the other SP family members, SP1 contains a C-terminal multimerization domain that mediates super-activation of promoter containing multiple adjacent SP sites.

SP1 is a eukaryotic specific factor and the full-length protein is highly conserved among mammalian species. While often described as a general transcription factor, Sp1-dependent transcription is highly regulated throughout development, cellular differentiation and tumorigenesis. Sp1 differentially regulates a large number of key factors that are important in a number of disease states, including cancer. It is overexpressed in a large number of tumors, including breast, gastric, pancreatic, lung, brain (glioma) and thyroid cancers. SP1 expression is known to have a strong correlation with aggressive disease and is considered as a potential negative prognostic factor for survival in some forms of cancer. SP1 overexpression was observed also in MB tumor and it was suggested that SP1 degradation could be a potential strategy for the treatment of this tumor type (Eslin et al., 2013).
Hanahan and Weinberg (2011) have reviewed all the cellular pathway that are essential for tumor formation and cancer progression. These include the major hallmarks of cancer: sustained proliferative signaling, replicative immortality, resistance to cell death, avoidance of immune destruction, induction of angiogenesis, invasion and metastasis, deregulation of cellular energetics. SP1 is critical for the regulation of genes whose products are responsible for each of these hallmarks. In addition, SP1 may influence inflammatory signaling and maintenance of genomic stability (Beishline and Azizkhan-Clifford, 2015).
All these findings make it interesting to explore the role of SP1 in *KCASH2* basal regulation in physiological and tumor contexts.

Interestingly, Mancarelli and colleagues (2010) have demonstrated that SP1 is necessary for the basal activity of *KCASH1* TATA-less promoter. On *KCASH1* promoter sequence there are six binding sites that are recognized by SP1, two of which are located near the TSS. Both KCASH1 and KCASH2 expression is strongly downregulated in sporadic MB, and SP1 contribution to *KCASH1* and *KCASH2* regulation could be a further control mechanism of Hh pathway that requires a fine-tuned balance of components at transcriptional and protein levels. This mechanism could guarantee the *KCASH1* or *KCASH2* basal transcription in all those pathological conditions characterized by one of the two genes lost, for LOH or for epigenetic events not yet characterized, ensuring a control of the pathway.

Figure 44. Identification of seven putative SP1 binding site on *KCASH2* promoter sequence

The sequences of SP1 binding sites on KCASH2 proximal promoter (named from A to G) are depicted in red rectangles. TSS is highlighted in red. (Genomatix software)

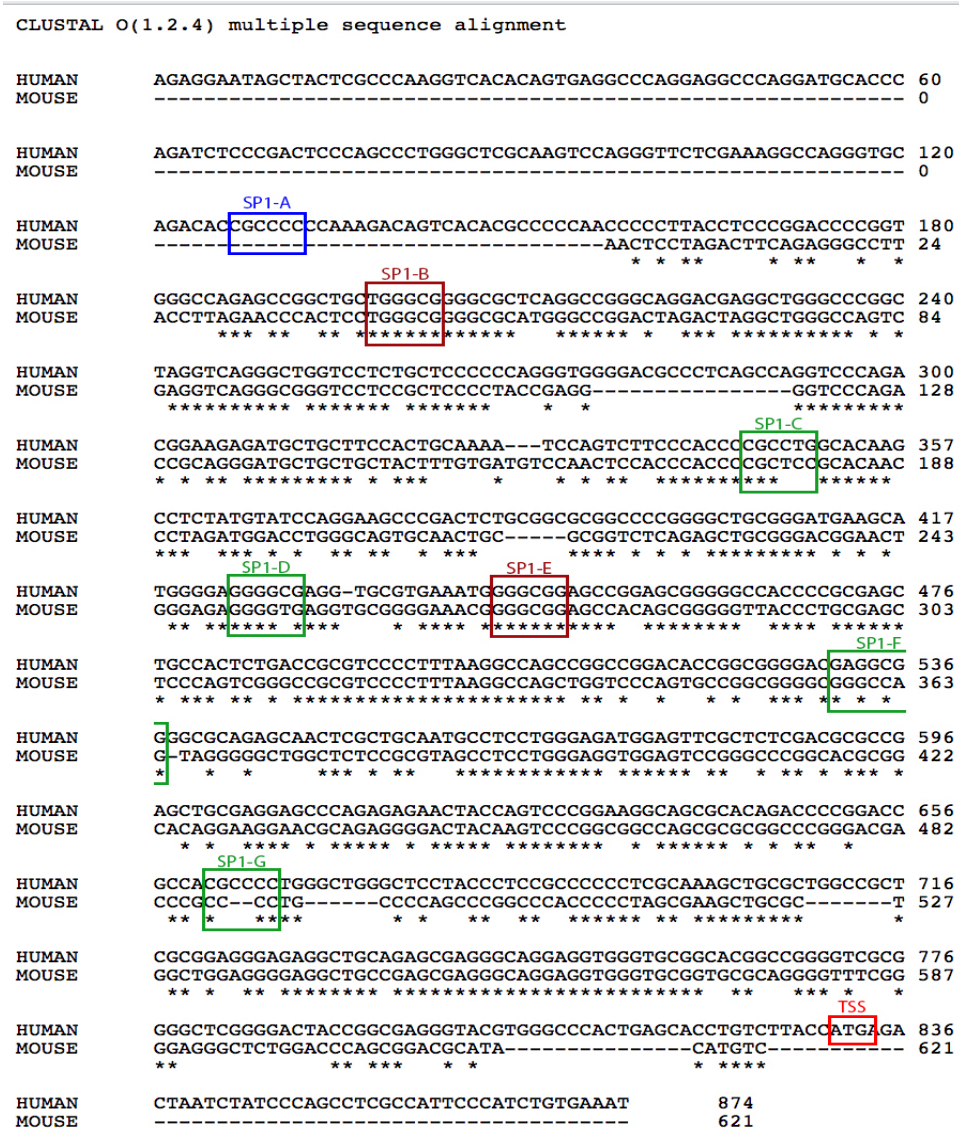

Figure 45. The SP1 binding sites on *KCASH2* promoter are highly conserved

Alignment of *KCASH2* proximal promoter sequence through mouse-human. CLUSTAL multiple sequence alignment by MUSCLE program.

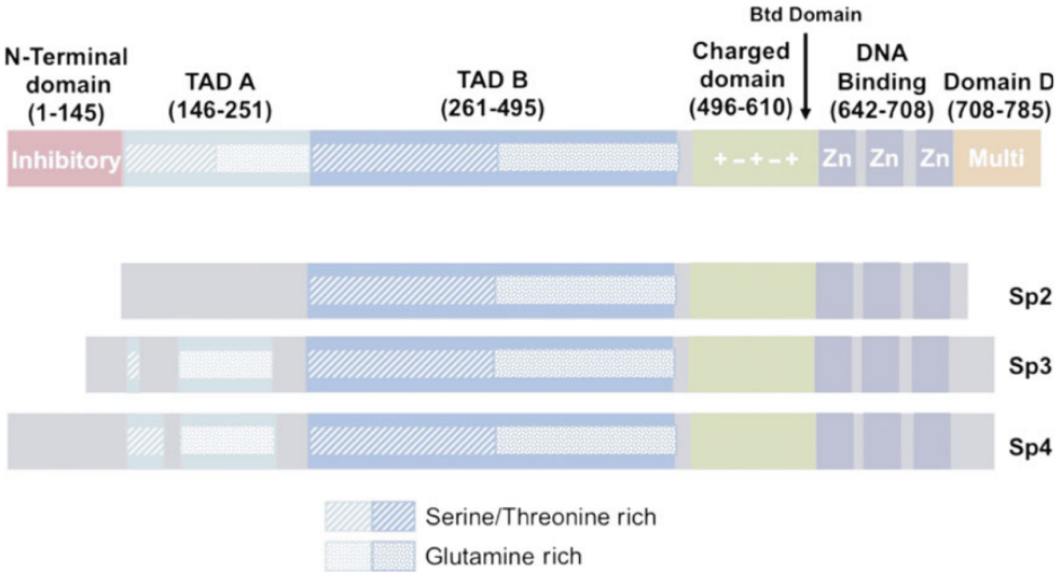

Figure 46. Transcription factor Sp1 and its closest related family members.

SP1 and its four closest family members are grouped together based on their Cys2His2 zinc finger DNA binding domains (purple) and transactivation domains (light and dark blue). The charged domain (green) promotes binding of the zinc fingers to their DNA target. Only SP1 contains a multimerization domain (beige) which facilitates interaction between multiple SP1 molecules. The position of the Buttonhead domain (Btd) is indicated. Grey regions lack similarity between proteins.

From Beishline and Azizkhan-Clifford, 2014.

3. SP1 activates basal transcriptional of *KCASH2* promoter in HEK293T cells

In order to understand the SP1 contribution to *KCASH2* transcription, we performed luciferase assay in HEK293T cells co-transfected with the *KCASH2* promoter luciferase reporter, in presence of control plasmid or plasmid expressing SP1 (**figure 47A**). As shown, SP1 overexpression significantly increases the *KCASH2* promoter luciferase activity in HEK293T.

To confirm this data, we treated HEK293T cells for 24 hours with different dosages (50-100-200-500 nM) of Mithramycin A (MTM), a gene selective SP1-inhibitor that binds to GC-rich DNA, displacing SP1 activity. The Western Blot of protein lysates shows a decrease of KCASH2 levels with increasing drug concentration, confirming the SP1 property to positively regulate the *KCASH2* transcription (**figure 47B**). Similarly, prolonged exposure times (24-48-72 hours) to MTM treatment (100nM) negatively affect KCASH2 mRNA levels (**figure 47C**).

Finally, we assessed the *in vivo* relevance of SP1-mediated regulation of *KCASH2* gene, performing ChIP-qPCR experiment for SP1 on HEK293T cells. We analyzed also the acetylation levels of K16 lysine of histone H4 (acH4K16) that is an epigenetic marker of transcriptional activation. As shown in **figure 47D (left panel),** SP1 binds strongly to *KCASH2* promoter in HEK293T, confirming that SP1 plays a pivotal role in regulating *KCASH2* gene expression, *in vivo*. Therefore, we demonstrated that the binding of acetylated-Histone4 to *KCASH2* promoter increases (**figure 47D, right panel**).

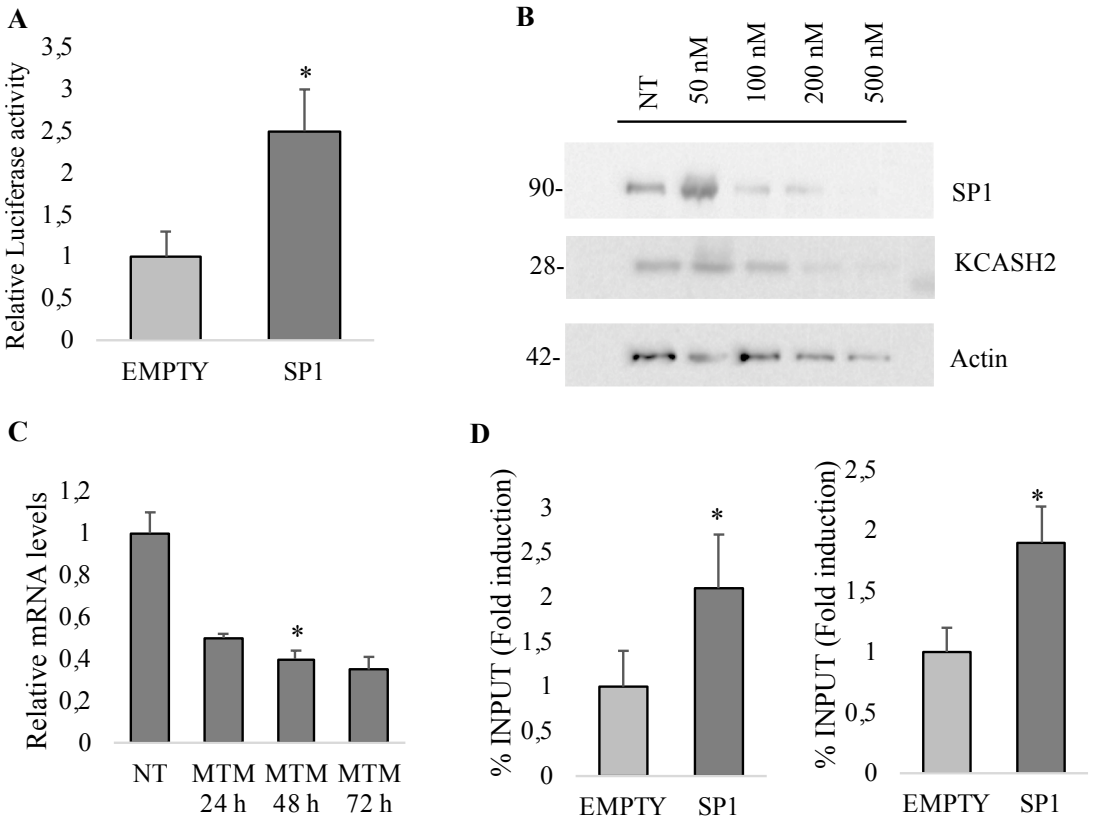

Figure 47. SP1 activates basal transcriptional of KCASH2 promoter in HEK293T cells

A) SP1 overexpression increases the KCASH2 promoter luciferase activity in HEK293T cells. HEK293T cells were co-transfected with empty luciferase vector or promoKCASH2pGL4.10[luc] and pRL-TK Renilla (as a normalizer). *p<0.05 versus control.

B) MTM treatment leads to a dose-dependent KCASH2 protein levels decrease. HEK293T cells were treated with increasing concentrations of MTM (gene selective SP1-inhibitor) and protein lysates were loaded and separated on SDS/PAGE. KCASH2 and SP1 were detected by respective antibodies. Actin was used as a loading control.

C) Prolonged exposure times to MTM treatment (200nM) negatively affect KCASH2 mRNA levels. Following MTM treatment at different time points (24-48-72h), KCASH2 mRNA levels were analyzed by Q-RT-PCR and normalized to the control (Ctr). *p<0.05 versus Ctr.

D) SP1 binds strongly to KCASH2 promoter in HEK293T. HEK293T cells were co-transfected with equal amounts of SP1 or empty vector. Crossed-linked chromatin was extracted and immunoprecipitated with anti-SP1 antibody (left panel) or AcH4K16 (right panel). Immunoprecipitated chromatin samples were analyzed by qPCR using KCASH2 promoter selective primers. Percentage of input was calculated by delta Ct analysis and it expressed as fold induction of SP1 transfection versus empty. *p<0.05 versus control.

4. SP1 negatively regulates *KCASH2* promoter in MB and colon cancer cells

In contrast with our results indicating a positive regulation of KCASH2 mediated by SP1, SP1 expression if generally found to be higher in most tumor types than the in non-tumor counterpart tissues, and a high SP1 expression in tumors is considered a negative prognostic factor for patient survival or correlated with a higher grade of malignancy (Maurer et al., 2007; Jiang et al., 2008; Lee et al., 2013). On the other side, *KCASH2* expression is reduced in a wide range of tumor types, related or not to Hh signaling deregulation.

Since SP1 is able to enhance or repress promoter activity, depending on which promoter it bind and the coregulators with whom they interact (Kaczynski et al, 2003; Fang et al., 2014), through R2 software, we looked for a correlation between KCASH2 and SP1 expression in publicly database of MB (Cavalli et al., 2017). As shown in **figure 48A**, there is a negative correlation between the expression of the two genes.

Therefore, we have evaluated in the SP1 contribution to *KCASH2* expression through luciferase assays in tumor cells.. In DAOY MB cell line, we observed a reduction of *KCASH2* expression following transfection with SP1 (**figure 48B**).

Similarly, we investigated the SP1 role in *KCASH2* regulation in HCT116 cell line. Luciferase assays highlight that SP1 overexpression in HCT116 cells is responsible of a decrease in *KCASH2* luciferase activity (**figure 48C**). To confirm this latter data, we treated HCT116 cells with MTM. We observe an increase of KCASH2 mRNA levels after 24h and 48h following drug exposition (**figure 48D**).

This data confirmed the hypothesis that SP1 may play a different regulatory role for *KCASH2* expression in normal and tumoral cellular contexts.

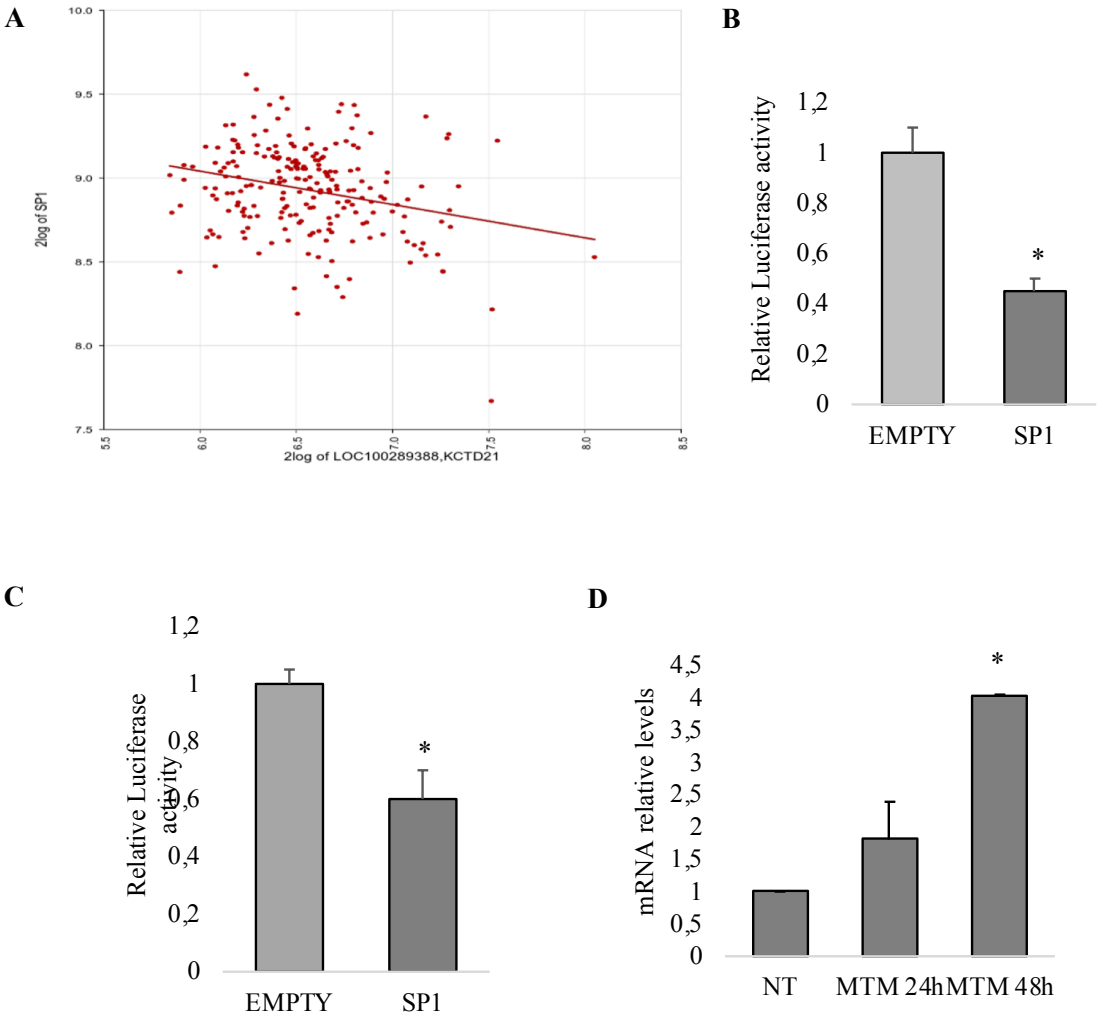

Figure 48. SP1 negatively regulates *KCASH2* transcription in DAOY and HCT116 cells

A) Negative correlation was observed (r: -0,204; p= 1.24e-08) between SP1 and KCASH2 expression analysis in human MB. R2 software, Cavalli et al., 2017.

B) SP1 overexpression decreases the KCASH2 promoter luciferase activity in DAOY cells. DAOY cells were co-transfected with empty luciferase vector or promoKCASH2pGL4.10[luc] and pRL-TK Renilla (as a normalizer). *p<0.05 versus control.

C) SP1 overexpression decreases the KCASH2 promoter luciferase activity in HCT116 cells. HCT116 cells were co-transfected with empty luciferase vector or promoKCASH2pGL4.10[luc] and pRL-TK Renilla (as a normalizer). *p<0.05 versus control.

D) Prolonged exposure times to MTM treatment (200nM) negatively affect KCASH2 mRNA levels. Following MTM treatment at different time points (24-48h), KCASH2 mRNA levels were analyzed by Q-RT-PCR and normalized to the control (Ctr). *p<0.05 versus Ctr.

5. SP1 overexpression negatively regulates *KCASH2* and leads to an increase of HCT116 cells proliferation

To assess the biological role of SP1 on tumor proliferation which may be mediated by *KCASH2* regulation, we abolished KCASH2 expression by transducing HCT116 cells with lentiviral particles expressing KCASH2 shRNA. We then transfected shKCASH2 and control cells with empty vector or SP1 encoding vector and we monitored cell proliferation for 42 hours.

As expected, in shKCASH2 HCT116 cells we observed an increase of cell proliferation compared to control cells (HCT116 shCtrl), coherently with the tumor suppressor role of KCASH2 (De Smaele et al., 2011). ShKCASH2 cells have the same proliferative behavior, regardless of SP1 expression, indicating that SP1 function in this context is mediated by KCASH2. Instead, SP1 overexpression is responsible of a decrease of cell proliferation in control cells (**figure 49**).

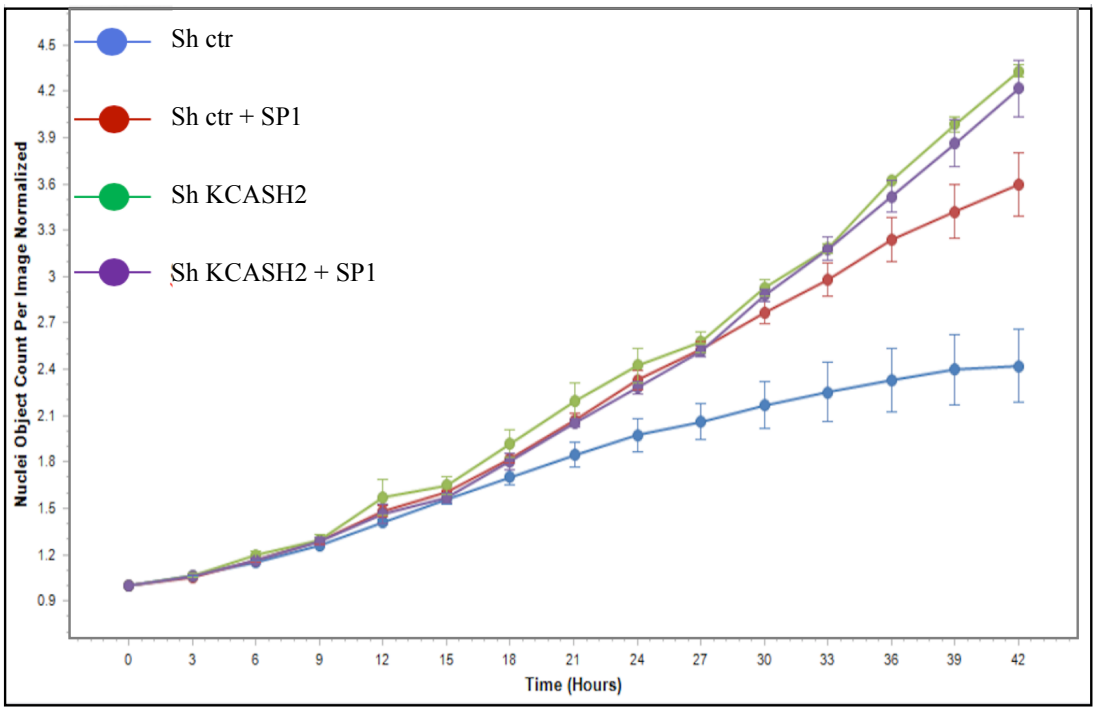

Figure 49. SP1 overexpression leads to an increase of HCT116 cells proliferation

SP1 overexpression, negatively regulating KCASH2, leads to an increase of cell proliferation. Transduced HCT116 cells with lentivirus expressing control and KCASH2 shRNA were co-transfected with vectors encoding SP1 or control and monitored cell proliferation for 42 hours. Proliferation was measured using quantitative kinetic processing metrics from time-lapse image acquisition and showed as percentage of culture confluence over time.

6. The seven SP1 binding sites contribute differently to the modulation of KCASH2 proximal promoter activity

SP1 is able to regulate genes whose promoter sequence has only one binding site for the TF.
Since we have observed two different regulation mechanisms of *KCASH2* transcription mediated by SP1 in tumor and non-tumor contexts, we hypothesized that the seven SP1 binding sites present on the *KCASH2* proximal promoter sequence contribute differently to the regulation of our gene.
To validate this hypothesis, we generated seven luciferase reporter constructs driven by the sequence of the *KCASH2* promoter, each carrying a mutation of one of the SP1 binding sites core sequence, and we assessed their basal luciferase activity in HEK293T (**figure 50**). Mutation of the fourth SP1 binding site mutant (referred as D) induces a significant increase of *KCASH2* promoter activity, indicating that this site could be mostly involved in negative regulation. The other sites, instead, seem to contribute differently to promote positively *KCASH2* transcription: in particular, mutation of the sites named B-C-F display an almost total abatement of *KCASH2* activity (**figure 51A**).
We evaluated also the effects of SP1 overexpression on the mutant promoters above indicated (**figure 51B**). Analyzing the assay, we observed that the promoter with mutation of the negative D binding site was not further upregulated by SP1 overexpression, probably since it has reached the plateau of activity. On the other side, the promoters exhibiting mutation of A or G binding sites, before identified as activators ones, maintain the capability, as mutants, to partially respond to SP1 overexpression, allowing us to hypothesize a positive contribution of the remaining sites.
In contrast, mutations of the B, C, E or F sites seems to have a dominant role, as the responsiveness of the promoter to Sp1 is abolished, and basal activity is close to null, suggesting the presence of further regulatory factors acting on or close to the SP1 binding sites. Modulations for site G are not significant.

These data allow us to assert that the second SP1 binding site (-632 to -626 bp upstream of the TSS) is crucial for negative *KCASH2* regulation SP1-mediated in HEK293T. However, the question of possible involvement of other TFs that could have overlapping or very close to SP1 binding site is still open.
Through bioinformatic analysis, we have searched for other putative TFs involved in *KCASH2* regulation whose sequence overlap or are localized closed to SP1 binding site (**figure 52**).
We have identified KLF, GliS3 and EGR TFs that overlap on SP1-A site.
E2F1 binds *KCASH2* promoter at the B-E-F SP1 binding site, the most preserved among evolution.
The SP1-C site is recognized also by EGF and KLF, while the D one only by KLF.

All mentioned TFs have been previously described by other research groups to act synergistically with SP1 regulating, positively or negatively, gene target transcription. Then, it will be necessary to study the involvement of these TFs on *KCASH2* regulation and analyze the relative contribution of single TFs and their combined action with SP1 to understand the *KCASH2* regulation in a deeper and more punctual manner in physio-pathological context.

However, the data produced so far assess SP1 contribution to *KCASH2* expression and represent a good starting point to further analysis.

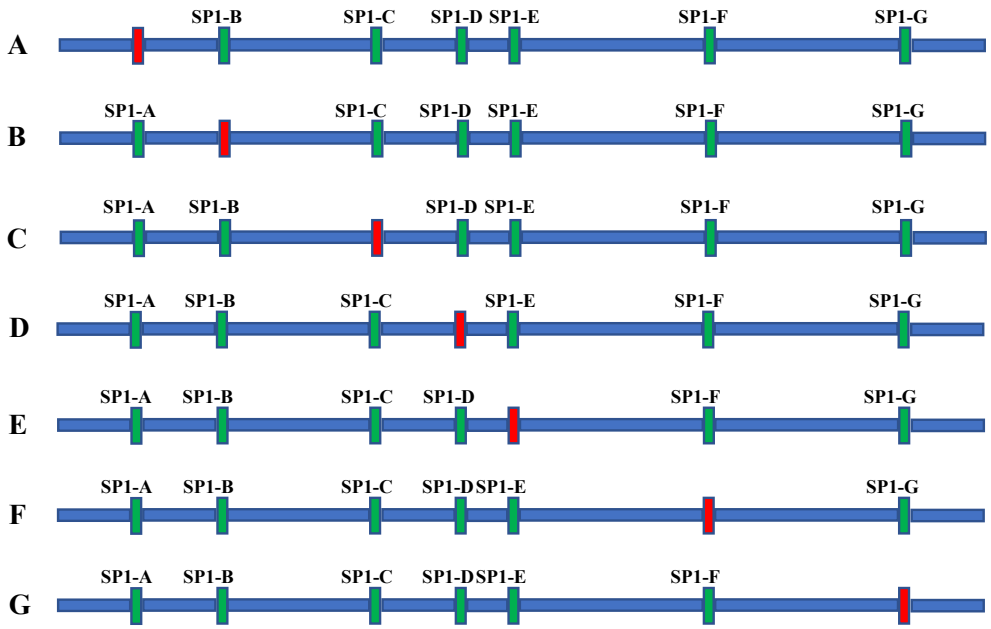

Figure 50. Schematic representation of the seven luciferase reporter constructs driven by the sequence of the *KCASH2* promoter, each carrying a mutation of one of the SP1 binding sites core sequence. Mutated site are shown in red.

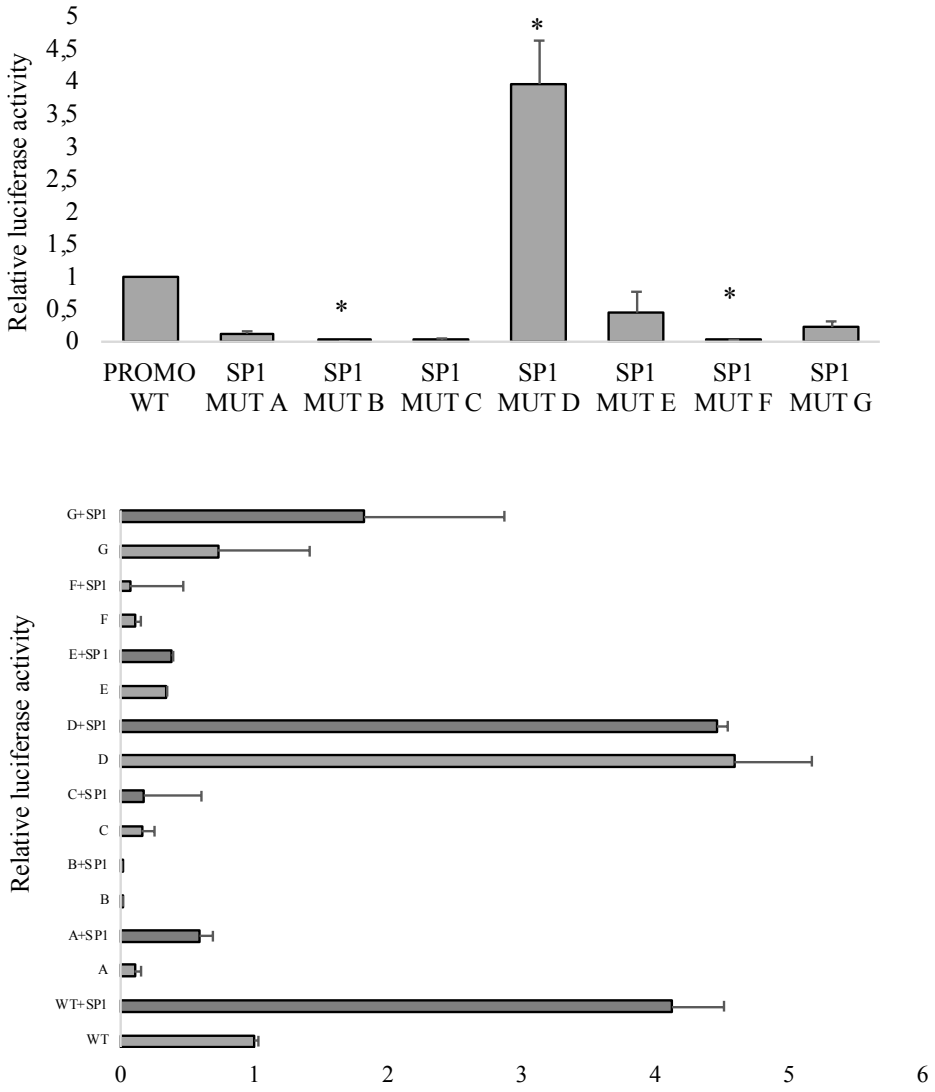

Figure 51. The seven SP1 binding sites contribute differently to the modulation of KCASH2 proximal promoter activity

A) The SP1 binding sites present on the KCASH2 proximal promoter sequence contribute differently to its regulation. HEK293T cells were co-transfected with seven luciferase reporter constructs driven by the sequence of the KCASH2 promoter, each carrying a mutation of one of the SP1 binding sites core sequence, and pRL-TK Renilla (as a normalizer). *$p<0.05$ versus control.

B) Prolonged exposure times to MTM treatment (200nM) negatively affect KCASH2 mRNA levels. Following MTM treatment at different time points (24-48h), KCASH2 mRNA levels were analyzed by Q-RT-PCR and normalized to the control (Ctr). *$p<0.05$ versus Ctr.

Figure 52. Identification of putative transcription factors that bind *KCASH2* promoter whose sequence overlap or are localized closed to SP1 binding site. Genomatix software

7. The use of demethylating agents does not increase the transcriptional activity of the KCASH2 promoter in tumor lines

DNA in somatic tissue is characterized by a bimodal pattern of methylation, which is established in the animal through a series of developmental events which are mainly associated with housekeeping genes. This genomic methylation pattern is broadly maintained during the life of the organism by maintenance methylation, and generally correlates with inhibition of gene expression (Siegfried et al., 1999). The SP-regulated promoters are often associated with GC-rich regions of the genome known as CpG islands, which are important for gene regulation (Macleod et al., 1994).
It was proposed that the balance between DNA methylation and SP1 binding to the promoter could represent a mechanism to regulate the tissue-specific expression pattern of *KCTD11*, since the treatment with demethylating agent increased *KCTD11* expression. It is noteworthy that the chromosomal region 17p13, where *KCTD11* localized, is frequently hypermethylated in cancer. Therefore, the strong down-regulation of KCTD11 in cancers may be due to promoter hypermethylation (Di Marcotullio et al., 2004; Mancarelli et al., 2010).

We wondered to assess if DNA methylation was involved in *KCASH2* regulation, with a mechanism that could flank or balance that one performed by SP1.
Through EMBOSS program (EMBL-EBI), we identified the presence of two putative CpG islands on *KCASH2* proximal promoter, situated to -538bp and -57bp upstream of the TSS (**figure 53A**). We treated HCT116 and DAOY cells with the demetilating agent 5-aza-2'-deoxycytidine (5-Aza) and analyzed by RT-qPCR the KCASH2 mRNA levels. Following 5-Aza treatment, KCASH2 mRNA levels are not upregulated (**figure 53B**), indicating that, in this context, DNA methylation is not involved in *KCASH2* regulation.

However, dedicated studies exploring methylation of 11q chromosome, where *KCASH2* is located, are sparse. It is of particular interest that changes in methylation appears to affect 11q chromosome surprisingly little (Mlakar et al., 2017; Fischer M. et al., 2010) and our data fit well with these observations.

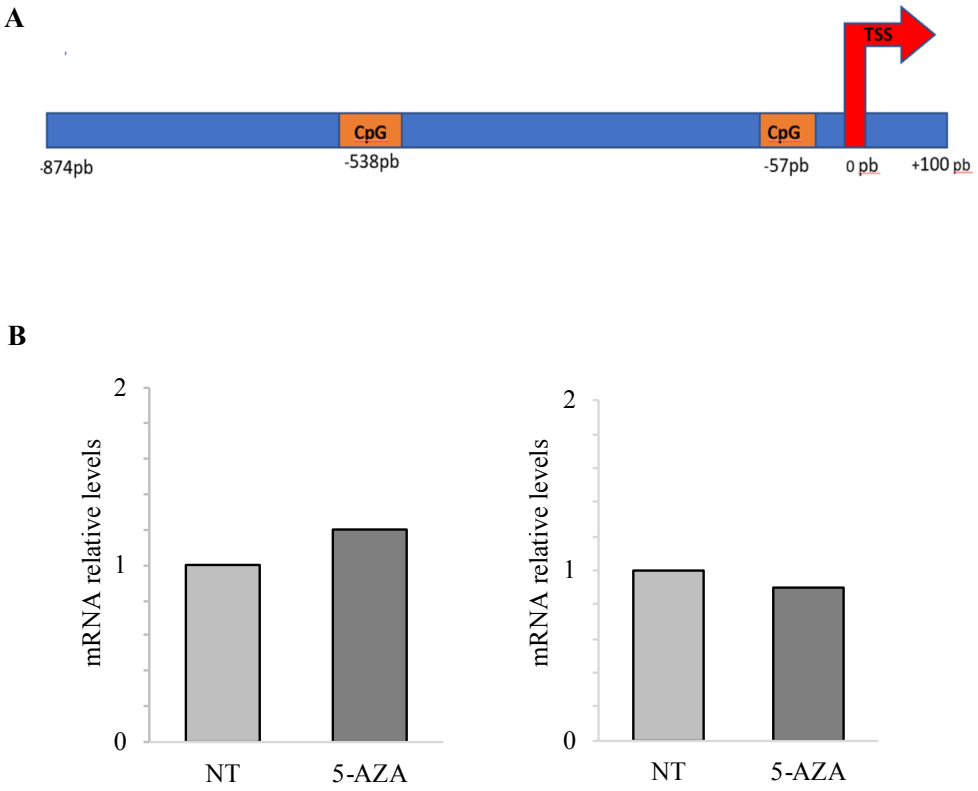

Figure 53: The use of demethylating agents does not increase the transcriptional activity of the KCASH2 promoter in tumor lines

A) Schematic representation of CpG islands on sequence of KCASH2 proximal promoter (EMBOSS program).

B) 5-AZA treatment of HCT116 (left panel) and DAOY (right panel) does not affect KCASH2 mRNA levels. Following 5-AZA treatment, KCASH2 mRNA levels were analyzed by Q-RT-PCR and normalized to the control (NT).

8. Discussion

We have investigated the KCASH2 transcriptional regulation aimed to discover new potential therapeutics mechanisms for all that tumor types in which KCASH2 is low expressed.
We have analyzed its proximal promoter region and performed bioinformatics analyses in order to identify putative transcription factors involved in KCASH2 regulation. Like most mammalian genes, transcription cellular machinery is not engaged on the KCASH2 promoter by TATA/CAAT consensus sequences, but rather by GC dinucleotides, bound by the TF SP1.
The involvement of SP1 perfectly fits into the fine-tuned control of the Hh pathway, since it regulates *KCASH1* (Mancarelli et al., 2010) and, following to our findings, *KCASH2* transcription.

Anyway, mechanisms with which SP1 regulates *KCASH1* and *KCASH2* expression are different: this divergence increases, on one hand, the complexity of the Hh signaling and, on the other one, represents a surveillance mechanism developed to increase the robustness of the signaling, resisting to all perturbations that lead to a decrease of KCASH1 or KCASH2 expression, events that promote tumorigenesis. Indeed, while KCASH1 transcription is the result of a punctual balance between DNA methylation and SP1 positive contribution, we demonstrated that SP1 regulates the KCASH2 promoter differently in tumor and non-tumor contexts. In the latter one, SP1 directly binds KCASH2 promoter and increases its basal KCASH2 transcription.
Otherwise, analyses performed on public database online show that SP1 and KCASH2 negatively correlate in MB tumors. The bland correlation observed may due to the fact that mRNA SP1 levels could be different from its protein levels, since transcriptional SP1 activity occurs largely at its post-translational level. Indeed, Sp1 is highly modified by almost all the common forms of PTMs, including phosphorylation, O-linked glycosylation, acetylation, SUMOylation, and ubiquitylation that affect SP1 activity and its stability, then its function.
In turn, in SHh-dependent MB DAOY cells and colorectal cancer HCT116 cells, SP1 overexpression leads to a decrease of KCASH2 promoter activity, promoting also HCT116 cells proliferation.
Nowadays, there are few data available on the SP1 role in tumorigenesis of both tumor types. In these tumors, data performed on sporadic MB human biopsies and database online of colon cancer show a low *KCASH2* expression compared to normal tissues. The analogous SP1 role in *KCASH2* regulation in two different tumors, in which the same pathways are not the main drivers, allow us to hypothesize that, most likely, in a non-physiological context SP1 undergoes certain PTMs and binds specific proteins, belonging to transcriptional machinery or chromatinic remodeling, that, as a final result, leads to *KCASH2* repression.

Here, we have identified SP1 as a key transcriptional regulator that is involved in *KCASH2* expression modulation in different cancers, on which the attention of several research groups is focused, since it is considered unanimously a hallmark of cancer.
SP1 presents a high expression in a large number of tumors, including MB, and has a strong link with aggressive disease, which makes it a candidate as a potential negative prognostic factor for survival. The highest SP1 expression in tumors correlates with low KCASH2 levels in correlation analysis performed on a large database of human sporadic MB.
KCASH2 proximal promoter sequence present seven highly conserved SP1 binding sites that contribute differently to KCASH2 transcription, perhaps recruiting other TFs that may or may not increase SP1 protein stability or act as co-factors, cooperating with SP1 and regulating KCASH2 expression in a space-time manner. Further data must be produced to evaluate the involvement of other TFs, which we only hypothesized following bioinformatic analysis.

SP1 could be an interesting pharmacological target for all those tumors characterized by a negative correlation between SP1 and KCASH2. In fact, researchers are developing an increasing number of small-molecule anticancer agents that decrease SP1 expression in cancer cells, contributing to efficacy of traditional tumor-specific therapies (Karki et al., 2018). Some SP1 inhibitors have already identified and characterized: one of these, tolfenamic acid (TA), has been proposed as anticancer agent in MB, targeting SP1 (Eslin et al., 2013).
In the future we aim to test *in vitro* and *in vivo*, through xenograft mouse model, the efficacy of the SP1 inhibitors known today in restoring KCASH2 levels in those types of tumor characterized by low expression of the latter.

CONCLUSION

Our research group has identified the KCASH family as a negative regulator of Hh/Gli signaling, acting in concert as native HDAC inhibitors and has demonstrated that their deficiency plays a role in sustaining Hh/Gli mediated tumorigenesis.

The presence of three KCASH members with common functions suggests a redundancy that makes the Hh regulation more solid and fine-tuned. KCASH proteins may act in concert but their role is not identical: these proteins possess a well conserved N-terminal BTB domain but an heterogenous C-terminus, suggesting the presence of peculiar functions or different mechanisms of functional regulation. For example, while KCASH1 and KCASH2 bind directly to HDAC1, KCASH3 requires the formation of heterodimers with KCASH1 (De Smaele et al., 2011), and is the unique member which is able to bind USP21.

This thesis shed light on unknown KCASH2 functions and increases the current knowledge of the biological systems in which it acts, not limited only to Hh signaling control.

Indeed, we observed that KCASH2 expression is reduced not only in Hh-dependent MB, but also in other tumor types not so far directly correlated to Hh signaling deregulation. Of note, chromosome 11q, where it is localized, is lost in several sporadic tumors, including neuroblastoma, leukemia and prostate cancer.

Moreover, the identification of KCASH2 regulation mechanisms are the first step in the development of new therapeutic approaches aimed to physiologically restore KCASH2 levels, preventing aberrant activation of Hh signaling.

Our findings identified two players, KCTD15 and SP1, that act on KCASH2, modulating its protein stability or its basal transcription, respectively. These findings may open the way for new strategies for treatment of Hh dependent tumors, or tumors characterized by low KCASH2 expression. Indeed, both proteins could be potential therapeutic targets for MB treatment, restoring physiological levels of KCASH2 and, consequentially, of downstream effectors.

In turn, a significant percentage of MB is resistant to treatment with SMO inhibitors due to the onset of drug-resistant receptor mutations or to the constitutive activation of Hh signaling downstream of SMO, at the level of the Gli1-3 transcription factors. This event limits the use of SMO inhibitors in MB treatment, highlighting the need to develop new therapeutic strategies acting at the level of Gli1-3.

KCASH2, which act on HDAC1, then downstream of the SMO co-receptor, is therefore a good candidate as alternative therapeutic target. The actual pharmacological HDAC inhibitors (HDACi)

induce cancer cell cycle arrest, differentiation and cell death, reduce angiogenesis and modulate immune response with different mechanisms depending on cancer type (Eckschlager et al., 2017). On the other side, given the wide range of potential HDAC targets, suppression of multiple HDACs in different cell types could lead to unwanted side effects. We hypothesize that a therapeutic strategy based on the restoration of physiological levels of an upstream key component of Hh signaling, like KCASH2, could be promising. Moreover, since KCASH2 acts specifically on HDAC1, the limitation of HDACi not to target selective HDACs could be overcame.
Further promises can be drawn by the observation that some SP1 inhibitors (which in tumors would upregulate KCASH2) have been identified and characterized and one of these, tolfenamic acid (TA), has been already proposed as anticancer agent in MB, although it was still unknown the biological mechanism underling SP1 contribution to MB tumorigenesis (Eslin et al., 2013).

The most exciting novelty is the identification of a novel function of KCASH2, a as a regulator of mitotic process, downregulating MAD2 protein levels. Although all the aspects of KCASH2 role on modulating MAD2 function during cell cycle and mitosis has to be better elucidated, the discovery of KCASH2's role in cell cycle regulation increases also the knowledge of genomic patterns that associate and/or synergize with aneuploid phenotypic profiles in promoting tumors development.
Such knowledge, complemented by the availability of rationally designed targeted agents, that could be SP1 inhibitors or molecules that mimic KCTD15 structure, will serve as a map for personalized synthetic lethal therapeutic strategies against all aneuploid tumors, that represent about 90% of solid tumors and 50% of hematological neoplasms.

The work presented here draw a more complex, although not yet complete, picture of the biological role of KCASH2, unveiling its additional functions as a new putative "guardian" of genomic stability and identifying two novel mechanism of regulation of its expression in KCTD15 and SP1.

MATERIALS AND METHODS

Human Tissue Samples

Human primary MB specimens were collected by surgical resections with the approval of Sapienza University institutional review board. Informed consent was obtained from all subjects. RNAs of normal human cerebella were purchased from Biocat (Heidelberg, Germany), Ambion (Applied Biosystems, Foster City, CA), and BD Biosciences (San Jose, CA).

Cell Culture, transfections and drugs treatment

Medulloblastoma cell line DAOY (ATCC® HTB-186™) was cultured in minimum essential medium (Gibco- Thermo Fisher Scientific, Waltham, MA, USA) supplemented with 10% heat-inactivated fetal bovine serum (FBS), 1% Sodium pyruvate, 1% non-essential amino acid solution, 1% L-glutamine and 1% penicillin/streptomycin. DAOY cells were transfected with Lipofectamine Plus, according to the manufacturer's instructions (Invitrogen- Thermo Fisher Scientific).

HEK293T (ATCC® CRL-3216™), HCT116 (ATCC® CCL-247™), hTERT RPE-1 (ATCC® CRL-4000™) were cultured in Dulbecco Modified Eagle Medium (Gibco) supplemented with 10% FBS, 1% L-glutamine and 1% penicillin/streptomycin. HEK293T and HCT116 cells were transfected with Lipofectamine 2000, according to the manufacturer's instructions (Invitrogen).

RPE-1 hTERT cell line expressing H2B-mCherry was a gift from S. Santaguida (IEO, Milan, IT).

Mycoplasma contamination in cells cultures were routinely screened by using PCR detection kit (Applied Biological Materials, Richmond, BC, Canada).

KCTD15 RNA interference (siRNA) was performed using Silencer® Select Pre-designed siRNA (30nM;94392420, Ambion- Thermo Fisher Scientific), transfected with Lipofectamine 2000 according to the manufacturer's instructions.

Proteasome inhibition was performed with 50 μM MG132 for 4 hours at 37°C.

For cell synchronization experiment, HCT116 cells were incubated with 5 mM thymidine for 24 hours at 37°C, 150 nM nocodazole for 16 hours at 37°C. hTERT RPE-1 were treated with 7.5 μM RO-3306 for 16 hours at 37°C. For both cell lines, reversine was used at a working concentration of 0.5 μM, as indicated in the text.

DAOY and HCT116 cells were treated with 2 μM of 5-Aza-2′-deoxycytidine (100nM) for 24 hours.

SP1 inhibition was performed with Mithramycin A, as indicated in the text.

All compounds were obtained from Sigma-Aldrich. All drugs were aliquoted, stored frozen, and thawed immediately before use.

Luciferase assay

Luciferase and Renilla activity were assayed with a dual-luciferase assay system, following manufacturer's instructions (Promega, Madison, WI, USA). Results are expressed as Luciferase/ Renilla ratios and represent the means ± SD of at least three biological replicates.

Plasmids and mutagenesis

The following vectors, expressing human KCTD15 or KCASHs, with or without tags: pCDNA3.1-KCTD15, pCXN2-KCTD15, pCXN2-Flag-GLI1, pGEX-KCASH2, pCXN2-KCASH2-Flag, pCXN2-BTB-KCASH2-Flag, pCXN2- ΔBTB-KCASH2-Flag were generated in our laboratory with standard cloning techniques and verified by sequencing.

The following plasmids were kindly provided by other laboratories: 12X Gli-Luc (R. Tofgard, Karolinska Institutet, Sweden), pCMV-HDAC1 (P.L. Puri, The Burnham Institute, CA), pCDNA Cul3-myc (M. Pagano, New York University School of Medicine, NY), pBB14 (pEGFP-N1, Brideau AD, 1998), HA-Ubiquitin construct (I. Dikic, Goethe University, Frankfurt, DEU), RSV-Sp1 (F. Zazzaroni, University of L'Aquila, IT), pCMV-Flag-MAD2 (R. Benezra, Addgene plasmid #16047), pRK-SMURF2-Myc (Y. Zhang, Addgene plasmid # 13678).

VSV-G pseudotyped third-generation self-inactivating bicistronic lentiviral vector encoding for EGFP under the control of the human CMV promoter (pTWEEN) was kindly provided by E. De Maria (Catholic University of the Sacred Heart and Gemelli Polyclinic). The pTWEEN plasmid was employed for the generation of pTWEEN- KCASH2-Flag, by cloning the hKCASH2 PCR-amplified CDS. PromoKCASH2 pGL4.10 [luc2] was generated cloning the human proximal promoter KCASH2 sequence PCR-amplified. All constructs were verified by sequencing.

The KCASH2 interference was performed using PLK0.1 plasmid expressing a specific shRNA (Mission shRNA-TRCN0000139768), and ShC002V as a control (SIGMA).

The MAD2-L13A, MAD2-V193N and MAD2R133A mutants were generated using hMAD2 PCR-amplified cDNA, cloned in pCMV-Flag vectors. The promoKCASH2 pGL4.10 [luc2] mutated in individual SP1-binding sites (from A to G) and all together were generated using the human proximal promoter KCASH2 sequence, cloned in pGL4.10 [luc2]. Residues were mutated by the Quickchange single/multi-site mutagenesis kit (Stratagene), according to manufacturer's protocols.

Lentivirus Production and Transduction of Target Cells

Sub confluent HEK293T cells were co-transfected using Calcium/Phosphate precipitation, with lentiviral constructs shKCASH2 and shC002, pTWEEN- KCASH2-Flag and pTWEEN-CTR. Virus titers in supernatants were determined by MOI assay. The HEK293T, HCT116 and hTERT RPE-1

cells were transduced with 1 x10^6 recombinant lentivirus-transducing units plus 8 μg/ml Polybrene for 24h. Cells transduced with lentiviral constructs shKCASH2 and shC002 were grown in medium supplemented with 1 μg/ml Puromycin (Sigma) for 5 days.

Flow cytometry (FACS) analysis

Transduced HCT116 cells were treated with Nocodazole. After 16h of treatment, round mitotic cells were recovered by gentle shaking of the culture dish, and then, were re-plated in fresh medium for different times (90'-180'-360'). For each time points, cells were collected, washed with PBS 10% FBS, fixed with PBS 2% formaldehyde (PFA) and then maintained in iced 70% ethanol. The fixed cells were then stained with PI staining solution (propidium iodide 20 μg/ml, Sigma, P4864) and RNase DNase-free (10 μg/ml) in PBS). Then stained cells were analyzed by flow cytometry (AccuriC6 instrument, BD Biosciences). The experiment was performed three times, and the data were collected using BD AccuriC6 acquisition software.

Transduced hTERT RPE-1 cells were treated with RO-3306. After 16h of treatment, cells were released in fresh medium or medium adding reversine and collected at different times (60'-90'-120'-150'). For each time points, cells were collected, washed with PBS 10% and fixed in chilled 70% ethanol. The harvested cells were then stained with PI staining solution (20 μg/ml) and RNase DNase-free (10 μg/ml in PBS) in the dark for 30' at room temperature. Then stained cells were analyzed by flow cytometry. Data analysis was performed with CellQuestPro software (BD Biosciences, Milan, Italy).

The forward and side scatter gates were set to exclude any dead cells from the analysis; 20000 events within this gate were acquired per sample. Data were statistically analyzed with paired two-tailed Student's τ-test. A P value of < 0.05 was considered statistically significant.

Time laps microscopy

Live cell imaging was performed using an inverted microscope (IX70; Nikon). Microscope was equipped with an incubation chamber maintained at 37°C in an atmosphere of 5% CO2. Unsynchronized HCT116 cells were cultured in the presence of thymidine. After wash-out of the drug, cells were placed into fresh medium or into medium adding reversine, right before the beginning of filming. Images were acquired every 5 min with a magnification objective of 10x to monitor cell mitotic timing, and every 10 min with a magnification objective of 20x to capture mis-segregation events.

Colony Assay

DAOY MB cells were transfected as indicated above, then plated in 10 cm-diameter dishes (1 x 104 cells per dish) and after 2 weeks of neomycin selection, as previously described (13), cell colonies were fixed and counted following crystal violet staining in 20% methanol. The number and size of the colonies were measured using the ImageJ plugins "colony-counter" (version 1.49v, Java 1.8.0_45, Wayen Rasband, U.S. National Institutes of Health, Bethesda, MD, USA; website: http://rsb.info.nih.gov/ij/downl oad.html). The colonies were splitted in Small (range 1-49 points), Medium (range 50-99 points) and Large (≥100 points) (1 points = 1 pixel = 0,03 mm). Experiment was performed in five biological replicates for each condition.

Proliferation and DNS assays

Proliferating DAOY cells transfected with plasmid encoding KCTD15 or empty vector were fluorescently labeled (4 hours) with the Click-iTTM EdU Alexa FluorTM 488 Imaging Kit (Life Technologies, C10337), in accordance with manufacturer's instructions.

For MTT assay, DAOY cells were plated at a density of 9,000 cells/well in 96-well plates containing complete medium. Cell proliferation was detected using CellTiter 96 Aqueous One Solution (Promega) at 24h following seeding. For cell proliferation measurement, 20 µl methanethiosulfonate reagent was added to the medium and incubated at 37℃ in a humidified 5% CO2 atmosphere. The absorbance was read at 490 nm.

For DNS assay, DAOY cells were cultured and transfected with indicated plasmids. After 48 hours, cells were incubated with PI (10 µM) and Hoechst 33342 (10 µM; U0334; Abnova, Germany) for 10 minutes. Images were acquired on a LEICA DM 2000 microscope.

HCT116 cells proliferation was quantified by counting the number of fluorescent nuclei over time to give true cell growth rates. Cells were labeled with nuclear-restricted non-perturbing fluorescent labels (IncuCyte® NucLight Green Lentivirus Reagent).

RNA isolation and Quantitative Real-time PCR

Total RNA from cells and tissues samples was extracted using TRIzol reagent, cDNA synthesis was performed using the High Capacity cDNA reverse transcription kit (Invitrogen) according to the manufacturer's instructions. Quantitative real-time PCR analysis of KCASH2, Gli1, N-myc, cyclin-D2, KCTD15, B- actin, GAPDH and HPRT messenger RNA (mRNA) was performed on cDNAs employing using TaqMan gene expression assay according to the manufacturer's instructions (Applied Biosystem- Thermo Fisher Scientific) and using the ViiATM 7 Real-Time PCR System (Applied Biosystem). Experiments were replicated biologically at least three times, with three

technical replicates each. All values were normalized to the endogenous controls GAPDH, HPRT and B-actin. mRNA quantification was expressed, in arbitrary units, as the ratio of the sample quantity to the mean values of control samples.

Chromatin Immunoprecipitation (ChIP)

HEK293T cells were crosslinked with formaldehyde 0.4% and the reaction was stopped by adding glycine 0.2M for 10 minutes at room temperature. Fixed cells were rinsed twice with PBS and resuspended in lysis buffer (10 mM EDTA pH 8, 50 mM Tris-HCl pH 8, SDS 1 %). Lysate was sonicated 5 min (30 sec on / 30 sec off) in Diagenode water bath-sonicator and centrifuged. The cleared supernatant was used immediately in ChIP experiments or stored at -80°C. 50-150 ug of sonicated chromatin was diluted 10 times in ChIP Dilution Buffer (SDS 0.01%, Triton X-100 1.1%, 1.2 mM EDTA pH 8, 16.7 mM Tris-HCl pH 8 and 167 mM NaCl) and pre-cleared for 1 hour, before the overnight incubation with 2-5ug of specific antibody anti SP1 (Abcam). The bound material was recovered, the beads were washed once in Low Salt Buffer (SDS 0.1%, Triton X100 1%, 2 mM EDTA pH 8, 20 mM Tris-HCl pH 8 and 150 mM NaCl), twice in High Salt Buffer (SDS 0.1%, Triton X-100 1%, 2 mM EDTA pH 8, 20 mM Tris-HCl pH 8 and 500 mM NaCl), twice in LiCl Buffer (0.25 M LiCl, NP-40 1%, Na Deoxycholate 1%, 1 mM EDTA pH8 and 10 mM Tris-HCl pH 8) and twice in TE. ChIPed material was eluted with 250 ul Elution Buffer (SDS 1%, 0.1 M NaHCO3). Chromatin was reverse-crosslinked by adding 20 ul of NaCl 5M and incubated at 65°C for 4 hours minimum and DNA was submitted to RNase and proteinase K digestion and extracted by phenol-chloroform. Chromatin immunoprecipitated was analyzed by qPCR using fluorescent dye SYBR Green in a ViiATM 7 Real-Time PCR System instrument (Applied Biosystem).

Primers are listed:

FW: 5'- TATGTATCCAGGAAGCCCGAC - 3'

RV: 5'- AGGAGGCATTGCAGCGAGTTG - 3'

Western Blot Analysis and Immunoprecipitation

Cells were lysed with buffer containing: 50 mM Tris-HCl (pH 7.6), 1% deoxycholic acid sodium salt, 150 mM NaCl, 1% NP40, 5 mM EDTA, 100 mM NaF, and protease inhibitors. Total protein extracts were then separated on a denaturing SDS-PAGE gel and evaluated by Western blot assay using the antibodies listed below.

For co-immunoprecipitation, lysates were incubated with agarose-conjugated Flag M2 beads (A2220; Sigma Aldrich-Merck, Darmstadt, Germany) for 2 hours at 4°C. For semi-endogenous IP assay, 1mg of protein was incubated with rabbit polyclonal antibody against Flag (SIGMA) O/N 4°C. Control

sample antibody was saturated with anti-Flag peptide (F3290; Sigma). Beads were washed extensively with lysis buffer, and the complexes were evaluated by Western blot analysis.

Antibody sources were as follows: mouse anti-tubulin polyclonal (SC- 8035; Santa Cruz Biotechnology, Heidelberg, Germany), mouse monoclonal antibody against β-actin (AC-15, A5441, SIGMA); goat anti-actin polyclonal (SC-8432; Santa Cruz Biotechnology); rabbit anti-KCTD15 polyclonal antibody (20128-1-AP; Proteintech, Manchester, UK); anti-Gli1 mouse monoclonal (2643; Cell Signaling Technology, Danvers, MA, USA); rabbit polyclonal anti-cleaved Caspase3 (9661S; Cell Signaling); rabbit anti-KCTD21/KCASH2 monoclonal (AB192259; Abcam, Cambridge, UK); rabbit polyclonal antibody against MAD2 (Santa Cruz Biotechnology); rabbit polyclonal antibody against Cyclin B1 (H-433, sc-752 Santa Cruz Biotechnology) and Cyclin A (H-432, sc-751, Santa Cruz Biotechnology); rabbit polyclonal anti-Sp1 (ab227383-Abcam), rabbit peroxidase conjugate against c-Myc (A5598, SIGMA); mouse anti-HA monoclonal (H6533; Sigma), mouse anti-Flag-M2 (A8592; Sigma), rabbit anti-Myc (A5598; Sigma).

Anti-acetylated Gli1 (K518) antibody rabbit polyclonal was a gift from G. Canettieri (La Sapienza, Rome, IT).

Secondary antibody anti–mouse (SC-516102) /rabbit (SC-2357)/goat IgG (SC-2354) conjugated with HRP were from Santa Cruz. Blots shown are representative of at least three independent experiments.

Statistical and bioinformatics analysis

For all luciferase, QPCR, MTT, FACS analysis, proliferation and apoptotic assays, colony formation assay experiments, the P values were determined using Student's t-test and statistical significance was set at $P<0.05$ or $P<0.01$. Data were assumed to have normal distribution. Results are expressed as mean ± S.D. P values for MB samples was calculated by Mann Whitney test. All experiments presented were representative of at least three biological replicas, except when specifically indicated. Correlation analysis was measured using GraphPad Prism 6 software (La Jolla, CA, USA).

Using database associated search tools (Genomatix, TF Search, EMBOSS), the human KCASH2 proximal promoter sequence was scanned for the presence of putative cis-acting regulatory elements. Sequences were aligned with CLUSTAL multiple sequence alignment by MUSCLE program. Correlation analysis were performed using software R2 (R2: Genomics Analysis and Visualization Platform (http://r2.amc.nl)).

BIBLIOGRAPHY

- Aaron R. Tipton A.R., Ji W., Sturt-Gillespie B., Bekier M.E., Wang K., Taylor W. R., Liu S. Monopolar Spindle 1 (MPS1) Kinase Promotes Production of Closed MAD2 (C-MAD2) Conformer and Assembly of the Mitotic Checkpoint Complex*An external file that holds a picture, illustration, etc. *J Biol Chem.* 2013 Dec 6; 288(49): 35149–35158.
- Abe Y., Tanaka N. Roles of the Hedgehog Signaling Pathway in Epidermal and Hair Follicle Development, Homeostasis, and Cancer. *J Dev Biol*. 2017 Nov 20;5(4)
- Ahn S., Joyner A.L. In vivo analysis of quiescent adult neural stem cells responding to Sonic hedgehog. *Nature.* 2005 Oct 6;437(7060):894-7.
- Almeida A.C., Maiato H. Chromokinesins. *Curr Biol.* 2018 Oct 8;28(19):R1131-R1135.
- Archer T.C., Mahoney E.L., Pomeroy S.L. Medulloblastoma: Molecular Classification-Based Personal Therapeutics. *Neurotherapeutics*. 2017 Apr;14(2):265-273.
- Argenti B., Gallo R., Di Marcotullio L., Ferretti E., Napolitano M., Canterini S., De Smaele E., Greco A., Fiorenza M.T., Maroder M., Screpanti I., Alesse E., Gulino A. Hedgehog antagonist REN(KCTD11) regulates proliferation and apoptosis of developing granule cell progenitors. *J Neurosci.* 2005 Sep 7;25(36):8338-46.
- Ayers K.L., Thérond P.P. Evaluating Smoothened as a G-protein-coupled receptor for Hedgehog signalling. *Trends Cell Biol*. 2010 May;20(5):287-98.
- Babu J.R., Jeganathan K.B., Baker D.J., Wu X., Kang-Decker N., van Deursen J.M. Rae1 is an essential mitotic checkpoint regulator that cooperates with Bub3 to prevent chromosome missegregation. *J Cell Biol.* 2003 Feb 3;160(3):341-53.
- Baker D.J, Jeganathan K.B., Cameron J.D., Thompson M., Juneja S., Kopecka A., Kumar R., Jenkins R.B., de Groen P.C., Roche P., van Deursen J.M. BubR1 insufficiency causes early onset of aging-associated phenotypes and infertility in mice. *Nat Genet.* 2004 Jul;36(7):744-9.
- Bangs F., Anderson K.V. Primary Cilia and Mammalian Hedgehog Signaling. *Cold Spring Harb Perspect Biol.* 2017 May 1;9(5).
- Bansal N., Farley N.J., Wu L., Lewis J., Youssoufian H., Bertino J.R. Darinaparsin inhibits prostate tumor-initiating cells and Du145 xenografts and is an inhibitor of hedgehog signaling. *Mol Cancer Ther*. 2015 Jan;14(1):23-30.
- Baranski T.J., Kraja A.T., Fink J.L., Feitosa M., Lenzini P.A., Borecki I.B., Liu C.T., Cupples L.A., North K.E., Province M.A. A high throughput, functional screen of human Body Mass Index GWAS loci using tissue-specific RNAi Drosophila melanogaster crosses. *PLoS Genet*. 2018 Apr 2;14(4):e1007222.

- Beachy P.A., Karhadkar S.S., Berman D.M. Tissue repair and stem cell renewal in carcinogenesis. *Nature*. 2004 Nov 18;432(7015):324-31.
- Beauchamp E, Bulut G, Abaan O, Chen K, Merchant A, Matsui W, Endo Y, Rubin JS, Toretsky J, Uren A. GLI1 is a direct transcriptional target of EWS-FLI1 oncoprotein. *J Biol Chem*. 2009 Apr 3;284(14):9074-82.
- Beishline K., Azizkhan-Clifford J. Interplay between the cell cycle and double-strand break response in mammalian cells. *Methods Mol Biol.* 2014;1170:41-59.
- Beishline K., Azizkhan-Clifford J. Sp1 and the 'hallmarks of cancer'. *FEBS J.* 2015 Jan;282(2):224-58.
- Bihannic L, Ayrault O. Insights into cerebellar development and medulloblastoma. *Bull Cancer.* 2016 Jan;103(1):30-40.
- Black B.E., Bassett E.A. The histone variant CENP-A and centromere specification. *Curr Opin Cell Biol.* 2008 Feb;20(1):91-100.
- Boveri T. Über mehrpolige Mitosen als Mittel zur Analyse des Zellkerns. *Verh. phys.-med*. 1902; Ges. 35: 67-90.
- Brechbiel J., Miller-Moslin K., Adjei A.A. Crosstalk between hedgehog and other signaling pathways as a basis for combination therapies in cancer. *Cancer Treat Rev*. 2014 Jul;40(6):750-9.
- Brownell I., Guevara E., Bai C.B., Loomis C.A., Joyner A.L. Nerve-derived sonic hedgehog defines a niche for hair follicle stem cells capable of becoming epidermal stem cells. *Cell Stem Cell*. 2011 May 6;8(5):552-65.
- Buonamici S., Williams J., Morrissey M., Wang A., Guo R., Vattay A., Hsiao K., Yuan J., Green J., Ospina B., Yu Q., Ostrom L., Fordjour P., Anderson D.L., Monahan J.E., Kelleher J.F., Peukert S., Pan S., Wu X., Maira S.M., García-Echeverría C., Briggs K.J., Watkins D.N., Yao Y.M., Lengauer C., Warmuth M., Sellers W.R., Dorsch M. Interfering with resistance to smoothened antagonists by inhibition of the PI3K pathway in medulloblastoma. *Sci Transl Med*. 2010 Sep 29;2(51):51ra70.
- Bürglin T.R. The Hedgehog protein family. *Genome Biol.* 2008;9(11):241.
- Canettieri G., Di Marcotullio L., Greco A., Coni S., Antonucci L., Infante P., Pietrosanti L., De Smaele E., Ferretti E, Miele E., Pelloni M., De Simone G., Pedone E.M., Gallinari P., Giorgi A., Steinkühler C., Vitagliano L., Pedone C., Schinin M.E., Screpanti I., Gulino A. Histone deacetylase and Cullin3-REN(KCTD11) ubiquitin ligase interplay regulates Hedgehog signalling through Gli acetylation. *Nat Cell Biol.* 2010 Feb;12(2):132-42.

- Carpenter R.L., Lo H.W. Hedgehog pathway and GLI1 isoforms in human cancer. *Discov Med*. 2012 Feb;13(69):105-13.
- Cavalli F.M.G., Remke M., Rampasek L., Peacock J., Shih D.J.H., Luu B., Garzia L., Torchia J., Nor C., Morrissy A.S., Agnihotri S., Taylor M.D. Intertumoral Heterogeneity within Medulloblastoma Subgroups. *Cancer Cell.* 2017 Jun 12;31(6):737-754.e6. *Cell Biosci*. 2013 Nov 24;3(1):45.
- Chang CH, Housepian EM, Herbert C Jr. An operative staging system and a megavoltage radiotherapeutic technic for cerebellar medulloblastomas. *Radiology*. 1969 Dec;93(6):1351-9.
- Chen C.M., Strapps W., Tomlinson A., Struhl G. Evidence that the cysteine-rich domain of Drosophila Frizzled family receptors is dispensable for transducing Wingless. *Proc. Natl. Acad. Sci. U.S.A.* (2004). 101(45): 15961-15966.
- Chen R.H. BubR1 is essential for kinetochore localization of other spindle checkpoint proteins and its phosphorylation requires Mad1. *J Cell Biol.* 2002 Aug 5;158(3):487-96.
- Cimini D. Merotelic kinetochore orientation, aneuploidy, and cancer. *Biochim Biophys Acta*. 2008 Sep;1786(1):32-40.
- Clarke T.K., Nymberg C., Schumann G. Genetic and environmental determinants of stress responding. *Alcohol Res.* 2012;34(4):484-94.
- Clement V, Sanchez P, de Tribolet N, Radovanovic I, Ruiz i Altaba A. HEDGEHOG-GLI1 signaling regulates human glioma growth, cancer stem cell self-renewal, and tumorigenicity. *Curr Biol*. 2007 Jan 23;17(2):165-72.
- Cloninger C.R. A new conceptual paradigm from genetics and psychobiology for the science of mental health. *Aust N Z J Psychiatry*. 1999 Apr;33(2):174-86.
- Coni S., Mancuso A.B., Di Magno L., Sdruscia G., Manni S., Serrao S.M., Rotili D., Spiombi E., Bufalieri F., Petroni M., Kusio-Kobialka M., De Smaele E., Ferretti E., Capalbo C., Mai A., Niewiadomski P., Screpanti I., Di Marcotullio L., Canettieri G. Selective targeting of HDAC1/2 elicits anticancer effects through Gli1 acetylation in preclinical models of SHh Medulloblastoma. *Sci Rep.* 2017 Apr 21;7:46645.
- Corbit K.C., Aanstad P., Singla V., Norman A.R., Stainier D.Y., Reiter J.F. Vertebrate Smoothened functions at the primary cilium. *Nature.* 2005 Oct 13;437(7061):1018-21.
- D'Alessandro G., Quaglio D., Monaco L., Lauro C., Ghirga F., Ingallina C., De Martino M., Fucile S., Porzia A., Di Castro M.A., Bellato F., Mastrotto F., Mori M., Infante P., Turano P., Salmaso S., Caliceti P., Di Marcotullio L., Botta B., Ghini V., Limatola C. (1)H-NMR metabolomics reveals the Glabrescione B exacerbation of glycolytic metabolism beside the cell growth inhibitory effect in glioma. *Cell Commun Signal*. 2019 Aug 28;17(1):108.

- Dahmane N., Ruiz i Altaba A. Sonic hedgehog regulates the growth and patterning of the cerebellum. *Development*. 1999 Jun;126(14):3089-100.
- Das T., Roy K.S., Chakrabarti T., Mukhopadhyay S., Roychoudhury S. Withaferin A modulates the Spindle assembly checkpoint by degradation of Mad2-Cdc20 complex in colorectal cancer cell lines. *Biochem Pharmacol*. 2014 Sep 1;91(1):31-9.
- de Crozé N., Maczkowiak F., Monsoro-Burq A.H. Reiterative AP2a activity controls sequential steps in the neural crest gene regulatory network. *Proc Natl Acad Sci U S A*. 2011 Jan 4;108(1):155-60.
- Dennler S, André J, Alexaki I, Li A, Magnaldo T, ten Dijke P, Wang XJ, Verrecchia F, Mauviel A. Induction of sonic hedgehog mediators by transforming growth factor-beta: Smad3-dependent activation of Gli2 and Gli1 expression in vitro and in vivo. *Cancer Res*. 2007 Jul 15;67(14):6981-6.
- De Smaele E., Di Marcotullio L., Ferretti E., Screpanti I., Alesse E., Gulino A. Chromosome 17p deletion in human medulloblastoma: a missing checkpoint in the Hedgehog pathway. *Cell Cycle.* 2004 Oct;3(10):1263-6.
- De Smaele E., Di Marcotullio L., Moretti M., Pelloni M., Occhione M.A., Infante P., Cucchi D., Greco A., Pietrosanti L., Todorovic J., Coni S., Canettieri G., Ferretti E., Bei R., Maroder M., Screpanti I., Gulino A. Identification and characterization of KCASH2 and KCASH3, 2 novel Cullin3 adaptors suppressing histone deacetylase and Hedgehog activity in medulloblastoma. *Neoplasia.* 2011 Apr;13(4):374-85.
- Dierks C., Grbic J., Zirlik K., Beigi R., Englund N.P., Guo G.R., Veelken H., Engelhardt M., Mertelsmann R., Kelleher J.F., Schultz P., Warmuth M. Essential role of stromally induced hedgehog signaling in B-cell malignancies. *Nat Med*. 2007 Aug;13(8):944-51.
- Di Marcotullio L., Ferretti E., De Smaele E., Argenti B., Mincione C., Zazzeroni F., Gallo R., Masuelli L., Napolitano M., Maroder M., Modesti A., Giangaspero F., Screpanti I., Alesse E., Gulino A. REN(KCTD11) is a suppressor of Hedgehog signaling and is deleted in human medulloblastoma. *Proc Natl Acad Sci U S A.* 2004 Jul 20;101(29):10833-8.
- Di Marcotullio L., Canettieri G., Infante P., Greco A., Gulino A. Protected from the inside: endogenous histone deacetylase inhibitors and the road to cancer. *Biochim Biophys Acta*. 2011 Apr;1815(2):241-52.
- Dlugosz A., Agrawal S., Kirkpatrick P. Vismodegib. *Nat Rev Drug Discov*. 2012 Jun 1;11(6):437-8.
- Dominguez-Brauer C., Thu K.L., Mason J.M., Blaser H., Bray M.R., Mak T.W. Targeting mitosis: emergening strategies. *Mol Cell.* 2015 Nov 19;60(4):524-36.

- Dorsky R.I., Moon R.T., Raible D.W. Control of neural crest cell fate by the Wnt signalling pathway. *Nature*. 1998 Nov 26;396(6709):370-3.
- Dutta S., Dawid I.B. Kctd15 inhibits neural crest formation by attenuating Wnt/beta-catenin signaling output. *Development*. 2010 Sep;137(18):3013-8.
- Echelard Y., Epstein D.J., St-Jacques B., Shen L., Mohler J., McMahon J.A., McMahon A.P. Sonic hedgehog, a member of a family of putative signaling molecules, is implicated in the regulation of CNS polarity. *Cell.* 1993 Dec 31;75(7):1417-30.
- Eckschlager T., Plch J., Stiborova M., Hrabeta J. Histone Deacetylase Inhibitors as Anticancer Drugs. *Int J Mol Sci*. 2017 Jul 1;18(7).
- Eslin D., Lee C., Sankpal U.T., Maliakal P., Sutphin R.M., Abraham L., Basha R. Anticancer activity of tolfenamic acid in medulloblastoma: a preclinical study. *Tumour Biol.* 2013 Oct;34(5):2781-9.
- Espeut J., Gaussen A., Bieling P., Morin V., Prieto S., Fesquet D., Surrey T., Abrieu A. Phosphorylation relieves autoinhibition of the kinetochore motor Cenp-E. *Mol Cell.* 2008 Mar 14;29(5):637-43.
- Faesen A.C., Thanasoula M., Maffini S., Breit C., Müller F., van Gerwen S., Bange T., Musacchio A. Basis of catalytic assembly of the mitotic checkpoint complex. *Nature.* 2017 Feb 23;542(7642):498-502.
- Fan Q., Gu D., He M., Liu H., Sheng T., Xie G., Li C.X., Zhang X., Wainwright B., Garrossian A., Garrossian M., Gardner D., Xie J. Tumor shrinkage by cyclopamine tartrate through inhibiting hedgehog signaling. *Chin J Cancer*. 2011 Jul;30(7):472-81.
- Fang Q., Yang W., Li H., Hu W., Chen L., Jiang S., Dong K., Song Q., Wang C., Chen S., Liu F., Jia W. Negative regulation of DsbA-L gene expression by the transcription factor Sp1. *Diabetes.* 2014 Dec;63(12):4165-71.
- Faryna M., Konermann C., Aulmann S., Bermejo J.L., Brugger M., Diederichs S., Rom J., Weichenhan D., Claus R., Rehli M., Schirmacher P., Sinn H.P., Plass C., Gerhauser C. Genome-wide methylation screen in low-grade breast cancer identifies novel epigenetically altered genes as potential biomarkers for tumor diagnosis. *FASEB J.* 2012 Dec;26(12):4937-50.
- Fava L.L., Kaulich M., Nigg E.A., Santamaria A. Probing the in vivo function of Mad1:C-Mad2 in the spindle assembly checkpoint. *EMBO J.* 2011 Jul 19;30(16):3322-36.
- Fenech M., Kirsch-Volders M., Natarajan A.T., Surralles J., Crott J.W., Parry J., Norppa H., Eastmond D.A., Tucker J.D., Thomas P. Molecular mechanisms of micronucleus, nucleoplasmic bridge and nuclear bud formation in mammalian and human cells. *Mutagenesis*. 2011 Jan;26(1):125-32.

- Fischer M., Bauer T., Oberthür A., Hero B., Theissen J., Ehrich M., Spitz R., Eils R., Westermann F., Brors B., König R., Berthold F. Integrated genomic profiling identifies two distinct molecular subtypes with divergent outcome in neuroblastoma with loss of chromosome 11q. *Oncogene*. 2010 Feb 11;29(6):865-75.
- Forrester H.B., Vidair C.A., Albright N., Ling C.C., Dewey W.C. Using computerized video time lapse for quantifying cell death of X-irradiated rat embryo cells transfected with c-myc or c-Ha-ras. *Cancer Res.* 1999 Feb 15;59(4):931-9.
- Fraschini R., Beretta A., Sironi L., Musacchio A., Lucchini G., Piatti S. Bub3 interaction with Mad2, Mad3 and Cdc20 is mediated by WD40 repeats and does not require intact kinetochores. *EMBO J.* 2001 Dec 3;20(23):6648-59.
- Gailani M.R., Bale A.E. Developmental genes and cancer: role of patched in basal cell carcinoma of the skin. *J Natl Cancer Inst*. 1997 Aug 6;89(15):1103-9.
- Gamero-Villarroel C., González L.M., Rodríguez-López R., Albuquerque D., Carrillo J.A., García-Herráiz A., Flores I., Gervasini G. Influence of TFAP2B and KCTD15 genetic variability on personality dimensions in anorexia and bulimia nervosa. *Brain Behav.* 2017 Sep; 7(9): e00784.
- Ganem N.J., Pellman D. Linking abnormal mitosis to the acquisition of DNA damage. *J Cell Biol*. 2012 Dec 10;199(6):871-81.
- Ge S., Skaar J.R., Pagano M. APC/C- and Mad2-mediated degradation of Cdc20 during spindle checkpoint activation. *Cell Cycle*. 2009 Jan 1;8(1):167-71.
- Glotzer M. Mitosis: don't get mad, get even. *Curr Biol*. 1996 Dec 1;6(12):1592-4.
- Gordon D.J., Resio B., Pellman D. Causes and consequences of aneuploidy in cancer. *Nat Rev Genet.* 2012 Jan 24;13(3):189-203.
- Gorrini C., Harris I.S., Mak T.W. Modulation of oxidative stress as an anticancer strategy. *Nat Rev Drug Discov.* 2013 Dec;12(12):931-47.
- Gu D., Xie J. Non-Canonical Hh Signaling in Cancer-Current Understanding and Future Directions. *Cancers (Basel)*. 2015 Aug 27;7(3):1684-98.
- Guardavaccaro D., Frescas D., Dorrello N.V., Peschiaroli A., Multani A.S., Cardozo T., Lasorella A., Iavarone A., Chang S., Hernando E., Pagano M. Control of chromosome stability by the beta-TrCP-REST-Mad2 axis. *Nature*. 2008 Mar 20;452(7185):365-9.
- Gulino A., Di Marcotullio L., Canettieri G., De Smaele E., Screpanti I. Hedgehog/Gli control by ubiquitination/acetylation interplay. *Vitam Horm.* 2012;88:211-27.

- Habu T., Matsumoto T. p31(comet) inactivates the chemically induced Mad2-dependent spindle assembly checkpoint and leads to resistance to anti-mitotic drugs. *Springerplus*. 2013 Oct 25;2:562.
- Hanahan D., Weinberg R.A. Hallmarks of cancer: the next generation. *Cell.* 2011 Mar 4;144(5):646-74.
- Hardwick K.G., Johnston R.C., Smith D.L., Murray A.W. MAD3 encodes a novel component of the spindle checkpoint which interacts with Bub3p, Cdc20p, and Mad2p. *J Cell Biol*. 2000 Mar 6;148(5):871-82.
- Hardwick K.G., Li R., Mistrot C., Chen R.H., Dann P., Rudner A., Murray A.W. Lesions in many different spindle components activate the spindle checkpoint in the budding yeast Saccharomyces cerevisiae. *Genetics.* 1999 Jun; 152(2): 509–518.
- Hassold T., Hunt P. To err (meiotically) is human: the genesis of human aneuploidy. *Nat Rev Genet*. 2001 Apr;2(4):280-91.
- Hegde G.V., Peterson K.J., Emanuel K., Mittal A.K., Joshi A.D., Dickinson J.D., Kollessery G.J., Bociek R.G., Bierman P., Vose J.M., Weisenburger D.D., Joshi S.S. Hedgehog-induced survival of B-cell chronic lymphocytic leukemia cells in a stromal cell microenvironment: a potential new therapeutic target. *Mol Cancer Res*. 2008 Dec;6(12):1928-36.
- Heride C., Rigden D.J, Bertsoulaki E., Cucchi D., De Smaele E., Clague M.J, Urbé S. The centrosomal deubiquitylase USP21 regulates Gli1 transcriptional activity and stability. *J Cell Sci.* 2016 Nov 1;129(21):4001-4013.
- Hernando E., Nahlé Z., Juan G., Diaz-Rodriguez E., Alaminos M., Hemann M., Michel L., Mittal V., Gerald W., Benezra R., Lowe S.W., Cordon-Cardo C. Rb inactivation promotes genomic instability by uncoupling cell cycle progression from mitotic control. *Nature.* 2004 Aug 12;430(7001):797-802.
- Hiruma Y., Koch A., Dharadhar S., Joosten R.P., Perrakis A. Structural basis of reversine selectivity in inhibiting Mps1 more potently than aurora B kinase. *Proteins*. 2016 Dec;84(12):1761-1766.
- Hodgkin J. Genetic suppression. *WormBook.* 2005 Dec 27:1-13.
- Howell B.J., Moree B., Farrar E.M., Stewart S., Fang G., Salmon E.D. Spindle checkpoint protein dynamics at kinetochores in living cells. *Curr Biol.* 2004 Jun 8;14(11):953-64.
- Huangfu D., Anderson K.V. Signaling from Smo to Ci/Gli: conservation and divergence of Hedgehog pathways from Drosophila to vertebrates. *Development.* 2006 Jan;133(1):3-14.

- Incardona J.P., Gaffield W., Kapur R.P., Roelink H. The teratogenic Veratrum alkaloid cyclopamine inhibits sonic hedgehog signal transduction. *Development*. 1998 Sep;125(18):3553-62.
- Infante P., Mori M., Alfonsi R., Ghirga F., Aiello F., Toscano S., Ingallina C., Siler M., Cucchi D., Po A., Miele E., D'Amico D., Canettieri G., De Smaele E., Ferretti E., Screpanti I., Uccello Barretta G., Botta M., Botta B., Gulino A., Di Marcotullio L. Gli1/DNA interaction is a druggable target for Hedgehog-dependent tumors. *EMBO J*. 2015 Jan 13;34(2):200-17.
- Infante P., Lospinoso Severini L., Bernardi F., Bufalieri F., Di Marcotullio L. Targeting Hedgehog Signalling through the Ubiquitylation Process: The Multiple Roles of the HECT-E3 Ligase Itch. *Cells*. 2019 Jan 29;8(2).
- Ingham P.W., McMahon A.P. Hedgehog signaling in animal development: paradigms and principles. *Genes Dev*. 2001 Dec 1;15(23):3059-87.
- Ingham P.W., Nakano Y., Seger C. Mechanisms and functions of Hedgehog signalling across the metazoa. *Nat Rev Genet*. 2011 Jun;12(6):393-406.
- Jiang J., Hui C.C. Hedgehog signaling in development and cancer. *Dev Cell*. 2008 Dec;15(6):801-12.
- Jiang NY1, Woda BA, Banner BF, Whalen GF, Dresser KA, Lu D. Sp1, a new biomarker that identifies a subset of aggressive pancreatic ductal adenocarcinoma. *Cancer Epidemiol Biomarkers Prev*. 2008 Jul;17(7):1648-52. doi: 10.1158/1055-9965.EPI-07-2791.
- Joglekar A.P. A Cell Biological Perspective on Past, Present and Future Investigations of the Spindle Assembly Checkpoint. *Biology (Basel)*. 2016 Nov 19;5(4).
- Johnson J.L., Hall T.E., Dyson J.M., Sonntag C., Ayers K., Berger S., Gautier P., Mitchell C., Hollway G.E., Currie P.D. Scube activity is necessary for Hedgehog signal transduction in vivo. *Dev Biol*. 2012 Aug 15;368(2):193-202.
- Johnson R.L., Rothman A.L., Xie J., Goodrich L.V., Bare J.W., Bonifas J.M., Quinn A.G., Myers R.M., Cox D.R., Epstein E.H. Jr, Scott M.P. Human homolog of patched, a candidate gene for the basal cell nevus syndrome. *Science*. 1996 Jun 14;272(5268):1668-71.
- Jordan M.A., Wilson L. Microtubules as a target for anticancer drugs. *Nat Rev Cancer*. 2004 Apr;4(4):253-65.
- Juraschka K., Taylor M.D. Medulloblastoma in the age of molecular subgroups: a review. *J Neurosurg Pediatr*. 2019 Oct 1;24(4):353-363.
- Kaczynski J., Cook T., Urrutia R. Sp1- and Krüppel-like transcription factors. *Genome Biol*. 2003;4(2):206.

- Kang M.I., Kobayashi A., Wakabayashi N., Kim S.G., Yamamoto M. Scaffolding of Keap1 to the actin cytoskeleton controls the function of Nrf2 as key regulator of cytoprotective phase 2 genes. *Proc Natl Acad Sci U S A.* 2004 Feb 17;101(7):2046-51.
- Karhadkar S.S., Bova G.S., Abdallah N., Dhara S., Gardner D., Maitra A., Isaacs J.T., Berman D.M., Beachy P.A. Hedgehog signaling in prostate regeneration, neoplasia and metastasis. *Nature*. 2004 Oct 7;431(7009):707-12.
- Karki K., Harishchandra S., Safe S. Bortezomib Targets Sp Transcription Factors in Cancer Cells. *Mol Pharmacol*. 2018 Oct;94(4):1187-1196.
- Katarzyna R., Lucyna B. Epigenetic therapies in patients with solid tumors: focus on monotherapy with deoxyribonucleic acid methyltransferase inhibitors and histone deacetylase inhibitors. *J Cancer Res Ther*. 2019 Jul-Sep;15(5):961-970.
- Knouse K.A., Wu J., Whittaker C.A., Amon A. Single cell sequencing reveals low levels of aneuploidy across mammalian tissues. *Proc Natl Acad Sci U S A*. 2014 Sep 16;111(37):13409-14.
- Koehler G.P.D. D.R., Sweezey N.B., Tanswell A.K., Hu J.: Lung inflammation as a therapeutic target in cystic fibrosis. *Cell Mol Biol*. 2004, 31: 377-381.
- Kok K., Naylor S.L., Buys C.H. Deletions of the short arm of chromosome 3 in solid tumors and the search for suppressor genes. *Adv Cancer Res.* 1997;71:27-92.
- Kong J.H., Siebold C., Rohatgi R. Biochemical mechanisms of vertebrate hedgehog signaling. *Development*. 2019 May 15;146(10).
- Kruse T., Larsen M.S., Sedgwick G.G., Sigurdsson J.O., Streicher W., Olsen J.V., Nilsson J. A direct role of Mad1 in the spindle assembly checkpoint beyond Mad2 kinetochore recruitment. *EMBO Rep*. 2014 Mar;15(3):282-90.
- Kulukian A., Han J.S., Cleveland D.W. Unattached kinetochores catalyze production of an anaphase inhibitor that requires a Mad2 template to prime Cdc20 for BubR1 binding. *Dev Cell.* 2009;16:105–117.
- Kuniyasu K., Iemura K., Tanaka K. Delayed Chromosome Alignment to the Spindle Equator Increases the Rate of Chromosome Missegregation in Cancer Cell Lines. *Biomolecules.* 2018 Dec 28;9(1).
- Lamont J.M., McManamy C.S., Pearson A.D., Clifford S.C., Ellison D.W. Combined histopathological and molecular cytogenetic stratification of medulloblastoma patients. *Clin Cancer Res*. 2004 Aug 15;10(16):5482-93.
- Lan W., Cleveland D.W. A chemical tool box defines mitotic and interphase roles for Mps1 kinase. *J Cell Biol.* 2010 Jul 12;190(1):21-4.

- Lauth M., Bergström A., Shimokawa T., Toftgård R. Inhibition of GLI-mediated transcription and tumor cell growth by small-molecule antagonists. *Proc Natl Acad Sci USA*. 2007 May 15;104(20):8455-60.
- Lee H.S., Park C.K., Oh E., Erkin Ö.C., Jung H.S., Cho M.H., Kwon M.J., Chae S.W., Kim S.H., Wang L.H., Park M.J., Lee S.Y., Yang H.B., Jia L., Choi Y.L., Shin Y.K. Low SP1 expression differentially affects intestinal-type compared with diffuse-type gastric adenocarcinoma. *PLoS One.* 2013;8(2):e55522.
- Lee P.R., Lasker R.D., Shapiro D.W., Bindman A.B. Managed care: provider profiling. *J Insur Med.* 1992 Fall;24(3):179-81.
- Lee R.T., Zhao Z., Ingham P.W. Hedgehog signalling. *Development*. 2016 Feb 1;143(3):367-72.
- Lescop S., Lellouch-Tubiana A., Vassal G., Besnard-Guerin C. Molecular genetic studies of chromosome 11 and chromosome 22q DNA sequences in pediatric medulloblastomas. *J Neurooncol*. 1999 Sep;44(2):119-27.
- Li R., Murray A.W. Feedback control of mitosis in budding yeast. *Cell*. 1991 Aug 9;66(3):519-31.
- Li X., Nicklas R.B. Mitotic forces control a cell-cycle checkpoint. *Nature*. 1995 Feb 16;373(6515):630-2.
- Li Y., Benezra R. Identification of a human mitotic checkpoint gene: hsMAD2. *Science* (1996) 274(5285):246-8.
- Lindsley D.L., Sandler L., Baker B.S., Carpenter A.T., Denell R.E., Hall J.C., Jacobs P.A., Miklos G.L., Davis B.K., Gethmann R.C., Hardy R.W., Steven A.H., Miller M., Nozawa H., Parry D.M., Gould-Somero M., Gould-Somero M. Segmental aneuploidy and the genetic gross structure of the Drosophila genome. *Genetics*. 1972 May;71(1):157-84.
- Lischetti T., Nilsson J. Regulation of mitotic progression by the spindle assembly checkpoint. *Mol Cell Oncol*. 2015 Jan-Mar; 2(1): e970484.
- List A., Beran M., DiPersio J., Slack J., Vey N., Rosenfeld C.S., Greenberg P. Opportunities for Trisenox (arsenic trioxide) in the treatment of myelodysplastic syndromes. *Leukemia*. 2003 Aug;17(8):1499-507.
- Liu Z., Xiang Y., Sun G. The KCTD family of proteins: structure, function, disease relevance. *Cell Biosci*. 2013 Nov 24;3(1):45.
- López-Maury L., Marguerat S., Bähler J. Tuning gene expression to changing environments: from rapid responses to evolutionary adaptation. *Nat Rev Genet.* 2008 Aug;9(8):583-93.

- Louis D.N., Ohgaki H., Wiestler O.D., Cavenee W.K., Burger P.C., Jouvet A., Scheithauer B.W., Kleihues P. The 2007 WHO classification of tumours of the central nervous system. *Acta Neuropathol*. 2007 Aug;114(2):97-109.
- Luo X., Fang G., Coldiron M., Lin Y., Yu H., Kirschner M.W., Wagner G. Structure of the Mad2 spindle assembly checkpoint protein and its interaction with Cdc20.*Nat Struct Biol* 2000 7(3):224-9.
- Luttikhuis M.E., Powell J.E., Rees S.A., Genus T., Chughtai S., Ramani P., Mann J.R., McConville C.M. Neuroblastomas with chromosome 11q loss and single copy MYCN comprise a biologically distinct group of tumours with adverse prognosis. *Br J Cancer*. 2001 Aug 17;85(4):531-7.
- Macleod D., Charlton J., Mullins J., Bird A.P. Sp1 sites in the mouse aprt gene promoter are required to prevent methylation of the CpG island. *Genes Dev*. 1994 Oct 1;8(19):2282-92.
- Maiato H., Gomes A.M., Sousa F., Barisic M. Mechanisms of Chromosome Congression during Mitosis. Biology (Basel). 2017 Feb 17;6(1).
- Malureanu L.A., Jeganathan K.B., Hamada M., Wasilewski L., Davenport J., van Deursen J.M. BubR1 N terminus acts as a soluble inhibitor of cyclin B degradation by APC/C(Cdc20) in interphase. *Dev Cell.* 2009 Jan;16(1):118-31.
- Mancarelli M.M., Zazzeroni F., Ciccocioppo L., Capece D., Po A., Murgo S., Di Camillo R., Rinaldi C., Ferretti E., Gulino A., Alesse E. The tumor suppressor gene KCTD11REN is regulated by Sp1 and methylation and its expression is reduced in tumors. *Mol Cancer.* 2010 Jun 30;9:172.
- Mapelli M., Filipp F.V., Rancati G., Massimiliano L., Nezi L., Stier G., Hagan R.S., Confalonieri S., Piatti S., Sattler M., Musacchio A. Determinants of conformational dimerization of Mad2 and its inhibition by p31comet. *EMBO J.* 2006 Mar 22;25(6):1273-84.
- Mapelli M., Musacchio A. MAD contortions: conformational dimerization boosts spindle checkpoint signaling. *Curr Opin Struct Biol.* 2007 Dec;17(6):716-25.
- Matson D.R., Stukenberg P.T. Spindle poisons and cell fate: a tale of two pathways. *Mol Interv*. 2011 Apr;11(2):141-50.
- Maurer G.D., Leupold J.H., Schewe D.M., Biller T., Kates R.E., Hornung H.M., Lau-Werner U., Post S., Allgayer H. Analysis of specific transcriptional regulators as early predictors of independent prognostic relevance in resected colorectal cancer. *Clin Cancer Res*. 2007 Feb 15;13(4):1123-32.
- McMahon A.P., Ingham P.W., Tabin C.J. Developmental roles and clinical significance of hedgehog signaling. *Curr Top Dev Biol.* 2003;53:1-114.

- McNeil D.E., Coté T.R., Clegg L., Rorke L.B. Incidence and trends in pediatric malignancies medulloblastoma/primitive neuroectodermal tumor: a SEER update. Surveillance Epidemiology and End Results. *Med Pediatr Oncol*. 2002 Sep;39(3):190-4.
- Melnick A., Ahmad K.F., Arai S., Polinger A., Ball H., Borden K.L., Carlile G.W., Prive G.G., Licht J.D. In-depth mutational analysis of the promyelocytic leukemia zinc finger BTB/POZ domain reveals motifs and residues required for biological and transcriptional functions. *Mol Cell Biol.* 2000 Sep;20(17):6550-67.
- Menssen A., Epanchintsev A., Lodygin D., Rezaei N., Jung P., Verdoodt B., Diebold J., Hermeking H. c-MYC delays prometaphase by direct transactivation of MAD2 and BubR1: identification of mechanisms underlying c-MYC-induced DNA damage and chromosomal instability. *Cell Cycle.* 2007 Feb 1;6(3):339-52.
- Michel L.S., Benezra R., Diaz-Rodriguez E. MAD2 dependent mitotic checkpoint defects in tumorigenesis and tumor cell death: a double-edged sword. *Cell Cycle.* 2004 Aug;3(8):990-2.
- Michel L.S., Liberal V., Chatterjee A., Kirchwegger R., Pasche B., Gerald W., Dobles M., Sorger P.K., Murty V.V., Benezra R. MAD2 haplo-insufficiency causes premature anaphase and chromosome instability in mammalian cells. *Nature.* 2001 Jan 18;409(6818):355-9.
- Millard N.E., De Braganca K.C. Medulloblastoma. *J Child Neurol*. 2016 Oct; 31(12):1341-53.
- Minor D.L., Lin Y.F., Mobley B.C., Avelar A., Jan Y.N., Jan L.Y., Berger J.M. The polar T1 interface is linked to conformational changes that open the voltage-gated potassium channel. *Cell.* 2000 Sep 1;102(5):657-70.
- Minucci S., Pelicci P.G. Histone deacetylase inhibitors and the promise of epigenetic (and more) treatments for cancer. *Nat Rev Cancer*. 2006 Jan;6(1):38-51.
- Mirsky R, Parmantier E, McMahon AP, Jessen KR. Schwann Cell-Derived Desert Hedgehog Signals Nerve Sheath Formation. *Ann N Y Acad Sci*. 1999 Oct;883(1):196-202.
- Mlakar V., Jurkovic Mlakar S., Lopez G., Maris J.M., Ansari M., Gumy-Pause F. 11q deletion in neuroblastoma: a review of biological and clinical implications. *Mol Cancer*. 2017 Jun 29;16(1):114.
- Mossaid I., Fahrenkrog B. Complex Commingling: Nucleoporins and the Spindle Assembly Checkpoint. *Cells.* 2015 Nov 3;4(4):706-25.
- Musacchio A., Salmon E.D. The spindle-assembly checkpoint in space and time. *Nat Rev Mol Cell Biol*. 2007 May;8(5):379-93.
- Myung K., Smith S., Kolodner R.D. Mitotic checkpoint function in the formation of gross chromosomal rearrangements in Saccharomyces cerevisiae. *Proc Natl Acad Sci U S A*. 2004 Nov 9;101(45):15980-5.

- Nicklas R.B., Ward S.C., Gorbsky G.J1. Kinetochore chemistry is sensitive to tension and may link mitotic forces to a cell cycle checkpoint. *J Cell Biol*. 1995 Aug;130(4):929-39.
- Nilsson J., Yekezare M., Minshull J., Pines J. The APC/C maintains the spindle assembly checkpoint by targeting Cdc20 for destruction. *Nat Cell Biol*. 2008 Dec;10(12):1411-20.
- Niyaz M., Khan MS., Mudassar S., Hedgehog Signaling: An Achilles Heel in Cancer. *Transl Oncol.* 2019 Jul 25;12(10):1334-1344.
- Northcott P.A., Shih D.J., Remke M., Cho Y.J., Kool M., Hawkins C., Eberhart C.G., Dubuc A., Guettouche T., Cardentey Y., Bouffet E., Pomeroy S.L., Marra M., Malkin D., Rutka J.T., Korshunov A., Pfister S., Taylor M.D. Rapid, reliable, and reproducible molecular sub-grouping of clinical medulloblastoma samples. *Acta Neuropathol*. 2012 Apr;123(4):615-26.
- Nüsslein-Volhard C., Wieschaus E. Mutations affecting segment number and polarity in Drosophila. *Nature* 1980;287:795–801.
- Ohashi A., Ohori M., Iwai K., Nakayama Y., Nambu T., Morishita D., Kawamoto T., Miyamoto M., Hirayama T., Okaniwa M., Banno H., Ishikawa T., Kandori H., Iwata K. Aneuploidy generates proteotoxic stress and DNA damage concurrently with p53-mediated post-mitotic apoptosis in SAC-impaired cells. *Nat Commun.* 2015 Jul 6;6:7668.
- Onishi H., Katano M. Hedgehog signaling pathway as a therapeutic target in various types of cancer. *Cancer Sci.* 2011 Oct;102(10):1756-60.
- Osmundson E.C., Ray D., Moore F.E., Gao Q., Thomsen G.H., Kiyokawa H. The HECT E3 ligase Smurf2 is required for Mad2-dependent spindle assembly checkpoint. *J Cell Biol.* 2008 Oct 20;183(2):267-77.
- Osmundson E.C., Ray D., Moore F.E., Kiyokawa H. Smurf2 as a novel mitotic regulator: From the spindle assembly checkpoint to tumorigenesis. Cell Div. 2009 Jul 7;4:14.
- Pampalona J., Roscioli E., Silkworth W.T., Bowden B., Genescà A., Tusell L., Cimini D. Chromosome Bridges Maintain Kinetochore-Microtubule Attachment throughout Mitosis and Rarely Break during Anaphase. *PLoS One*. 2016 Jan 19;11(1):e0147420.
- Pan S., Wu X., Jiang J., Gao W., Wan Y., Cheng D., Han D., Liu J., Englund N.P., Wang Y., Peukert S., Miller-Moslin K., Yuan J., Guo R., Matsumoto M., Vattay A., Jiang Y., Tsao J., Sun F., Pferdekamper A.C., Dodd S., Tuntland T., Maniara W., Kelleher J.F. 3rd, Yao Y.M., Warmuth M., Williams J., Dorsch M. Discovery of NVP-LDE225, a Potent and Selective Smoothened Antagonist. *ACS Med Chem Lett*. 2010 Mar 16;1(3):130-4.
- Parmantier E., Lynn B., Lawson D., Turmaine M., Namini S.S., Chakrabarti L., McMahon A.P., Jessen K.R., Mirsky R. Schwann cell-derived Desert hedgehog controls the development of peripheral nerve sheaths. *Neuron*. 1999 Aug;23(4):713-24.

- Pelullo M, Zema S, Nardozza F, Checquolo S, Screpanti I, Bellavia D. Wnt, Notch, and TGF-β Pathways Impinge on Hedgehog Signaling Complexity: An Open Window on Cancer. *Front Genet*. 2019 Aug 21;10:711.
- Peng Y. C., Levine C. M., Zahid S., Wilson E.L. Joyner A. L. Sonic hedgehog signals to multiple prostate stromal stem cells that replenish distinct stromal subtypes during regeneration. *Proc. Natl. Acad. Sci. USA*. 2013. 110, 20611-20616.
- Percy M.J., Myrie K.A., Neeley C.K., Azim J.N., Ethier S.P., Petty E.M. Expression and mutational analyses of the human MAD2L1 gene in breast cancer cells. *Genes Chromosomes Cancer*. 2000 Dec;29(4):356-62.
- Pérez de Castro I., de Cárcer G., Malumbres M. A census of mitotic cancer genes: new insights into tumor cell biology and cancer therapy. *Carcinogenesis.* 2007 May;28(5):899-912.
- Persson H., Søkilde R., Häkkinen J., Pirona A.C., Vallon-Christersson J., Kvist A., Mertens F., Borg Å., Mitelman F., Höglund M., Rovira C. Frequent miRNA-convergent fusion gene events in breast cancer. *Nat Commun.* 2017 Oct 5;8(1):788.
- Petrova R., Joyner AL. Roles for Hedgehog signaling in adult organ homeostasis and repair. *Development.* 2014 Sep;141(18):3445-57.
- Pinkas D.M., Sanvitale C.E., Bufton J.C., Sorrell F.J., Solcan N., Chalk R., Doutch J., Bullock A.N. Structural complexity in the KCTD family of Cullin3-dependent E3 ubiquitin ligases. *Biochem J.* 2017 Nov 1;474(22):3747-3761.
- Po A., Ferretti E., Miele E., De Smaele E., Paganelli A., Canettieri G., Coni S., Di Marcotullio L., Biffoni M., Massimi L., Di Rocco C., Screpanti I., Gulino A. Hedgehog controls neural stem cells through p53-independent regulation of Nanog. *EMBO J.* 2010 Aug 4;29(15):2646-58.
- Po A., Silvano M., Miele E., Capalbo C., Eramo A., Salvati V., Todaro M., Besharat Z.M., Catanzaro G., Cucchi D., Coni S., Di Marcotullio L., Canettieri G., Vacca A., Stassi G., De Smaele E., Tartaglia M., Screpanti I., De Maria R., Ferretti E. Noncanonical GLI1 signaling promotes stemness features and in vivo growth in lung adenocarcinoma. *Oncogene.* 2017 Aug 10;36(32):4641-4652.
- Poddar A., Stukenberg P.T., Burke D.J. Two complexes of spindle checkpoint proteins containing Cdc20 and Mad2 assemble during mitosis independently of the kinetochore in Saccharomyces cerevisiae. *Eukaryot Cell.* 2005 May;4(5):867-78.
- Prencipe M., Fitzpatrick P., Gorman S., Tosetto M., Klinger R., Furlong F., Harrison M., O'Connor D., Roninson I.B., O'Sullivan J., McCann A. Cellular senescence induced by aberrant MAD2 levels impacts on paclitaxel responsiveness in vitro. *Br J Cancer.* 2009 Dec 1;101(11):1900-8.

- Reardon D.A., Jenkins J.J., Sublett J.E., Burger P.C., Kun L.K. Multiple genomic alterations including N-myc amplification in a primary large cell medulloblastoma. *Pediatr Neurosurg*. 2000 Apr;32(4):187-91.
- Reddy S.K., Rape M., Margansky W.A., Kirschner M.W. Ubiquitination by the anaphase-promoting complex drives spindle checkpoint inactivation. *Nature.* 2007 Apr 19;446(7138):921-5.
- Riddle R.D., Johnson R.L., Laufer E., Tabin C. Sonic hedgehog mediates the polarizing activity of the ZPA. *Cell.* 1993 Dec 31;75(7):1401-16.
- Ried T., Hu Y., Difilippantonio M.J., Ghadimi B.M., Grade M., Camps J. The consequences of chromosomal aneuploidy on the transcriptome of cancer cells. *Biochim Biophys Acta*. 2012 Jul;1819(7):784-93.
- Rimkus T.K., Carpenter R.L., Qasem S., Chan M., Lo H.W. Targeting the Sonic Hedgehog Signaling Pathway: Review of Smoothened and GLI Inhibitors. *Cancers (Basel*). 2016 Feb 15;8(2).
- Rodriguez-Bravo V., Maciejowski J., Corona J., Buch H.K., Collin P., Kanemaki M.T., Shah J.V., Jallepalli P.V. Nuclear pores protect genome integrity by assembling a premitotic and Mad1-dependent anaphase inhibitor. *Cell.* 2014 Feb 27;156(5):1017-31.
- Rosenberg S.C., Corbett K.D. The multifaceted roles of the HORMA domain in cellular signaling. *J Cell Biol* (2015) 211(4):745-55.
- Rossi A., Caracciolo V., Russo G., Reiss K., Giordano A. Medulloblastoma: from molecular pathology to therapy. *Clin Cancer Res.* 2008 Feb 15;14(4):971-6.
- Ruat M., Roudaut H., Ferent J., Traiffort E. Hedgehog trafficking, cilia and brain functions. *Differentiation*. 2012 Feb;83(2):S97-104.
- Rubin L.L., de Sauvage F.J. Targeting the Hedgehog pathway in cancer. *Nat Rev Drug Discov*. 2006 Dec;5(12):1026-33.
- Sansregret L., Swanton C. The Role of Aneuploidy in Cancer Evolution. *Cold Spring Harb Perspect Med*. 2017 Jan 3;7(1).
- Santaguida S., Amon A. Short- and long-term effects of chromosome mis-segregation and aneuploidy. *Nat Rev Mol Cell Biol.* 2015 Aug;16(8):473-85.
- Santaguida S., Vasile E., White E., Amon A. Aneuploidy-induced cellular stresses limit autophagic degradation. *Genes Dev*. 2015 Oct 1;29(19):2010-21.
- Santaguida S., Tighe A., D'Alise A.M., Taylor S.S., Musacchio A. Dissecting the role of MPS1 in chromosome biorientation and the spindle checkpoint through the small molecule inhibitor reversine. *J Cell Biol.* 2010 Jul 12;190(1):73-87.

- Scales SJ, de Sauvage FJ. Mechanisms of Hedgehog pathway activation in cancer and implications for therapy. *Trends Pharmacol Sci*. 2009 Jun;30(6):303-12.
- Schibler A., Koutelou E., Tomida J., Wilson-Pham M., Wang L., Lu Y., Cabrera A.P., Chosed R.J., Li W., Li B., Shi X., Wood R.D., Dent S.Y. Histone H3K4 methylation regulates deactivation of the spindle assembly checkpoint through direct binding of Mad2. *Genes Dev.* 2016 May 15;30(10):1187-97.
- Schleutker J., Baffoe-Bonnie A.B., Gillanders E., Kainu T., Jones M.P., Freas-Lutz D., Markey C., Gildea D., Riedesel E., Albertus J., Gibbs K.D. Jr., Matikainen M., Koivisto P.A., Tammela T., Bailey-Wilson J.E., Trent J.M., Kallioniemi O.P. Genome-wide scan for linkage in finnish hereditary prostate cancer (HPC) families identifies novel susceptibility loci at 11q14 and 3p25-26. *Prostate.* 2003 Dec 1;57(4):280-9.
- Schuyler S.C., Wu Y.F., Kuan V.J. The Mad1-Mad2 balancing act--a damaged spindle checkpoint in chromosome instability and cancer. *J Cell Sci.* 2012 Sep 15;125(Pt 18):4197-206.
- Schvartzman J.M., Duijf P.H., Sotillo R., Coker C., Benezra R. Mad2 is a critical mediator of the chromosome instability observed upon Rb and p53 pathway inhibition. *Cancer Cell.* 2011 Jun 14;19(6):701-14.
- Seddik R., Jungblut S.P., Silander O.K., Rajalu M., Fritzius T., Besseyrias V., Jacquier V., Fakler B., Gassmann M., Bettler B. Opposite effects of KCTD subunit domains on GABA(B) receptor-mediated desensitization. *J Biol Chem.* 2012 Nov 16;287(47):39869-77.
- Shah J.V., Botvinick E., Bonday Z., Furnari F., Berns M., Cleveland D.W. Dynamics of centromere and kinetochore proteins; implications for checkpoint signaling and silencing. *Curr Biol.* 2004 Jun 8;14(11):942-52.
- Shandilya J., Roberts S.G. A role of WT1 in cell division and genomic stability. *Cell Cycle*. 2015;14(9):1358-64.
- Sharpe H.J., Pau G., Dijkgraaf G.J., Basset-Seguin N., Modrusan Z., Januario T., Tsui V., Durham A.B., Dlugosz A.A., Haverty P.M. Genomic analysis of smoothened inhibitor resistance in basal cell carcinoma. *Cancer Cell*. 2015, 27, 327–341.
- Shin K., Lee J., Guo N., Kim J., Lim A., Qu L., Mysorekar I. U., Beachy P. A. Hedgehog/Wnt feedback supports regenerative proliferation of epithelial stem cells in bladder. *Nature.* 2011. 472, 110-114.
- Sicklick J.K., Li Y.X., Jayaraman A., Kannangai R., Qi Y., Vivekanandan P., Ludlow J.W., Owzar K., Chen W., Torbenson M.S., Diehl A.M. Dysregulation of the Hedgehog pathway in human hepatocarcinogenesis. *Carcinogenesis*. 2006 Apr;27(4):748-57.

- Siegfried Z., Eden S., Mendelsohn M., Feng X., Tsuberi B.Z., Cedar H. DNA methylation represses transcription in vivo. *Nat Genet*. 1999 Jun;22(2):203-6.
- Simonetti G., Bruno S., Padella A., Tenti E., Martinelli G. Aneuploidy: Cancer strength or vulnerability? *Int J Cancer*. 2019 Jan 1;144(1):8-25.
- Sironi L., Mapelli M., Knapp S., De Antoni A., Jeang K-T., Musacchio A. Crystal structure of the tetrameric Mad1–Mad2 core complex: implications of a 'safety belt' binding mechanism for the spindle checkpoint. *EMBO J.* 2002 May 15; 21(10): 2496–2506.
- Sitry-Shevah D., Kaisari S., Teichner A., Miniowitz-Shemtov S., Hershko A. Role of ubiquitylation of components of mitotic checkpoint complex in their dissociation from anaphase-promoting complex/cyclosome. *Proc Natl Acad Sci U S A*. 2018 Feb 20;115(8):1777-1782.
- Smaldone G., Pirone L., Balasco N., Di Gaetano S., Pedone E.M., Vitagliano L. Cullin 3 Recognition Is Not a Universal Property among KCTD Proteins. *PLoS One.* 2015 May 14;10(5):e0126808.
- Smith J.J., Deane N.G., Wu F., Merchant N.B., Zhang B., Jiang A., Lu P., Johnson J.C., Schmidt C., Bailey C.E., Eschrich S., Kis C., Levy S., Washington M.K., Heslin M.J., Coffey R.J., Yeatman T.J., Shyr Y., Beauchamp R.D. Experimentally derived metastasis gene expression profile predicts recurrence and death in patients with colon cancer. *Gastroenterology*. 2010 Mar;138(3):958-68.
- Somers W.G., Saint R. A RhoGEF and Rho family GTPase-activating protein complex links the contractile ring to cortical microtubules at the onset of cytokinesis. *Dev Cell.* 2003 Jan;4(1):29-39.
- Sotillo R., Hernando E., Díaz-Rodríguez E., Teruya-Feldstein J., Cordón-Cardo C., Lowe S.W., Benezra R. Mad2 overexpression promotes aneuploidy and tumorigenesis in mice. *Cancer Cell.* 2007 Jan;11(1):9-23.
- Spiombi E., Angrisani A., Fonte S., De Feudis G., Fabretti F., Danilo C., Izzo M., Infante P., Miele E., Po A., Di Magno L., Magliozzi R., Guardavaccaro D., Maroder M., Canettieri G., Giannini G., Ferretti E., Gulino A., Di Marcotullio L., Moretti M., De Smaele E. KCTD15 inhibits the Hedgehog pathway in Medulloblastoma cells by increasing protein levels of the oncosuppressor KCASH2. Oncogenesis. 20192019 Nov 4;8(11):64.
- Srivastava R.K., Kaylani S.Z., Edrees N., Li C., Talwelkar S.S., Xu J., Palle K., Pressey J.G., Athar M. GLI inhibitor GANT-61 diminishes embryonal and alveolar rhabdomyosarcoma growth by inhibiting Shh/AKT-mTOR axis. *Oncotarget*. 2014 Dec 15;5(23):12151-65.

- St-Jacques B., Hammerschmidt M., McMahon A.P. Indian hedgehog signaling regulates proliferation and differentiation of chondrocytes and is essential for bone formation. *Genes Dev*. 1999 Aug 15;13(16):2072-86.
- Stankovic T., Skowronska A. The role of ATM mutations and 11q deletions in disease progression in chronic lymphocytic leukemia. *Leuk Lymphoma.* 2014 Jun;55(6):1227-39.
- Stecca B., Ruiz I Altaba A. Context-dependent regulation of the GLI code in cancer by HEDGEHOG and non-HEDGEHOG signals. *J Mol Cell Biol*. 2010 Apr;2(2):84-95.
- Stegmeier F., Rape M., Draviam V.M., Nalepa G., Sowa M.E., Ang X.L., McDonald E.R., Li M.Z., Hannon G.J., Sorger P.K., Kirschner M.W., Harper J.W., Elledge S.J. Anaphase initiation is regulated by antagonistic ubiquitination and deubiquitination activities. *Nature.* 2007 Apr 19;446(7138):876-81.
- Strumillo M., Beltrao P. Towards the computational design of protein post-translational regulation. *Bioorg Med Chem*. 2015 Jun 15;23(12):2877-82.
- Sudakin V., Chan G.K., Yen T.J. Checkpoint inhibition of the APC/C in HeLa cells is mediated by a complex of BUBR1, BUB3, CDC20, and MAD2. *J Cell Biol*. 2001 Sep 3;154(5):925-36.
- Sugimoto I., Murakami H., Tonami Y., Moriyama A., Nakanishi M. DNA replication checkpoint control mediated by the spindle checkpoint protein Mad2p in fission yeast. *J Biol Chem*. 2004 Nov 5;279(45):47372-8.
- Sun Z., Lu J., Wu M., Li M., Bai L., Shi Z., Hao L., Wu Y. Deficiency of PTEN leads to aberrant chromosome segregation through downregulation of MAD2. *Mol Med Rep*. 2019 Nov;20(5):4235-4243.
- Takahashi C., Suzuki T., Nishida E., Kusakabe M. Identification and characterization of Xenopus kctd15, an ectodermal gene repressed by the FGF pathway. *Int J Dev Biol.* 2012;56(5):393-402.
- Tanaka K., Hirota T. Chromosomal instability: A common feature and a therapeutic target of cancer. *Biochim Biophys Acta.* 2016 Aug;1866(1):64-75.
- Teglund S., Toftgård R. Hedgehog beyond medulloblastoma and basal cell carcinoma. *Biochim Biophys Acta.* 2010 Apr;1805(2):181-208.
- Teichner A., Eytan E., Sitry-Shevah D., Miniowitz-Shemtov S., Dumin E., Gromis J., Hershko A. p31comet promotes disassembly of the mitotic checkpoint complex in an ATP-dependent process. *Proc Natl Acad Sci U S A.* 2011 Feb 22; 108(8): 3187–3192.
- Thompson S.L., Compton D.A. Proliferation of aneuploid human cells is limited by a p53-dependent mechanism. *J Cell Biol.* 2010 Feb 8;188(3):369-81.
- Thorleifsson G., Walters G.B., Gudbjartsson D.F., Steinthorsdottir V., Sulem P., Helgadottir A., Styrkarsdottir U., Gretarsdottir S., Thorlacius S., Jonsdottir I., Stefansson K. Genome-wide

association yields new sequence variants at seven loci that associate with measures of obesity. *Nat Genet.* 2009 Jan;41(1):18-24.

- Tipton A.R., Tipton M., Yen T., Liu S.T. Closed MAD2 (C-MAD2) is selectively incorporated into the mitotic checkpoint complex (MCC). *Cell Cycle.* 2011 Nov 1;10(21):3740-50.
- Tukachinsky H., Kuzmickas R.P., Jao C.Y., Liu J., Salic A. Dispatched and scube mediate the efficient secretion of the cholesterol-modified hedgehog ligand. *Cell Rep.* 2012 Aug 30;2(2):308-20.
- Utani K., Kohno Y., Okamoto A., Shimizu N. Emergence of micronuclei and their effects on the fate of cells under replication stress. *PLoS One*. 2010 Apr 8;5(4):e10089.
- Valind A., Jin Y., Baldetorp B., Gisselsson D. Whole chromosome gain does not in itself confer cancer-like chromosomal instability. *Proc Natl Acad Sci U S A*. 2013 Dec 24;110(52):21119-23.
- Van den Brink G.R., Bleuming S.A., Hardwick J.C., Schepman B.L., Offerhaus G.J., Keller J.J., Nielsen C., Gaffield W., van Deventer S.J., Roberts D.J., Peppelenbosch M.P. Indian Hedgehog is an antagonist of Wnt signaling in colonic epithelial cell differentiation. *Nat Genet*. 2004 Mar;36(3):277-82.
- Varetti G., Guida C., Santaguida S., Chiroli E., Musacchio A. Homeostatic control of mitotic arrest. *Moll Cell.* 44, 710-720.
- Varjosalo M. and Taipale J. Hedgehog: functions and mechanisms. *Genes & Dev*. 2008. 22: 2454-2472.
- Waalen J. The genetics of human obesity. *Transl Res*. 2014 Oct;164(4):293-301.
- Walczak C.E., Heald R. Mechanisms of mitotic spindle assembly and function. *Int Rev Cytol*. 2008;265:111-58.
- Wang Q., Hirohashi Y., Furuuchi K., Zhao H., Liu Q., Zhang H., Murali R., Berezov A., Du X., Li B., Greene M.I. The centrosome in normal and transformed cells. *DNA Cell Biol.* 2004 Aug;23(8):475-89.
- Weaver B.A., Silk A.D., Cleveland D.W. Cell biology: nondisjunction, aneuploidy and tetraploidy. *Nature*. 2006 Aug 17;442(7104):E9-10.
- Wechsler-Reya R.J., Scott M.P. Control of neuronal precursor proliferation in the cerebellum by Sonic Hedgehog. *Neuron*. 1999 Jan;22(1):103-14.
- Willer C.J., Speliotes E.K., Loos R.J., Li S., Lindgren C.M., Heid I.M., Berndt S.I., Elliott A.L., Jackson A.U., Lamina C., Hirschhorn J.N. Six new loci associated with body mass index highlight a neuronal influence on body weight regulation. *Nat Genet*. 2009 Jan;41(1):25-34.

- Williams B.R., Prabhu V.R., Hunter K.E., Glazier C.M., Whittaker C.A., Housman D.E., Amon A. Aneuploidy affects proliferation and spontaneous immortalization in mammalian cells. *Science.* 2008 Oct 31;322(5902):703-9.
- Wood K.W., Cornwell W.D., Jackson J.R. Past and future of the mitotic spindle as an oncology target. *Curr Opin Pharmacol.* 2001 Aug;1(4):370-7.
- Yoganathan P., Karunakaran S., Ho M.M., Clee S.M. Nutritional regulation of genome-wide association obesity genes in a tissue-dependent manner. *Nutr Metab (Lond)*. 2012 Jul 10;9(1):65.
- Xie J., Murone M., Luoh S.M., Ryan A., Gu Q., Zhang C., Bonifas J.M., Lam C.W., Hynes M., Goddard A., Rosenthal A., Epstein E.H. Jr, de Sauvage F.J. Activating Smoothened mutations in sporadic basal-cell carcinoma. *Nature*. 1998 Jan 1;391(6662):90-2.
- Yue F., Jiang Y., Pan Y., Li L., Li L., Liu R., Wang R. Molecular cytogenetic characterization of partial monosomy 2p and trisomy 16q in a newborn: A case report. *Exp Ther Med.* 2019 Aug;18(2):1267-1275.
- Zainolabidin N., Kamath S.P., Thanawalla A.R., Chen Al. Distinct Activities of Tfap2A and Tfap2B in the Specification of GABAergic Interneurons in the Developing Cerebellum. *Front Mol Neurosci*. 2017 Aug 31;10:281.
- Zarelli V.E., Dawid I.B. The BTB-containing protein Kctd15 is SUMOylated in vivo. *PLoS One.* 2013 Sep 24;8(9):e75016.
- Zheng Y., Guo J., Li X., Xie Y., Hou M., Fu X., Dai S., Diao R., Miao Y., Ren J. An integrated overview of spatiotemporal organization and regulation in mitosis in terms of the proteins in the functional supercomplexes. *Front Microbiol*. 2014 Oct 29;5:573.

ABBREVIATIONS

APC/C: Anaphase Promoting Complex/Cyclosome

Aza: 5'-Aza-2'-deoxycytidine

BTB: broad-complex, Tramtrack, and Bric à brac

BUB: budding uninhibited by benzimidazole

CDC20: Cell Division Cycle 20

CDK1: cyclin-dependent kinase 1

CENP-A/E: centromere protein A/E

CIN: chromosome instability

Co-IP: Co-Immunoprecipitation

CUL3: Cullin3

DHH: Desert Hedgheog

ED: Eating Disorders

GIN: genomic instability

GWAS: Genome-wide association studies

HDAC: histone deacetylase

HDACi: HDAC inhibitors

KCASH: KCTD Containing-Cullin3 Adaptors, Suppressors of Hedgehog

KCTD: potassium (K+) Channel Tetramerization Domain

KCTD15: Potassium Channel Tetramerization Domain Containing 15 protein

IHH: Indian Hedgehog

INM: inner nuclear membrane

LOH: loss of heterozygosity

MAD2: Mitotic Arrest Deficient

MB: Medulloblastoma

MCC: Mitotic Checkpoint Complex

MN: micronuclei

MPS1: Monopolar Spindle 1

MS: Mass Spectrometry

MTA: Microtubule-targeting agents

MTM: Mithramycin A

MTOCs: microtubule organizing centers

NC: neural crest

NE: nuclear envelope

NEBD: nuclear envelope breakdown

NPC: nuclear pore complex

PI: propidium iodide

PTM: post translational modifications

RE: responsive element

ROS: reactive oxygen species

SAC: Spindle Assembly Checkpoint

SHH: Sonic Hedgehog

SMURF2: SMAD Specific E3 Ubiquitin Protein Ligase 2

SP1: specific protein 1

SRR: sterol recognition region

TF: Transcription Factor

TFAP2β: Transcription Factor AP-2 Beta

TP53: Tumor Protein P53

TSS: transcription start site